

UNIVERSIDADE FEDERAL DE MINAS GERAIS
INSTITUTO DE CIÊNCIAS BIOLÓGICAS
PROGRAMA DE PÓS-GRADUAÇÃO EM BIOLOGIA CELULAR

Dissertação de Mestrado

**Caracterização ultraestrutural das brânquias de *Limnoperna fortunei*
frente à exposição aos biocidas Dicloroisocianurato de sódio (NaDCC) e
MXD-100**

Amanda Maria Siqueira Moreira

Belo Horizonte-MG

2022

Amanda Maria Siqueira Moreira

**Caracterização ultraestrutural das brânquias de *Limnoperna fortunei*
frente à exposição aos biocidas Dicloroisocianurato de sódio (NaDCC) e
MXD-100**

Dissertação apresentada ao Programa de Pós-Graduação em Biologia Celular, do Instituto de Ciências Biológicas, da Universidade Federal de Minas Gerais, como requisito parcial para obtenção do título de Mestre em Ciências.

Orientadora: Profa. Dra. Erika Cristina Jorge

Belo Horizonte - MG

Maio de 2022

043

Moreira, Amanda Maria Siqueira.

Caracterização ultraestrutural das brânquias de *Limnoperna fortunei* frente à exposição aos biocidas Dicloroisocianurato de sódio (NaDCC) e MXD-100 [manuscrito] / Amanda Maria Siqueira Moreira. – 2022.

119 f. : il. ; 29,5 cm.

Orientadora: Erika Cristina Jorge.

Dissertação (mestrado) – Universidade Federal de Minas Gerais, Instituto de Ciências Biológicas. Programa de Pós-Graduação em Biologia Celular.

1. Biologia Celular. 2. Biomarcadores. 3. Agentes de Controle Biológico. 4. Mexilhão-dourado. I. Jorge, Erika Cristina. II. Universidade Federal de Minas Gerais. Instituto de Ciências Biológicas. III. Título.

CDU: 576



UNIVERSIDADE FEDERAL DE MINAS GERAIS
 INSTITUTO DE CIÊNCIAS BIOLÓGICAS
 PROGRAMA DE PÓS-GRADUAÇÃO EM BIOLOGIA CELULAR

ATA DA DEFESA DE DISSERTAÇÃO DE MESTRADO DE AMANDA MARIA SIQUEIRA MOREIRA

Às **nove horas** do dia **20 de maio de 2022**, reuniu-se, no Instituto de Ciências Biológicas da UFMG, a Comissão Examinadora da Dissertação, indicada pelo Colegiado do Programa, para julgar, em exame final, o trabalho final intitulado: "**CARACTERIZAÇÃO ULTRAESTRUTURAL DAS BRÂNQUIAS DE LIMNOPERNA FORTUNEI FRENTE À EXPOSIÇÃO AOS BIOCIDAS DICLOROISACIANURATO SÓDICO (NADCC) E MXD-100**", requisito final para obtenção do grau de Mestre em Biologia Celular. Abrindo a sessão, a Presidente da Comissão, **Dra. Erika Cristina Jorge**, após dar a conhecer aos presentes o teor das Normas Regulamentares do Trabalho Final, passou a palavra à candidata, para apresentação de seu trabalho. Seguiu-se a arguição pelos examinadores, com a respectiva defesa da candidata. Logo após, a Comissão se reuniu, sem a presença da candidata e do público, para julgamento e expedição de resultado final. Foram atribuídas as seguintes indicações:

Prof./Pesq.	Instituição	Indicação
Dra. Erika Cristina Jorge	UFMG	Aprovada
Dra. Samyra Maria dos Santos Nassif Lacerda	UFMG	Aprovada
Dra. Lucília Souza Miranda	UFMG	Aprovada

Pelas indicações, a candidata foi considerada: APROVADA

O resultado final foi comunicado publicamente à candidata pela Presidente da Comissão. Nada mais havendo a tratar, a Presidente encerrou a reunião e lavrou a presente ATA, que será assinada por todos os membros participantes da Comissão Examinadora. **Belo Horizonte, 20 de maio de 2022.**

Dr^a. Erika Cristina Jorge (Orientadora)

Dr^a. Samyra Maria dos Santos Nassif Lacerda

Dr^a. Lucília Souza Miranda

Obs: Este documento não terá validade sem a assinatura do Coordenador



Documento assinado eletronicamente por **Fernanda Radicchi Campos Lobato de Almeida**, **Coordenador(a)**, em 20/05/2022, às 14:40, conforme horário oficial de Brasília, com fundamento no art. 5º do [Decreto nº 10.543, de 13 de novembro de 2020](#).

Documento assinado eletronicamente por **Erika Cristina Jorge**, **Professora do Magistério Superior**, em 20/05/2022, às 14:46, conforme horário oficial de Brasília, com fundamento no art. 5º do



[Decreto nº 10.543, de 13 de novembro de 2020.](#)



Documento assinado eletronicamente por **Lucilia Souza Miranda, Professora do Magistério Superior**, em 20/05/2022, às 15:35, conforme horário oficial de Brasília, com fundamento no art. 5º do [Decreto nº 10.543, de 13 de novembro de 2020.](#)



Documento assinado eletronicamente por **Samyra Maria dos Santos Nassif Lacerda, Professora do Magistério Superior**, em 23/05/2022, às 13:36, conforme horário oficial de Brasília, com fundamento no art. 5º do [Decreto nº 10.543, de 13 de novembro de 2020.](#)



A autenticidade deste documento pode ser conferida no site https://sei.ufmg.br/sei/controlador_externo.php?acao=documento_conferir&id_orgao_acesso_externo=0, informando o código verificador **1471887** e o código CRC **ECC651EA**.

AGRADECIMENTOS

Agradecimento especialmente à DEUS, o responsável por me dar forças para superar as dificuldades, e aos meus familiares por todo suporte e carinho durante esta jornada.

Agradeço também aos meus orientadores Profa. Dra. Erika Jorge, Prof. Dr. Antônio Valadão Cardoso e Dr. Érico Freitas por terem compartilhado comigo seus conhecimentos, contribuindo assim para minha formação pessoal e acadêmica.

Aos meus colegas Julia Meireles, Mariana de Paula e Newton Ulhoa por estarem sempre prontos a ajudar e pelas sugestões neste trabalho, em especial ao meu amigo Rayan de Paula por ser meu braço direito durante todo o projeto.

À toda equipe do Laboratório de Biologia Oral e do Desenvolvimento (LABODE) pelo suporte e aprendizado durante os ensaios laboratoriais e à equipe do Centro de Biengenharia de Espécies Invasoras (CBEIH) pela experiência e conhecimento do universo de espécies invasoras, que me permitiram compreender o estudo do mexilhão-dourado.

Agradeço também à Universidade Federal de Minas Gerais e ao Programa de Pós-graduação em Biologia Celular pela oportunidade de concluir mais esta etapa de meus estudos.

*“Não se apavore, nem se desanime, pois o Senhor, o seu Deus, estará com você por onde
você andar.”*

(Josué 1:6-9)

RESUMO

Limnoperna fortunei (Dunker 1857), conhecido como mexilhão-dourado, é um molusco bivalve nativo da Ásia que invadiu a América do Sul na década de 1990. Esta espécie é responsável por danos ecológicos e econômicos devido à sua capacidade incrustante. Entre os métodos utilizados em seu combate, os biocidas MXD-100, composto por taninos e amônia quaternária, e o dicloroisocianurato de sódio (NaDCC), composto orgânico oxidante, são frequentemente utilizados para controlar a infestação em sistemas hidráulicos. O presente trabalho teve como objetivo caracterizar morfológicamente as brânquias de *L. fortunei* e investigar os efeitos dos biocidas MXD-100 e dicloroisocianurato de sódio nestas estruturas, por meio de análises morfológicas e moleculares. Em um primeiro momento, as brânquias foram caracterizadas para consolidar o padrão morfológico da estrutura e, em seguida, os animais foram expostos a NaDCC (1,5mg/L) e MXD-100 (0,56 mg/L) sob condições laboratoriais controladas por 24, 48 e 72h. Achados morfológicos no epitélio branquial demonstraram processos relacionados à captura e seleção de partículas, como estruturas ciliares altamente organizadas, diferenciação entre mucopolissacarídeos neutros e ácidos e abundância de organelas relacionadas à alta demanda energética. A exposição ao NaDCC promoveu mudanças morfológicas progressivas e um aumento da expressão gênica de *SOD* e *HSP70* durante 24 horas, enquanto o MXD-100 levou a alterações morfológicas severas, além do aumento da expressão de *SOD*, *CAT*, *HSP70*, *CYP* durante 24 horas e diminuição da enzima *CAT* durante 48 horas. Assim, NaDCC (1,5 mg/L) apresentou danos letais após 72 horas de exposição sendo necessário exposição contínua para alcançar o controle da espécie, já o tratamento com MXD-100 (5,6 mg/L) mostrou vários efeitos durante as primeiras 24 horas, apresentando uma toxicidade aguda em menor período de tempo. Além de melhorar a compreensão da biologia e estrutura das brânquias de *L. Fortunei*, este trabalho também permitiu determinar os períodos de ação mais eficientes dos biocidas mais comumente

utilizados no controle de incrustações, sem gastos extras ou eventuais desperdícios desses produtos químicos na natureza.

Palavras-chave: biocidas; biomarcadores moleculares; brânquias; mexilhão-dourado; morfologia.

ABSTRACT

Limnoperna fortunei (Dunker 1857), known as the golden mussel, is a bivalve mollusc native to Asia that invaded South America in the 1990s. This species is responsible for ecological and economic damage due to its fouling capacity. Among the methods used to combat it, the biocides MXD-100, composed of tannins and quaternary ammonia, and sodium dichloroisocyanurate (NaDCC), an organic oxidizing compound, are often used to control the infestation in hydraulic systems. This work aimed to characterize the wild *L. fortunei* gills and to investigate the effects of MXD-100 and sodium dichloroisocyanurate on these structures, by morphological and molecular analyses. At first, the gills were characterized to consolidate the morphological pattern of the structure and then, the animals were exposed to NaDCC (1.5mg/L) and MXD-100 (0.56mg/L) under controlled laboratory conditions, for 24, 48 and 72 hours. Morphological findings in the gill epithelium demonstrated processes related to particle capture and selection, such as highly organized ciliary structures, differentiation between neutral and acidic mucopolysaccharides and abundance of organelles related to high energy demand. Exposure to NaDCC promoted progressive morphological changes and an increase in *SOD* and *HSP70* gene expression during 24 hours, while MXD-100 led to severe morphological changes, in addition to increased expression of *SOD*, *CAT*, *HSP70*, *CYP* during 24 hours and decrease in *CAT* enzyme for 48 hours. Thus, NaDCC (1.5 mg/L) showed lethal damage after 72 hours of exposure, requiring continuous exposure to achieve control of the species, while treatment with MXD-100 (5.6 mg/L) showed several effects during the first 24 hours, presenting an acute toxicity in a shorter period of time. Besides to improving the understanding of the biology and structure of the gills of *L. Fortunei*, this work also allowed us to determine the most efficient periods of action of the most commonly used biocides in fouling control, without extra expenses or eventual waste of these chemicals in nature.

Key words: biocides; gills; golden mussel; molecular biomarkers; morphology.

Sumário

1.	Introdução Geral	13
2.	Objetivos.....	16
2.1	Objetivos Específicos	16
3.	Capítulo 1.....	17
3.1	Abstract.....	20
	Background.....	20
	Results.....	20
	Conclusions.....	20
3.2	Background.....	21
3.3	Results.....	24
	Gills Microstructure.....	24
	Gills Ultrastructure	24
3.4	Discussion.....	26
3.5	Conclusions.....	29
3.6	Methods	29
	Light Microscopy.....	29
	Electron Microscopy.....	30
	Scanning Electron Microscopy (SEM).....	30
	Transmission Electron Microscopy (TEM)	31
	Structural Analysis.....	31
3.7	List of abbreviations	33
3.8	References.....	36
3.9	Figure Legends	43
3.10	Supplementary Information	53
4.	Capítulo 2.....	60
4.1	Abstract.....	62
4.2	Introduction.....	63
4.3	Materials And Methods	65
	Mussel Management.....	65
	Exposure To Biocides.....	65
	Histological Analysis.....	66
	Morphometry	66
	Mucous Cell Analysis.....	66

	Scanning Electron Microscopy (SEM) Preparations	66
	Transmission Electron Microscopy (TEM) Preparations	67
	Molecular Analysis	67
	Statistical Analysis.....	68
4.4	Results.....	69
	Changes From Exposure To Sodium Dichloroisocyanurate (Nadcc).....	69
	Changes From Exposure To MXD-100.....	70
4.5	Discussion	71
4.6	Conclusions.....	75
4.7	Acknowledgments	75
4.8	References.....	76
4.9	List of Abbreviation.....	85
4.10	Fugure Legends.....	86
4.11	Tables.....	100
5.	Considerações Finais	102
6.	Referências Bibliográficas	103
7.	Anexo 1.....	105

1. INTRODUÇÃO GERAL

Espécies exóticas correspondem aquelas presentes em um ecossistema de onde não são originárias. Quando a espécie estabelecida possui abundância ou dispersão geográfica que interferem na capacidade de sobrevivência de outras espécies, esta é considerada uma espécie invasora (FERNANDES et al., 2012). A chegada de espécies não nativas a novos ecossistemas propicia alterações na biodiversidade natural, e o estabelecimento de organismos invasores em um novo ambiente pode resultar em uma mudança irreversível na estrutura de suas comunidades biológicas e acarretar a extinção de espécies nativas (SILVA et al., 2016).

O *Limnoperna fortunei*, espécie considerada um problema ecológico, é responsável também por impactos econômicos no setor hidrelétrico devido à volumosas incrustações causadas pelo seu modo de vida gregário (FERNANDES et al., 2012). Conhecido como mexilhão-dourado, é um bivalve nativo de rios da China que foi reportado como espécie invasora na América do sul no Rio de La Plata na década de 90, provavelmente introduzido via águas de lastros carregados por navios cargueiros provenientes da Ásia (DARRIGRAM; PASTORINO, 1993; MANSUR et al., 2003).

Considerando as dimensões continentais do Brasil, a introdução de espécies com potencial invasivo se torna comum de uma bacia hidrográfica em outra na qual não ocorria (FERNANDES et al., 2012). Sendo assim, o mexilhão-dourado foi registrado no Brasil em 2001, na Barragem de Itaipu (ZANELLA; MARENDA, 2002), e se espalhou ao norte atingindo hidrovias como o Rio Paranaíba em 2004 e o Rio grande, na barragem e Volta grande, em 2011 (OLIVEIRA et al., 2015).

O mexilhão-dourado é uma espécie invertebrada e filtradora, pertencente ao filo Mollusca, classe Bivalvia e família Mytilidae. Possui duas válvulas articuladas por ligamento, corpo revestido por manto, um único pé e dois pares de brânquias (Ctenídeos) (BOGAN, 2007). As brânquias dispõem de estrutura dupla lamelar compostas por vários filamentos justapostos (lamelibrânquias) (fig.1) que auxiliam na captura de partículas alimentares suspensas na água e nas trocas gasosas (MANSUR et al., 2012). Dessa forma, em bivalves como *L. fortunei*, este órgão cumpre os papéis de respiração, captura e transporte de partículas (MORTON, 2015).

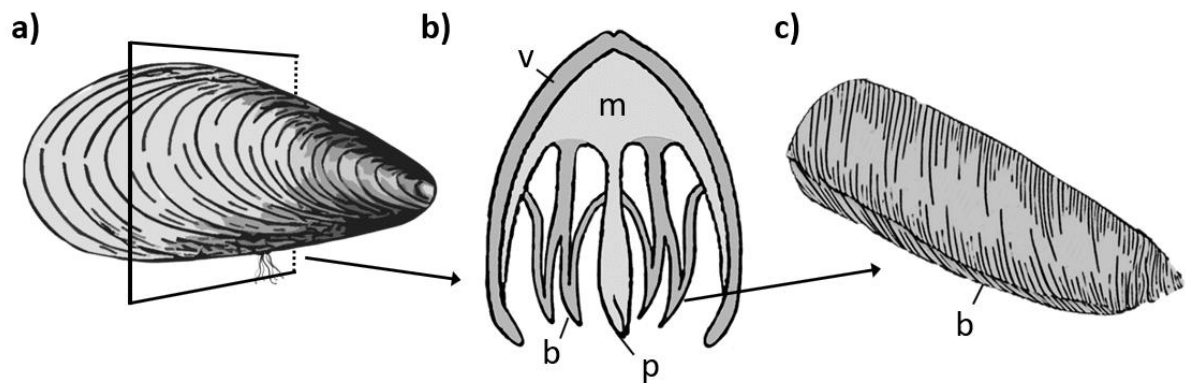


Figura 1 Esquema ilustrativo dos principais órgãos do *L. fortunei*. (a) Vista externa da concha. (b) Corte transversal da metade do animal. (c) Vista lateral das brânquias (ctenídeos). [b] brânquias, [m] manto, [p] pé, [v] válvula.

O estabelecimento do mexilhão-dourado como espécie invasora pode gerar mudanças irreversíveis no ambiente. Além dos impactos ambientais significativos, usinas hidrelétricas têm sofrido diversos prejuízos em seus sistemas, como obstruções de tubulações e entupimento de filtros dos sistemas de arrefecimento das turbinas que demandam manutenções específicas e frequentes, e envolvem custos consideráveis (DE RESENDE, 2007; HAUBROCK et al., 2021).

Entre os métodos de controle de população utilizados, os compostos químicos, também conhecidos como biocidas oxidantes e não-oxidantes, são comumente usados na tentativa de controlar a bioincrustação em sistemas industriais, sendo imprescindível compreender seus mecanismos de ação bem como as reações do organismo quando expostos a esses químicos de controle (CLOETE et al., 1998; DARRIGRAN; DAMBORENEA, 2005).

Deste modo, o presente trabalho investigou os efeitos de ação de dois biocidas, comumente usados em sistemas hidrelétricos - dicloroisocianurato de sódio (NaDCC) e MXD-100, sobre as brânquias do *Limnoperna fortunei*, por meio de análises morfológicas e moleculares. Inicialmente foi realizada a caracterização do epitélio branquial estabelecendo assim um padrão morfológico da espécie, e em um segundo momento, foi feita a exposição aguda à agentes biocidas, em diferentes tempos e as alterações brânquias avaliadas.

O primeiro capítulo desta dissertação traz o artigo intitulado ‘Ultrastructure of the gill ciliary epithelium of *Limnoperna fortunei* (Dunker 1857), the invasive golden mussel’, publicado na revista BMC Zoology em 17 de janeiro de 2022, no qual descrevemos pela

primeira vez, por meio de análises microscópicas de luz e eletrônica, a ultraestrutura do epitélio branquial em mexilhões adultos.

O segundo capítulo, organizado também em formato de artigo, traz os efeitos de dois dos principais biocidas usados no controle de mexilhões em usinas hidrelétricas no país, o dicloroisocianurato de sódio (NaDCC) e MXD-100. Espécimes de mexilhões adultos foram expostos a diferentes tempos em ambos os tratamentos, e as alterações branquiais avaliadas, por análises morfológicas e moleculares, com o intuito de verificar modificações fisiológicas e metabólicas que possam justificar os efeitos nas brânquias consequentes da exposição. Desta forma, esse trabalho apontou os períodos necessários do uso dos agentes biocidas NaDCC e MXD-100, a partir de concentrações pré-estabelecidas, para que haja alterações irreversíveis nas brânquias, e o controle seja eficiente.

2. OBJETIVOS

O presente trabalho teve como objetivo caracterizar a ultraestrutura das brânquias do *Limnoperna fortunei* e investigar os efeitos de diferentes períodos dos biocidas dicloroisocianurato sódio (NaDCC) e MXD-100 sobre este órgão desta espécie.

2.1 OBJETIVOS ESPECÍFICOS

- I- Caracterizar morfológicamente o epitélio mucociliar das brânquias, por meio de análises ultraestruturais de microscopia eletrônica de transmissão e varredura;
- II- Expor espécimes de mexilhões adultos aos biocidas NaDCC e MXD-100, em diferentes tempos de exposição;
- III- Avaliar histologicamente as brânquias dos animais expostos e controle, com o intuito de verificar alterações morfológicas em sua estrutura;
- IV- Verificar possíveis alterações celulares nas brânquias dos animais expostos e controle, utilizando a microscopia eletrônica de transmissão e de varredura;
- V- Analisar, por PCRq, a expressão relativa dos genes *SOD*, *CAT*, *HSP70* e *CYP* que poderiam justificar as modificações fisiológicas consequentes da exposição aos biocidas no tecido branquial exposto ou não aos agentes biocidas.

3. CAPÍTULO 1

ULTRASTRUCTURE OF THE GILL CILIARY EPITHELIUM OF *LIMNOPERNA FORTUNEI* (DUNKER 1857), THE INVASIVE GOLDEN MUSSEL

Ultrastructure of the gill ciliary epithelium of *Limnoperna fortunei* (Dunker 1857), the invasive golden mussel

Erico Tadeu Fraga Freitas^{1,2,3*†}, Amanda Maria Siqueira Moreira^{1,4*}, Rayan Silva de Paula^{1,4}, Gabriela Rabelo Andrade¹, Marcela David de Carvalho⁵, Paulo Santos Assis³, Antônio Valadão Cardoso^{1,6}, Erika Cristina Jorge⁴

1 Centro de Bioengenharia de Espécies Invasoras de Hidrelétricas (CBEIH), Belo Horizonte, MG, 31035-536, Brazil.

2 Universidade Federal de Minas Gerais (UFMG), Centro de Microscopia, Belo Horizonte, MG, 31270-901, Brazil.

3 Universidade Federal de Ouro Preto (UFOP), FIMAT, Ouro Preto, MG, 35400-000, Brazil.

4 Universidade Federal de Minas Gerais (UFMG), Instituto de Ciências Biológicas, Belo Horizonte, MG, 31270-901, Brazil.

5 Companhia Energética de Minas Gerais SA (CEMIG), Belo Horizonte, MG, 30190-131, Brazil.

6 Universidade do Estado de Minas Gerais (UEMG), Escola de Design, Belo Horizonte, MG, 30140-091, Brazil.

* Both authors contributed in the same way to the work

†Corresponding Author: E. Tadeu Fraga Freitas ericotadeu@ufmg.br

Itrastructure of the gill ciliary epithelium of *Limnoperna fortunei* (Dunker 1857), the invasive golden mussel

Erico Tadeu Fraga Freitas^{1,2,3*†}, Amanda Maria Siqueira Moreira^{1,4*}, Rayan Silva de Paula^{1,4}, Gabriela Rabelo Andrade¹, Marcela David de Carvalho⁵, Paulo Santos Assis³, Antônio Valadão Cardoso^{1,6}, Erika Cristina Jorge⁴

¹ Centro de Bioengenharia de Espécies Invasoras de Hidrelétricas (CBEIH), Belo Horizonte, MG, 31035-536, Brazil.

² Universidade Federal de Minas Gerais (UFMG), Centro de Microscopia, Belo Horizonte, MG, 31270-901, Brazil.

³ Universidade Federal de Ouro Preto (UFOP), FIMAT, Ouro Preto, MG, 35400-000, Brazil.

⁴ Universidade Federal de Minas Gerais (UFMG), Instituto de Ciências Biológicas, Belo Horizonte, MG, 31270-901, Brazil.

⁵ Companhia Energética de Minas Gerais SA (CEMIG), Belo Horizonte, MG, 30190-131, Brazil.

⁶ Universidade do Estado de Minas Gerais (UEMG), Escola de Design, Belo Horizonte, MG, 30140-091, Brazil.

* Both authors contributed in the same way to the work

†Corresponding Author:

E. Tadeu Fraga Freitas ericotadeu@ufmg.br

3.1 ABSTRACT

Background

Limnoperna fortunei is a freshwater bivalve mollusc originally from southern Asia that invaded South America in the 1990's. Due to its highly efficient water pumping and filtering, and its capacity to form strong adhesions to a variety of substrates by byssus thread, this invasive species has been able to adapt to several environments across South America, causing significant ecological and economic damages. By gaining a deeper understanding of the biological and ecological aspects of *L. fortunei* we will be able to establish more effective strategies to manage its invasion. The gills of the mollusc are key structures responsible for several biological functions, including respiration and feeding. In this work, we characterized the ultrastructure of *L. fortunei* gills and its ciliary epithelium using light microscopy, transmission and scanning electron microscopies. This is the first report of the morphology of the epithelial cells and cilia of the gill of *L. fortunei* visualized in high resolution.

Results

The analysis showed highly organized and abundant ciliary structures (lateral cilia, laterofrontal cirri and frontal cilia) on the entire length of the branchial epithelium. Mitochondria, smooth endoplasmic reticulum and glycogen granules were abundantly found in the epithelial cells of the gills, demonstrating the energy-demanding function of these structures. Neutral mucopolysaccharides (low viscosity mucus) were observed on the frontal surface of the gill filaments and acid mucopolysaccharides (high viscosity mucus) were observed to be spread out, mainly on the lateral tract. Spherical vesicles, possibly containing mucus, could also be observed in these cells. These findings demonstrate the importance of the mucociliary processes in particle capture and selection.

Conclusions

Our data suggest that the mechanism used by this mollusc for particle capture and selection could contribute to a better understanding of key aspects of invasion and also in the establishment of more efficient and economically viable strategies of population control.

Key words: golden mussel, invasive species, mussel gill, suspension-feeding, branchial epithelium, electron microscopy

3.2 BACKGROUND

Biological invasions of alien animals and plants are one of the most critical threats to biodiversity in aquatic ecosystems. Among the known invasive species, bivalve molluscs are responsible for causing both significant environmental and economic damages [1]. *Limnoperna fortunei* (Dunker 1857) and *Corbicula fluminea* (Müller 1774) are among those bivalves known to have become established invaders in South America [2, 3]. *Limnoperna fortunei* is a bivalve belonging to the family Mytilidae (subclass Pteriomorpha and order Mytiloida) and is originally native to Southeast Asia (including China and South Korea) [4]. The arrival of this invasive mollusc in South America occurred in the early 1990's, possibly transported by ballast waters from cargo ships originating in Asia due to the increase in trade routes between the two continents [5].

Limnoperna fortunei can inhabit waters with a wide range of temperatures and salinity and cope with long periods of air exposure [6, 7]. Understanding the morphological aspects of *L. fortunei* structures is key to further understanding these biological invasions. Some recent studies focused on the morphology and function of the cilia on the *L. fortunei* foot, used to promote adhesion to substrates [8], and on its shell microstructure in adults [9]. As a prolific suspension feeder, *L. fortunei* has one of the highest reported clearance rates for suspension-feeding bivalves, including other invasive species such as *Dreissena polymorpha* (Pallas 1771), *Dreissena bugensis* (Andrusov 1897) and *C. fluminea*. This filtering capacity was analyzed under laboratory conditions using cells from the alga *Chlorella vulgaris*. That also makes *L. fortunei* able to function as a bioindicator and sentinel of metal pollution and pollution monitoring, already observed in other bivalves such as the blue mussel *Mytilus edulis* (Linnaeus 1758) [10, 11, 12]. Indeed, this attribute has already been evaluated in studies involving the accumulation and dynamics of microplastics [13] and herbicides, such as glyphosate [14, 15].

Further understanding of the invasive mussels' morphology can reveal their role in varying ecosystems and also provide insight into possible methods of population control in invaded areas [16]. A thorough morphological description of the *L. fortunei* anatomy has been reported by Morton [17]. *Limnoperna fortunei* has a single foot, two pairs of gills (ctenidia) and is gonochoric with external fertilization. Both juvenile and adult individuals have two valves surrounding the body, mainly composed of calcium carbonate [18] and its polymorphs

aragonite and amorphous calcium carbonate [9]. The outermost part of the shell has a proteinaceous layer, known as periostracum. Adult shell length can reach 4.5 cm [17].

Limnoperna fortunei adult gills are flat, homorhabdic and filibranchiate [17], being in direct contact with the environment. In the presence of environmental contaminants chemicals, such as chlorothalonil, the bivalve gills are key in xenobiotics biotransformation, antioxidant response, innate immune response and osmoregulation [19]. Moreover, a giant virus belonging to the Marseilleviridae family was recently found in *L. fortunei* gills, as the morphophysiological structure of the gills favours microorganism bioaccumulation such as amoebas and viruses [20]. Bivalve gills are located in the mantle cavity [21]. After the post larvae stage, the gills are quite well formed in Mytilidae and Pectinidae, although they continue growing and developing until adulthood [22]. Each gill comprises two demibranchs, the outer and inner demibranchs, a double-lamellar macrostructure, namely ascending and descending lamellae [21]. The gill of the *L. fortunei* is type B(I) [17, 23], showing a W-shape in transverse sections, such as in *M. edulis* and other representatives of Mytilidae [22, 23]. The ventral margin of each demibranch has a deep groove, the marginal food groove [23]. Similar to *D. polymorpha* (Dreissenidae), the outer demibranch of *L. fortunei* is longer than the inner [17, 23]. This arrangement increases the efficiency of transfer of material from the marginal food grooves to the labial palps [17]. Each lamella comprises several parallel tubular filaments, the spaces between which form the interfilament channels. On the lateral surface of each individual filament there are ciliary bands, known as water-pumping cilia or lateral cilia (lc), responsible for the main water flow through the gills [17, 24]. Similar to other Mytiloida, there are frontal cilia (fc) at the frontal tract of the filaments, and laterofrontal cirri (lfc) located at the frontal margin of each filament frontal surface, in between the lc and fc. Each laterofrontal cirrus is a compound ciliary structure, and the action of the lfc facilitates particle capture [25, 26]. The fc transfer the captured particles towards the marginal food groove and then to the labial palps [17, 22, 24, 27-30]. Thereby, in addition to its respiratory function, this organ also fulfils the capturing and transportation of particles [17, 22].

Particle transportation on the gill filaments is mediated to a great extent by mucus [30-34]. The contact of captured particles to the fc of the gill filaments in *Ostrea edulis* (Linnaeus 1758) might cause the goblet cells to secrete mucus, trapping the particles within them [30]. Particles that require large amounts of mucus to cover them would be less likely to be ingested, while those demanding less mucus would be more likely to enter the labial palps [31]. In *M.*

edulis, *Venerupis pullastra* (Montagu 1803) and *Cerastoderma edule* (Linnaeus 1758) an increase in mucus secretion was observed when particles were added to filtered sea water, and strings of mucus-particles could be observed [32]. Mucus mediating particle selection or rejection would be size dependent. High mass particles caused an instantaneous mucus discharge on the coarse frontal tracts of *Crassostrea virginia* (Gmelin 1791), in which the particles were entangled [33]. Mucus discharge would be triggered by a type of tactile stimulation. The smaller particles, on the other hand, would not cause such discharge to occur in the fine frontal tract [33]. A detailed mechanism of selection and rejection of mucus-particles strings by the labial palps in bivalves can be found in the works of Foster-Smith [32, 34] and Beninger and colleagues [35]. The mechanisms of particle capture were reviewed and discussed by Riisgård and Larsen [36] and the works of Ward and Shumway [37] and Rosa and colleagues [38] present great reviews of the present understanding of particle processing by suspension feeders.

The mechanism of particle processing and the further understanding of the physiological aspects of suspension-feeding bivalves greatly depend upon the knowledge of their morphology. *Limnoperna fortunei* morphology has been described in Morton [17]. Additionally, Paolucci and colleagues [39] reported the association between genetic variability and macro- and micro-structural morphology of *L. fortunei* populations across South America. However, few information about the ultrastructure of the golden mussel gills is available thus far. In this current work, for the first time, we characterized the ultrastructure of the gills epithelium of adult *L. fortunei*. These results will assist us to better understand the morphological aspects of the gills, which are vital for respiration and feeding.

3.3 RESULTS

Gills microstructure

The *L. fortunei* gills of adult individuals have a large surface area fitting the mantle cavity space. Each pair of gills has a leaf-like shape (Fig. 1) and is located at both sides of the viscera. Each gill comprises two demibranchs, known as inner- and outer- demibranchs, in a double lamellar structure joined by the gill axis (Fig. 2a). Each demibranch has nearly 75 filaments. Ventrally, the outer demibranch is longer than the inner, but it shortens laterally, close to the labial palps.

At the margins of the frontal surface of each filament, different ciliary projections were observed: lc and lfc, and, on the frontal surface, fc (Fig. 3, 4 and 5 and Additional file 1). Each laterofrontal cirrus has approximately 18-28 pairs of cilia (see Additional file 1). Ciliary discs (cd) were observed at the lateral surface of the filaments (Fig. 3), measuring approximately 16 x 10 μm and cross-connecting individual filaments. TEM images showed that lc, lfc, and fc have the type 9+2 axoneme microtubule-based cytoskeleton (Additional files 1, 2 and 3, Fig. 6 and 7). Pro-laterofrontal cirri (p-lfc) could not be observed between the lfc and fc in the SEM and TEM images. Several adhering particles (<15 μm) could be observed on the frontal surface of the filaments (Fig. 3). A larger particle (nearly 20 μm) could be observed at the lateral tract (Fig. 3) and several smaller particles were observed attached to the lc and lfc (Fig. 3c-d). The smallest particles (200-300 nm) were found to be spherical vesicles and clearly seen on TEM images (Fig. 7b-c, Additional files 1 and 2). Particles of almost 4-5 μm are probably the size of algae cells.

Gills ultrastructure

Light microscopy (LM) images show transverse and longitudinal sections of gill filaments (Fig. 4). The lc, lfc and fc can be clearly observed in the transverse section (Fig. 4a-b). Based on the combined alcian blue and periodic acid Schiff (AB-PAS) staining, we could observe the presence of different types of mucocytes in the gills filaments sections. Acid and neutral mucopolysaccharides were also observed. Larger amounts of neutral mucopolysaccharides (NMPS) were found at the apex of the frontal surface (Fig. 4c-d - stained in pink), while acid mucopolysaccharides (AMPS) were found, in small numbers, spread out in the whole filament (Fig. 4c-d - stained in blue).

TEM image of the transverse section of one filament showed many ciliated epithelial cells (see Additional file 6). Backscattered electron (BSE) SEM images of the longitudinal section of filaments are shown in Fig. 5, with an inverse contrast resembling TEM images. At the dorsal part of the filament epithelium, the basal membrane is smooth (Fig. 5 and Additional file 2). It is supported by a collagenous structure, which also surrounds the hemolymph vessel (Fig. 5). Close to the marginal food groove, a V-shaped collagenous structure could be observed (Fig. 5a). It is apparent that the central hemolymph vessel has no collagenous supporting structure, apart from the marginal food groove. Hemocytes were observed in the central hemolymph (Fig. 5a-b), while more elongated hemocytes could be observed in the region below the basal epithelium (Fig. 5a-c). Three types of cells were observed, Two of them (cells I and II) located at the apical epithelium and the other (cell III) at the basal region (Fig. 5c and Additional file 7). The cell I narrows at the apex of the epithelium and has an elongated dark nucleus that occupies a large volume in the cell and contains more dispersed heterochromatin. Each laterofrontal cirrus arises from a single cell I, as can be seen in the 3D model (see Additional file 7). In between these cells, we could observe the cell II, which has a goblet shape also with an elongated dark nucleus, but with less dispersed heterochromatin. Cell II enlarges at the apex of the epithelium and possesses microvilli, 880 ± 150 nm long (Fig. 5c Additional file 7). The microvilli were also observed on the surface of the lateral tract of the filaments, below the lc around the cd (Fig. 3b-c). Numerous mucins were observed in the cells II (Additional file 8). The cells III have a lobed bright nucleus and were mostly found present at the basal epithelium (Fig. 4d and 5c). Vacuoles occupy a large volume of epithelium and interconnect the basal membrane to the apical region (Fig. 5c).

Gill epithelial cells are shown in Fig. 6 and 7. In Fig. 6a, some fc lay longitudinally to the demibranch filament, suggesting that the fc are stiffer in that portion of the filament, as also observed in Fig. 3c and Additional file 5. In Fig. 6c, the fc were observed in cross-section, which means most of them are bent. Many mitochondria could be observed, mainly in the region close to the insertion site of gill cilia (Fig. 6c-d), while the smooth endoplasmic reticulum could be found in the apical region (Fig. 6d). Surrounding the smooth reticulum, we could also observe several nearly 70 nm electron dense glycogen granules (Fig. 6d). Cell junctions could clearly be seen in the portion of the epithelium observed in TEM images (Fig. 6 and 7) and several septate junctions were observed adjacent to the region with glycogen granules and smooth endoplasmic reticulum (Fig. 6d, 7b-d). In addition, numerous vesicles (201 ± 29 nm), possibly containing mucus, could also be observed in this region (Fig. 6b-c, 7c-d).

3.4 DISCUSSION

In this work, we have characterized the ultrastructure of the mucociliary epithelium of *L. fortunei* gills in order to describe the cellular traits of this important biological structure, mainly responsible for feeding and respiration. The gills of suspension feeders are in direct contact with the environment and understanding their morphology is fundamental to the establishment of new strategies to manage this invasive species in the environment.

Adult gills size from the specimens used in the present work did not significantly differ from the population of *L. fortunei* studied by Paolucci and colleagues [39]. In this work, we could observe a slightly longer mean cilia length of fc of the Volta Grande (VG) specimen, and a slightly lower mean of filament width for the Paranaíba river (PR) one, both compared with *L. fortunei* populations of South America [39]. Morphometric differences found for both VG and PR specimens might be due to different environmental conditions in which they had grown and adapted to.

Classically, the two main functions of the gills in bivalves are feeding and respiration. The thin structure of the gill epithelium may allow the exchange of gases such as oxygen and carbon dioxide by passive diffusion, in response to partial gas pressures. Also, it allows ion exchange between the external environment and the hemolymphatic vessels [40]. The observed microvilli at the apical pole of goblet cells of *L. fortunei* are now evidence that gills might also present a trophic function. The outermost gill epithelium might have a large surface area due to the microvilli, which may assist the direct uptake of dissolved or particulate organic matter. This trait was also suggested for the bivalve *Placopecten magellanicus* (Gmelin 1791) [41, 42]. Furthermore, these cells present vacuoles interconnecting the apical region to the basal membrane of the epithelium, which suggests that transport and diffusion of nutrients might be occurring [42]. We also found endoplasmic reticulum and Golgi complex, organelles that produce and excrete mucus in the goblet cells. These cells look similar to the ones found in *M. edulis* [43] and *P. magellanicus* [42]. As described for the Brazilian endemic bivalve *Diplodon expansus* (Küster 1856) [44], the production of mucus in this apical region of the gills might be associated with lubrication, in order to reduce the frictional resistance in water flow along the epithelium. In *D. expansus*, the mucus layer is highly viscous and difficult to hydrate, ensuring the efficiency of the mucus as a lubricant. The mucus associated with the ciliary tracts might change the local fluid mechanical properties and, in fact, only a small amount of mucus is

needed for the viscosity of the medium transport [45]. It is unlikely that captured particles can be kept in this confined local current produced by the cilia beating without the intervention of mucus in mytiloids homorhabdic gills [36, 46]. Particles covered by intermediate-viscosity mucus are transported close to the frontal gill epithelium in *M. edulis*, in such enclosed space [32, 44]. Our own results are evidence of that in *L. fortunei*. Numerous vesicles, mucus and likely mucus strings were observed in the fc tract of *L. fortunei*. The LM images of sections stained with AB-PAS showed mixed-secreted (neutral and acid) mucopolysaccharide in the gill filaments, with NMPS being abundant on the frontal surface of the filaments. This result corroborates other studies in *M. edulis* [45] and in the oyster *Crassostrea gigas* (Thunberg 1793) [47]. The particles bound to NMPS or mixed (acid + neutral) mucopolysaccharides are transferred to the marginal groove by the frontal cilia and then transported to the labial palps, where they are sorted and either ingested or rejected as pseudofeces.

The mechanisms of particle capture and their transport in suspension-feeding molluscs are almost exclusively ciliary dependent. The lc are responsible for pumping water through the gill interfilament channels towards the suprabranchial cavity [24, 27, 42]. One of the functions of the lfc in Mytilidae and Pectinidae is ascribed to the particle capture [13, 22, 24, 27], which is accomplished by the lfc [27, 28], or through currents produced as the lfc beat against the main water current [24]. Captured particles are then transported towards the marginal food groove by the action of fc, which seems to be autonomous mechanical processes. However, *in vivo* endoscopic observations in many bivalves have shown that the transportation of particles depends either on mucociliary and hydrodynamic mechanisms [25, 26]. Particle rejection or ingestion, on the other hand, is based on physicochemical interactions that can be sensed in the labial palps [13, 42].

Particle selection mechanism is not fully resolved. Some works show that it depends on particle characteristics such as size, shape and surface properties, which affect their ingestion or rejection [37, 38]. Rejected particles are bound to cohesive mucus, deposited in specific sites of the mantle and then transported to the cilia, for their expulsion as pseudofeces [25]. Additionally, the mucus covering feeding organs might mediate particle selection [13, 33, 49]. For *P. magellanicus*, it has been shown that reduced mucus-particles viscosity are more likely to be ingested, while high viscosity mucus-particles are more likely rejected (AMPS) [49]. Our own results show evidence that the mucus produced and excreted in the gills epithelium also plays a role in the mechanism of particle capture itself.

Our data suggested that the mucus in *L. fortunei* gill filaments might be correlated to the fc beating. A larger number of mucus-containing vesicles in the epithelium cells were observed when the fc were bent and, conversely, less mucus-containing vesicles were observed when fc were stiffer, being longitudinal to the gill filament. Such correlation is rather difficult to ensure based on images of TEM sections only and it would need to be investigated by volume electron microscopy. TEM images suggested that the mucus are packed and sent to the apical region. Indeed, we observed mucus and spherical vesicles above the epithelial cells in between the fc and lfc and also mucus covering a food particle. This might be an ongoing process, in which the mucus carried by vesicles towards the gill cilia might be available to interact with the surface of an upcoming particle that will be captured and further transported to the labial palps to be physicochemically sensed and discriminated [13, 42], and then rejected or selected by the feeding organs [13]. The mucus produced by epithelial cells is modified by the Golgi complex, near the nucleus, playing a key role in sorting newly synthesized and recycled molecules towards their final destinations [50], the apical region of the epithelium. TEM images also showed mitochondria with extensive lamellar cristae, arranged in parallel juxtaposed sheets that occupy most of the organelle volume, which is common of high energy-demanding tissues [51] such as the gill ciliary epithelium [52]. The smooth reticulum was also present and among several cellular functions, it participates in glycogen metabolism [52]. The glycogen granules are important components for the bivalve metabolism [54]. Indeed, several septate junctions were observed interconnecting the cell rich in mucus vesicles to the cell where glycogen granules and smooth reticulum were observed. The presence of the septate junctions in this portion of the epithelium is evidence of the active intercellular communication and transport of molecules between them [55, 56]. This energetic apparatus is related to the morpho-functional structure of the ciliary epithelium and its analysis allowed us inferring the correlation between the mucus in gill filaments to the beat of the cilia. Such correlation is quite hard to confirm by single TEM sections, though. This would require a 3D reconstruction of the ciliary epithelium at high spatial resolution. This will be further investigated by volume electron microscopy techniques, to better understand such dynamical processes as this.

3.5 CONCLUSIONS

Understanding the *L. fortunei* morphology is the first step towards the establishment of strategies to control this invasive species and, to the authors' knowledge, this is the first time high-resolution ultrastructure of *L. fortunei* gills epithelium have been reported. Our data showed the microstructure of the gill filaments and cilia in high spatial resolution and also evidence of the production and release of mucus and spherical vesicles in ciliary cells. This might have implications to the process of selection and discrimination of particles to be ingested or rejected by mussels.

3.6 METHODS

Gills preparation

Specimens of adult *L. fortunei* were collected in February 2019 in the fish farming reservoir of the Volta Grande (VG specimen), on the border between the states of Minas Gerais and São Paulo, Brazil (20°01'54.0"S, 48°13'10.0"W), where measured water parameters were 29.2 °C, pH 7.5, dissolved oxygen 3.2 mg L⁻¹, and turbidity 0.1 NTU. Specimens were packed in cloth bags (to decrease overlapping individuals) and during transport, they were submerged in water at constant aeration. In the laboratory at the *Centro de Bioengenharia de Espécies Invasoras de Hidrelétricas* (CBEIH), nearly 200 animals were acclimated for 3 weeks in an aquarium with 36 L capacity containing artesian water well, pH 7.7, dissolved oxygen 6.8 mg L⁻¹ and turbidity 1.68 NTU, at constant aeration and temperature of 18 to 20 °C to minimize stress. After acclimation, the molluscs were kept under the same conditions and temperature of 22 ± 1 °C.

Light microscopy

Adult *L. fortunei* specimens (n=10) were taken out of the aquarium and immersed in Bouin's fixative for 24 h. After this, the gills were dissected, dehydrated in a progressive series of ethanol, cleared in xylene and then embedded in paraffin. Longitudinal and transverse histological sections of the gills were cut with 5 µm thickness, using a MRS 3500 Microtome. Sections were dewaxed in xylene, hydrated in graded ethanol and stained accordingly: to determine the general structure of gills filaments, sections were stained with hematoxylin-eosin

[57]; to demonstrate the existence of polysaccharides, periodic acid Schiff (PAS), combined with alcian blue (AB), at pH 2.5, were used [58], which allowed us differentiating between neutral (stained pink) and acid polysaccharides (stained blue). In addition, the Masson's trichrome method [59] was used to allow the identification of structures that had connective tissue.

Electron microscopy

For the purpose of this work, an adult specimen, with a shell length of approximately 1.5 cm long, was taken out of the aquarium so its valves could be kept partially open with the help of a short piece of metal (1 mm diameter). Next, the specimen was rapidly submerged in a 1.5 mL Eppendorf[®] tube, filled with modified Karnovsky fixative solution (2% paraformaldehyde and 2.5% glutaraldehyde), and incubated for 3 days. The valves were then carefully opened and the gills dissected using forceps, to further process for scanning electron microscopy (SEM) and transmission electron microscopy (TEM). Dissected gills were placed into 1.5 mL Eppendorf[®] tubes containing phosphate buffer solution (PBS). In this present work, we also used unreported TEM and SEM data of the gills from another pristine adult specimen that was collected in Paranaíba river (PR), downstream the confluence with Barreiro's river, near the municipality of Paranaíba (Mato Grosso do Sul, Brazil). Sample preparation details about this latter specimen can be found in Andrade et al. [8]. The two specimens used in the work were named after the place they were collected, as VG and PR specimens.

Scanning electron microscopy (SEM)

Immediately before the secondary fixation, PBS excess volume was first removed and replaced by an appropriate volume of a fresh PBS and incubated for 10 min. This washing process was performed three times. PBS was then replaced by an appropriate volume of 1% osmium tetroxide (OsO₄) in PBS (pH 7.3 ± 0.1) in the fume hood and incubated for 1 h in darkness and room temperature (RT). The sample was washed with PBS and incubated for 10 min, three times. Excess PBS was removed and replaced by 1% tannic acid (C₇₆H₅₂O₄₆) solution and incubated for 20 min at RT. After washing with PBS three times, the solution was replaced by 1% OsO₄ solution and incubated for 1h in darkness and RT. The samples were then washed in distilled water three times and dehydrated in a sequence of alcohol solutions (35%, 50%, 70%, 85%, 95% and 100%), 10 min each. The last step with absolute alcohol was performed twice. The sample was critical point dried with CO₂ (using a Leica EM CPD 030), placed on

an aluminium SEM stub with a carbon tape and finally coated with gold nanoparticles (5 nm thickness) in a sputter coater (Bal-tec MED 020). The VG sample was analysed in a field emission scanning electron microscope (FEI Quanta 200), operated at 5 kV and 15 kV.

Transmission electron microscopy (TEM)

For TEM analysis, samples were firstly washed three times in PBS, for 10 min each time. PBS was replaced by 2% OsO₄ in PBS (pH 7.3 ± 0.1) and incubated for 2h in darkness at RT. Samples were then washed with deionized water four times, for 10 min each time. Distilled water was then replaced by 2% uranyl acetate (C₄H₈O₆U) solution and incubated overnight at 6°C in darkness. Samples were again washed with deionized water, three times, for 5min each, followed by dehydration in a sequence of alcohol solutions (35%, 50%, 70%, 85%, 95% and 100%). Absolute alcohol was replaced by acetone and incubated for 20min. Acetone was then replaced by EponTM resin in three steps, using different dilutions of acetone in resin (2:1, 1:1, and 1:2). In each of these three steps, the tube was enclosed and homogeneously agitated (using a Norte Científica NH2200) for at least 2h. After drying the excess acetone/resin with a filter paper, samples were transferred to a new polypropylene tube containing EponTM resin prepared with DMP-3 (Sigma Aldrich) and incubated at 40°C for 1h. Samples were carefully embedded to obtain longitudinal sections of the lateral surface of the gills' filament. Ultrathin sections (60 nm) were obtained using an ultramicrotome (Leica EM UC6) and a diamond knife Ultra 45° (Diatome), with the sections being transferred to C-film Cu-TEM grids. Series of ultrathin sections (100 nm) array was also obtained and deposited in a clean silicon wafer. The surface of the silicon wafer was previously glow discharged so to become more hydrophilic. Sections were post-stained using a 2% uranyl acetate and lead citrate. TEM analysis was performed in a thermionic W-filament transmission electron microscope (FEI Tecnai Spirit G2-12 BioTwin), operated at 120 kV. SEM and TEM samples preparations and their analysis were performed at the Center of Microscopy at the Universidade Federal de Minas Gerais (UFMG).

Structural analysis

The micro-morphological analysis of the *L. fortunei* gills structure was performed using SEM images. Electron microscopy of thin sections was used to describe the ultrastructural morphology of the ciliary gill epithelium. When suitable, measurements of the gill filaments were performed using transmitted light microscopy images (Additional file 4), taken in a Leica DM4500 microscope, with the same plastic embedded blocks for TEM preparation. Filament

width, interfilament space, and filament linear density (number of filaments per linear distance) were obtained from SEM images. Data are shown in the Additional file 9. Cilia length was obtained in SEM images and the cilia diameter and linear density (number of cilia onto the filament over the linear distance along the filament) using the TEM images. Measurements were performed using the free software FIJI / ImageJ v. 1.52p (Wayne Rasband - National Institutes of Health, USA) and the DigitalMicrograph® v. 3.41.2916.1 (Gatan, Inc).

3.7 LIST OF ABBREVIATIONS

3D – three dimensional

AB-PAS – alcian blue and periodic acid Schiff

AMPS – acid mucopolysaccharides

BSE – Backscattered electron

CBEIH – Centro de Bioengenharia de Espécies Invasoras de Hidrelétricas

cd – ciliary discs

fc – frontal cilia

lc – lateral cilia

lfc – laterofrontal cirri

LM – Light Microscopy

NMPS – neutral mucopolysaccharides

PBS – phosphate buffer solution

p-lfc – pro-laterofrontal cirri

PR – Paranaíba river

SEM – Scanning Electron Microscopy

TEM – Transmission Electron Microscopy

VG – Volta Grande

Declarations

Ethics approval and consent to participate: The experiments have been conducted in compliance with the Brazilian law nº 11.794, of 08/10/2008, (available at http://www.planalto.gov.br/ccivil_03/_ato2007-2010/2008/lei/111794.htm), that concerns laboratory and field experiments involving animals and following the orientation of the Ethical Committee of the Universidade Federal of Minas Gerais (UFMG), which follows the Brazilian regulations on the matter (available at <https://www.ufmg.br/bioetica/ceua/>). The law ruling the animal experiment is concerned about those animals pertaining to the Phylum Chordata and the subphylum Vertebrata. For all the other cases, the submission of the proposal to the above-mentioned ethical committee is waived. Even though there are no specific rules about experiments using invertebrates, our work was carried out in compliance with international standards in ethical research and recent scientific concerns, as those expressed in Drinkwater et al (*Methods Ecol Evol*, 2019, 10(8):1265-1273. doi:10.1111/2041-210X.13208), and ASAB (*Animal Behaviour*, 2020, 159:I-XI. doi:10.1016/j.anbehav.2019.11.002).

Our experiments were performed using adult *L. fortunei* specimens (which are molluscs of the class *Bivalvia*). The collection, transport and maintenance of the molluscs in the laboratory have been authorized by the environmental agency ICMBio, linked to the Ministry of the Environment under code 72222-2 (and can be accessed in <https://drive.google.com/file/d/1SVsAlcTtghxozTmYpyVu9JhEvKX0eMQx/view?usp=sharing>).

Consent for publication: Not applicable.

Availability of data and materials: All data generated or analyzed during this study are included in this published article (and its supplementary information files).

Competing interests: We declare no competing interests.

Funding: This work was supported by Agência Nacional de Energia Elétrica (Anel) / Cemig-GT S.A. under the Project GT-604. The funder supported the CBEIH laboratory infrastructure and all the experiments performed to carry out this work.

Author's contribution: Mr. ETFF performed the electron microscopy analyses and compiled the data. Ms. AMSM collected the samples at the CBEIH laboratory and did the pre-fixation.

Mr. ETFF, Ms. AMSM, and Mr. RSdP contributed to the data analysis and to the written part of the manuscript. Ms. GRA helped in the image treatment, manuscript review and agreed to give non-published electron microscopy images of *L. fortunei* gills she investigated earlier. Mrs. MDdC is the project manager and Professor Mr. PSA the coordinator of the R&D Aneel/Cemig GT-604. Professor Mr. AVC is the research group leader who had the idea of studying the *L. fortunei* gills and revised this manuscript. Professor Mrs. ECJ did the throughout review of the manuscript. All the authors read and approved the manuscript.

Acknowledgments: This work was supported by the Companhia Energética de Minas Gerais (Cemig) GT/ANEEL R&Ds GT-0604. Erico T. F. Freitas received a scholarship from the Universidade Federal de Ouro Preto / Cemig GT S.A. Erika C. Jorge received a scholarship from Conselho Nacional de Desenvolvimento Científico e Tecnológico (CNPq). Author are grateful for the support given by Renato Brito and Kelly Carneiro at the CBEIH laboratory, and by Altair Mendes dos Santos, Flávia Kelly Moreira da Silva, and Marilene Luiza de Oliveira for the sample preparation assistance at the Center of Microscopy at UFMG. This work is dedicated to the memory of Brian Morton (1942-2021), professor emeritus of marine ecology, The University of Hong Kong.

3.8 REFERENCES

1. Fernandes FdC, Mansur M, Pereira D, Fernandes L, Campos S, Danelos O. Abordagem conceitual dos moluscos invasores nos ecossistemas límnicos brasileiros. In: Mansur MCD, Santos CPd, Pereira D, Paz ICP, Zurita MLL, Rodriguez MTR, Nehrke MV, Bergonci PEA, organizadores. Moluscos límnicos invasores no Brasil: biologia, prevenção e controle. Porto Alegre: Redes Editora. 2012; p.19-23.
2. Ituarte C. Primera noticia acerca de la introducción de pelecípodos asiáticos en el área rioplatense (Mollusca: Corbiculidae). *Neotropica*. 1981; 27(77):79-82.
3. Darrigran G, Pastorino G. Bivalvos invasores en el Río de la Plata, Argentina. *Comun Soc Malacol Urug*. 1993; 7:309-13.
4. Xu M. Distribution and spread of *Limnoperna fortunei* in China. In: *Invading nature – Springer series in invasion ecology*. Springer. 2015; doi:10.1007/978-3-319-13494-9_17.
5. Oliveira MD, Campos MC, Paolucci EM, Mansur MC, Hamilton SK. Colonization and spread of *Limnoperna fortunei* in South America. In: *Invading nature – Springer series in invasion ecology*. Springer. 2015; doi:10.1007/978-3-319-13494-9_19.
6. Uliano-Silva M, Americo JA, Brindeiro R, Dondero F, Prosdocimi F, de Freitas Rebelo M. Gene discovery through transcriptome sequencing for the invasive mussel *Limnoperna fortunei*. *PLoS One* 9. 2014; doi:10.1371/journal.pone.0102973.
7. de Andrade JTM, Cordeiro NIS, Montresor LC, da Luz DMR, de Faria Viana EM, Martinez CB, Vidigal THDA. Tolerance of *Limnoperna fortunei* (Dunker, 1857) (Bivalvia: Mytilidae) to aerial exposure at different temperatures. *Hydrobiologia*. 2020; doi:10.1007/s10750-020-04191-4.
8. Andrade GR, de Araújo JLF, Nakamura Filho A, Guañabens AC, Carvalho MDd, Cardoso AV. Functional Surface of the golden mussel's foot: morphology, structures and the role of cilia on underwater adhesion. *Mat Sci Eng C*. 2015; doi:10.1016/j.msec.2015.04.032.

9. Nakamura Filho A, Almeida ACd, Riera HE, Araújo JLFd, Gouveia VJP, Carvalho MDd, Cardoso AV. Polymorphism of CaCO₃ and microstructure of the shell of a Brazilian invasive mollusc (*Limnoperna fortunei*). *Mater Res*. 2014; doi:10.1590/S1516-14392014005000044.
10. Sylvester F, Dorado J, Boltovskoy D, Juárez Á, Cataldo D. Filtration rates of the invasive pest bivalve *Limnoperna fortunei* as a function of size and temperature. *Hydrobiologia*. 2005; doi:10.1007/s10750-004-1322-3.
11. Waykar B, Deshmukh G. Evaluation of bivalves as bioindicators of metal pollution in freshwater. *Bull Environ Contam Toxicol*. 2012; doi:10.1007/s00128-011-0447-0.
12. Schøyen M, Allan IJ, Ruus A, Håvardstun J, Hjermann DØ, Beyer J. Comparison of caged and native blue mussels (*Mytilus edulis* spp.) for environmental monitoring of PAH, PCB and trace metals. *Mar Environ Res*. 2017; doi:10.1016/j.marenvres.2017.07.025.
13. Ward JE, Rosa M, Shumway SE. Capture, ingestion, and egestion of microplastics by suspension-feeding bivalves: a 40-year history. *Anthropocene Coasts*. 2019; doi:10.1139/anc-2018-0027.
14. Di Fiori E, Pizarro H, dos Santos Afonso M, Cataldo D. Impact of the invasive mussel *Limnoperna fortunei* on glyphosate concentration in water. *Ecotox Environ Safe*. 2012; doi:10.1016/j.ecoenv.2012.04.024.
15. Vargas RPF, Saad JF, Graziano M, dos Santos Afonso M, Izaguirre I, Cataldo D. Bacterial composition of the biofilm on valves of *Limnoperna fortunei* and its role in glyphosate degradation in water. *Aquat Microb Ecol*. 2019; doi:10.3354/ame01907.
16. Mansur M. Bivalves invasores límnicos: morfologia comparada de *Limnoperna fortunei* e espécies de *Corbicula* spp. In: Mansur MCD, Santos CPd, Pereira D, Paz ICP, Zurita MLL, Rodriguez MTR, Nehrke MV, Bergonci PEA, organizadores. *Moluscos límnicos Invasores no Brasil: biologia, prevenção, controle*. Porto Alegre: Redes Editora; 2012. p.61-74.
17. Morton B. The biology and anatomy of *Limnoperna fortunei*, a significant freshwater bioinvader: blueprints for success. In: *Invading nature – Springer series in invasion ecology*. Springer. 2015; doi: 10.1007/978-3-319-13494-9_1.

18. Bogan AE. Global diversity of freshwater mussels (Mollusca, Bivalvia) in freshwater. In: Balian EV, Lévêque C, Segers H, Martens K, editors. Freshwater animal diversity assessment. Springer. 2008; doi:10.1007/978-1-4020-8259-7_16.
19. Guerreiro AdS, Monteiro JS, Medeiros ID, Sandrini JZ. First evidence of transcriptional modulation by chlorothalonil in mussel *Perna perna*. *Chemosphere*. 2020; doi:10.1016/j.chemosphere.2020.126947.
20. dos Santos RN, Campos FS, de Albuquerque NRM, Finoketti F, Correa RA, Cano-Ortiz L, Assis FL, Arantes TS, Roehe PM, Franco AC. A new marseillevirus isolated in Southern Brazil from *Limnoperna fortunei*. *Sci Rep*. 2016; doi:10.1038/srep35237.
21. Ridewood WD. On the structure of the gills of the lamellibranchia. *Philos Trans R Soc B*. 1903; doi:10.1098/rstb.1903.0005.
22. Cannuel R, Beninger PG, McCombie H, Boudry P. Gill development and its functional and evolutionary implications in the blue mussel *Mytilus edulis* (Bivalvia: Mytilidae). *Biol Bull*. 2009; doi: 10.1086/BBLv217n2p173.
23. Atkins D. On the ciliary mechanisms and interrelationships of lamellibranchs. Part III: types of lamellibranch gills and their food currents. *J Cell Sci*. 1937; doi: 10.1242/jcs.s2-79.315.375.
24. Riisgård HU, Funch P, Larsen PS. The mussel filter–pump–present understanding, with a re-examination of gill preparations. *Acta Zool*. 2015; doi:10.1111/azo.12110.
25. Ward, JE. Biodynamics of suspension-feeding in adult bivalves molluscs: particle capture, processing and fate. *Invert. Bio*. 1996; doi:10.2307/3226932.
26. Ward, JE, Sanford LP, Newell RIE, MacDonald BA. A new explanation of particle capture in suspension-feeding bivalve molluscs. *Limnol. Oceanogr*. 1998; doi:10.4319/lo.1998.43.5.0741.
27. Atkins D. On the ciliary mechanisms and interrelationships of lamellibranchs. Part VI: latero-frontal cilia of the gill filaments and their phylogenetic value. *J Cell Sci*. 1938; doi:10.1242/jcs.s2-80.319.345.

28. Silverman H, Lynn JW, Achberger EC, Dietz TH. Gill structure in zebra mussels: bacterial-sized particle filtration. *Am Zool.* 1996; doi:10.1093/icb/36.3.373.
29. Owen G. Classification and the bivalve gill. *Phil Trans R Soc Lond B.* 1978; doi:10.1098/rstb.1978.0075.
30. Yonge C. Structure and physiology of the organs of feeding and digestion in *Ostrea edulis*. *J Mar Biolog Assoc UK.* 1926; doi:10.1017/S002531540000789X.
31. Atkins D. On the ciliary mechanisms and interrelationships of lamellibranchs. Part II: sorting devices on the gills. *J Cell Sci.* 1937; doi:10.1242/jcs.s2-79.315.339.
32. Foster-Smith RL. The role of mucus in the mechanism of feeding in three filter-feeding bivalves. *Proc Malac Soc Lond.* 1975; doi:10.1093/oxfordjournals.mollus.a065307.
33. Ribelin BW, Collier A. Studies on the gill ciliation of the American oyster *Crassostea virginica* (Gmelin). *J Morph.* 1977; doi:10.1002/jmor.1051510308.
34. Foster-Smith RL. The function of the pallial organs of bivalves in controlling ingestion. *J Moll Stud.* 1978; doi:1093/oxfordjournals.mollus.a065419.
35. Beninger PG, Le Pennec M, Donval A. Mode of particle ingestion in five species of suspension-feeding bivalve molluscs. *Mar Biol.* 1991; doi:10.1007/BF01344340.
36. Riisgård HU, Larsen PS. Particle capture mechanisms in suspension-feeding invertebrates. *Mar Ecol Progr Ser.* 2010; doi:10.3354/meps08755.
37. Ward JE, Shumway SE. Separating the grain from the chaff: particle selection in suspension-and deposit-feeding bivalves. *J Exp Mar Biol Ecol.* 2004; doi:10.1016/j.jembe.2004.03.002.
38. Rosa M, Ward JE, Shumway SE. Selective capture and ingestion of particles by suspension-feeding bivalve molluscs: a review. *J Shellfish Res.* 2018; doi:10.2983/035.037.0405.
39. Paolucci E, Sardiña P, Sylvester F, Perepelizin PV, Zhan A, Ghabooli S, Cristescu ME, Oliveira MD, MacIsaac HJ. Morphological and genetic variability in an alien invasive mussel

across an environmental gradient in South America *Limnol Oceanogr.* 2014; doi:10.4319/lo.2014.59.2.0400.

40. Rodriguez C, Prieto GI, Vega IA, Castro-Vazquez A. Functional and evolutionary perspectives on gill structures of an obligate air-breathing, aquatic snail. *PeerJ* 2019; doi: 10.7717/peerj.7342.

41. Beninger PG, Le Pennec M, Salaün M. New observations of the gills of *Placopecten magellanicus* (Mollusca: Bivalvia), and implications for nutrition. I. General anatomy and surface microanatomy. *Mar Biol.* 1988; doi:10.1007/BF00392659.

42. Le Pennec M, Beninger PG, Herry A. New observations of the gills of *Placopecten magellanicus* (Mollusca: Bivalvia), and implications for nutrition. II. Internal anatomy and microanatomy. *Mar Biol.* 1988; doi:10.1007/BF00391199.

43. Owen G. Studies on the gill of *Mytilus edulis*: the eu-latero-frontal cirri. *Proc R Soc Lond B.* 1974; doi:10.1098/rspb.1974.0062.

44. Nogarol LR, Brossi-Garcia AL, de Oliveira David JA, Fontanetti CS. Morphological and Histochemical Characterization of Gill Filaments of the Brazilian Endemic Bivalve *Diplodon expansus* (Küster, 1856) (Mollusca, Bivalvia, Hyriidae). *Microsc Microanal.* 2012; doi:10.1017/S1431927612013992.

45. Beninger PG, Decottignies P. Worth a second look: gill structure in *Hemipecten forbesianus* (Adam & Reeve, 1849) and taxonomic implications for the Pectinidae. *J Molluscan Stud.* 2008; doi:10.1093/mollus/eyn001.

46. Beninger PG, St-Jean S, Poussart Y, Ward JE. Gill function and mucocyte distribution in *Placopecten magellanicus* and *Mytilus edulis* (Mollusca: Bivalvia): the role of mucus in particle transport. *Mar Eco Progr Ser.* 1993; doi:10.3354/meps098275.

47. Beninger PG, Cannuel R, Jaunet S. Particle processing on the gill plicae of the oyster *Crassostrea gigas*: fine-scale mucocyte distribution and functional correlates. *Mar Eco Progr Ser.* 2005; doi:10.3354/meps295191.

48. Garrido M, Chaparro O, Thompson R, Garrido O, Navarro J. Particle sorting and formation and elimination of pseudofaeces in the bivalves *Mulinia edulis* (siphonate) and *Mytilus chilensis* (asiphonate). *Mar Biol.* 2012; doi:10.1007/s00227-012-1879-8.
49. Beninger PG, Le Pennec M. Scallop structure and function. *Dev Aquacult Fish Sci.* 2016; doi:10.1016/B978-0-444-62710-0.00003-1.
50. Zappa F, Failli M, Matteis MA. The Golgi complex in disease and therapy. *Curr Opin Cell Biol.* 2018; doi:10.1016/j.ceb.2018.03.005.
51. Fontanesi F. Mitochondria: structure and role in respiration. *eLS.* 2001; doi:10.1002/9780470015902.a0001380.pub2.
52. Jones HD, Richards OG, Hutchinson S. The role of ctenidial abfrontal cilia in water pumping in *Mytilus edulis* L. *J Exp Mar Biol Ecol.* 1990; doi:10.1016/0022-0981(90)90108-O.
53. Alberts B, Dennis B, Karen H. *Fundamentos da Biologia Celular 4.* Porto Alegre: Artmed Editora; 2006.
54. Berthelin C, Kellner K, Mathieu M. Histological characterization and glucose incorporation into glycogen of the Pacific oyster *Crassostrea gigas* storage cells. *Mar biotechnol.* 2000; doi:10.1007/s101269900017.
55. Gilula NB, Satir P. Septate and gap junctions in molluscan gill epithelium. *J Cell Biol.* 1971; doi:10.1083/jcb.51.3.869.
56. Alexander DB, Goldberg GS. Transfer of biologically important molecules between cells through gap junction channels. *Curr Med Chem.* 2005; doi:10.2174/0929867033456927.X1.
57. Bancroft JD, Layton C. 10 - The hematoxylin and eosin, Editors: Suvarna SK, Layton C, Bancroft JD. *Bancroft's theory and practice of histological techniques.* 2012; doi:10.1016/B978-0-7020-4226-3.00010-X.
58. Yamabayashi S. Periodic acid-Schiff-Alcian Blue: A method for the differential staining of glycoproteins. *Histochem J.* 1987; doi:10.1007/BF01687364.

59. Ferro AB, Alves I, Silva MA, Carrujo O. Optimização da técnica do tricrómio de Masson. Mícron. 2006; <http://hdl.handle.net/10400.21/5458>.

3.9 FIGURE LEGENDS:

Fig. 1 Digitally Colored SEM images of *L. fortunei* with the left valve removed, showing one ciliated gill (inner and outer demibrach), the labial palps, the foot and byssus threads, and parts of the shell structure.

Fig. 2 SEM images of the *L. fortunei* gills. (a) Dorsal view of the gill showing the lamellae, the inner- and outer- demibranch [id and od] joined by the gill axis [ga]. The od is behind and folded under the id. Its ventral margin appears at the lower left of the image. (b) Frontal view of one lamella [lm] showing its ventral aspect. (c) Longitudinal view of one filament demibranch [f] showing its lateral aspect. The marginal food groove [mfg] at the lamella's edge is pointed out by the arrowheads in images (b,c).

Fig. 3 SEM images of the *L. fortunei* gills. (a) View in perspective of a set of filaments [f], showing ciliary discs [cd], lateral cilia [lc], laterofrontal cirri [lfc] and frontal cilia [fc]. The outlined arrowheads indicate likely mucus-strings on the frontal tract. The outlined and filled open arrowheads indicate larger particles on the frontal and lateral tract, respectively. Images (b) and (c, d) show in detail a cd, the lc and lfc, respectively. Microvilli [mv] are present below the lc and around the cd. Several spherical particles of about 200-300 nm and one of nearly 4-5 μm size were observed attached to the lfc. (e) View in perspective of one filament showing its lateral aspect and the detailed lfc at the top frontal margin. (f) Higher magnification image of the region marked with the rectangle in (e). Each individual cilia of the laterofrontal cirrus bent at the top, thus having a shape of a comb.

Fig. 4 LM images showing the transverse (a, b, c) and coronal (c, d) sections of a gill filament of *L. fortunei*. Filaments stained with hematoxylin and eosin are shown in the images (a, e). The filaments stained with Alcian Blue/PAS shown in images (c, d, f), and stained with Masson's trichrome in image (b). Neutral mucopolysaccharides (NMPS) are coloured in pink and acid mucopolysaccharides (AMPS) are coloured in blue. Lateral cilia [lc], laterofrontal cirri [lfc], frontal cilia [fc], marginal food groove [mfg], and collagenous structure [cs] are indicated.

Fig. 5 (a) Backscattered electron SEM images (with inverse contrast) of a thin section longitudinal to the gill filament close to the marginal food groove (at the top, not visible). The collagenous structure [cs] supporting the hemolymph vessel of the epithelium, the smooth basal membrane [bm], and hemocytes [h] are shown. (b, c) Higher magnification images of the squares shown in (a). A lobed hemocyte in the central hemolymph shown in (b). Large vacuoles [vc], cs and bm are shown in (c). Three types of cells are indicated, types I and II with a dark nuclei, and the type III with a bright nucleus. The filled arrowheads indicate the microvilli on the apex of cells of type II. The lfc that arise from the cells of type I are also shown.

Fig. 6 Bright-field TEM images of the epithelial cells of *L. fortunei*, showing coronal sections of a gill filament. In image (a), many frontal cilia [fc] are observed longitudinal to the gill filament, and in image (c) the fc are observed in cross-section. (b, d) Epithelial cells at higher magnification, displaying the nucleus [n], mitochondria [m], Golgi complex [g], vesicles [v], smooth reticulum [r], and glycogen granules [gg]. The region highlighted in image (c) shows possibly mucus in between the fc. The filled arrowheads in images (b, d) point out some vesicles, mitochondria, and glycogen granules. The open arrowheads in (b) indicate apparent non-junctional regions of the cell membranes with a slightly increased space. The open arrowheads in (d) indicate the septate junctions.

Fig. 7 Bright-field TEM images of the epithelial cells of *L. fortunei*, showing transversal sections of the gill filament. (a) Epithelial cells of the frontal tract, displaying the nucleus [n], Golgi complex [g] and smooth reticulum [r]. (b) Cells at the margin of the frontal tract showing the laterofrontal cirri [lfc] and spherical vesicles [v] above the epithelium. (c) Cells of the lateral tract that bears the lateral cilia [lc]. Spherical vesicles are also present in between the lc. (d) Higher magnification image of the square in (c) showing vesicle possibly containing mucus, and the septate junction in detail [sj]. The open arrowheads in images (b, c) indicate septate junctions. The outlined arrowheads point out non-junctional regions of the cell membranes with increased space

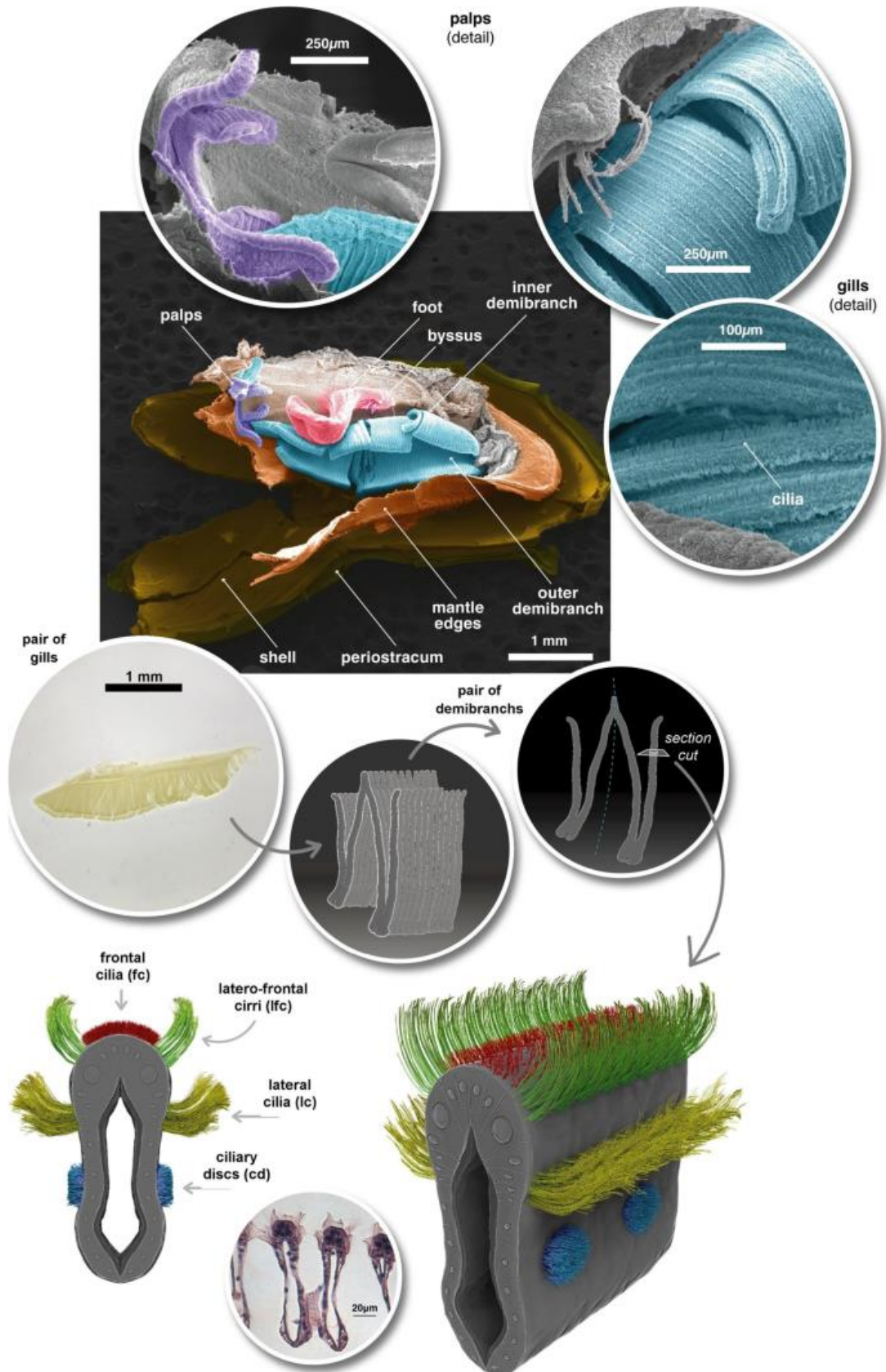


Figure 1 Digitally Colored SEM images of *L. fortunei* with the left valve removed, showing one ciliated gill (inner and outer demibranch), the labial palps, the foot and byssus threads, and parts of the shell structure.

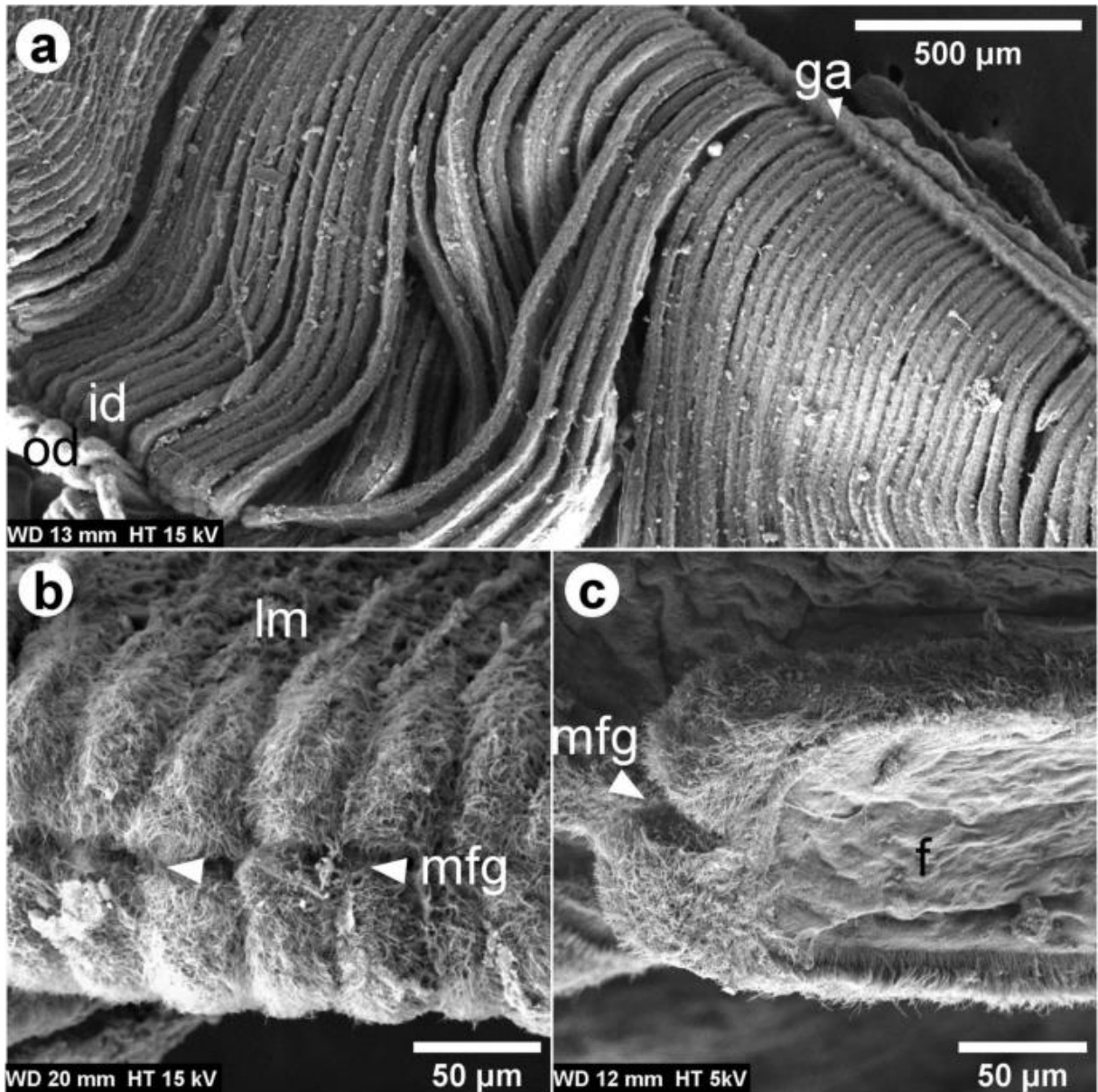


Figure 2 SEM images of the *L. fortunei* gills. (a) Dorsal view of the gill showing the lamellae, the inner- and outer- demibranch [id and od] joined by the gill axis [ga]. The od is behind and folded under the id. Its ventral margin appears at the lower left of the image. (b) Frontal view of one lamella [lm] showing its ventral aspect. (c) Longitudinal view of one filament demibranch [f] showing its lateral aspect. The marginal food groove [mfg] at the lamella's edge is pointed out by the arrowheads in images (b,c).

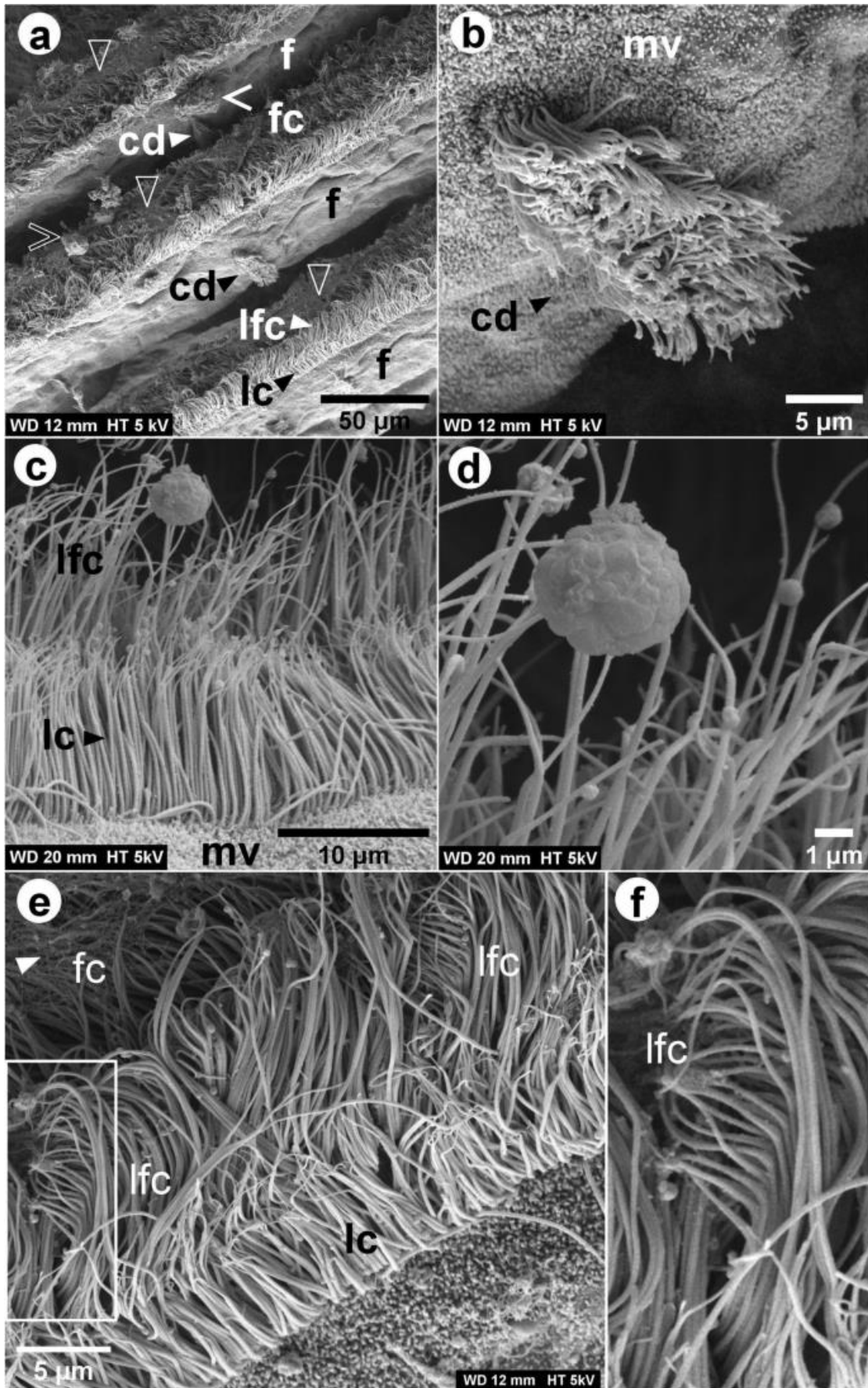


Figure 3 SEM images of the *L. fortunei* gills. (a) View in perspective of a set of filaments [f], showing ciliary discs [cd], lateral cilia [lc], laterofrontal cirri [lfc] and frontal cilia [fc]. The outlined arrowheads indicate likely mucus-strings on the frontal tract. The outlined and filled open arrowheads indicate larger particles on the frontal and lateral tract, respectively. Images (b) and (c, d) show in detail a cd, the lc and lfc, respectively. Microvilli [mv] are present below the lc and around the cd. Several spherical particles of about 200-300 nm and one of nearly 4-5 μm size were observed attached to the lfc. (e) View in perspective of one filament showing its lateral aspect and the detailed lfc at the top frontal margin. (f) Higher magnification image of the region marked with the rectangle in (e). Each individual cilia of the laterofrontal cirrus bent at the top, thus having a shape of a comb.

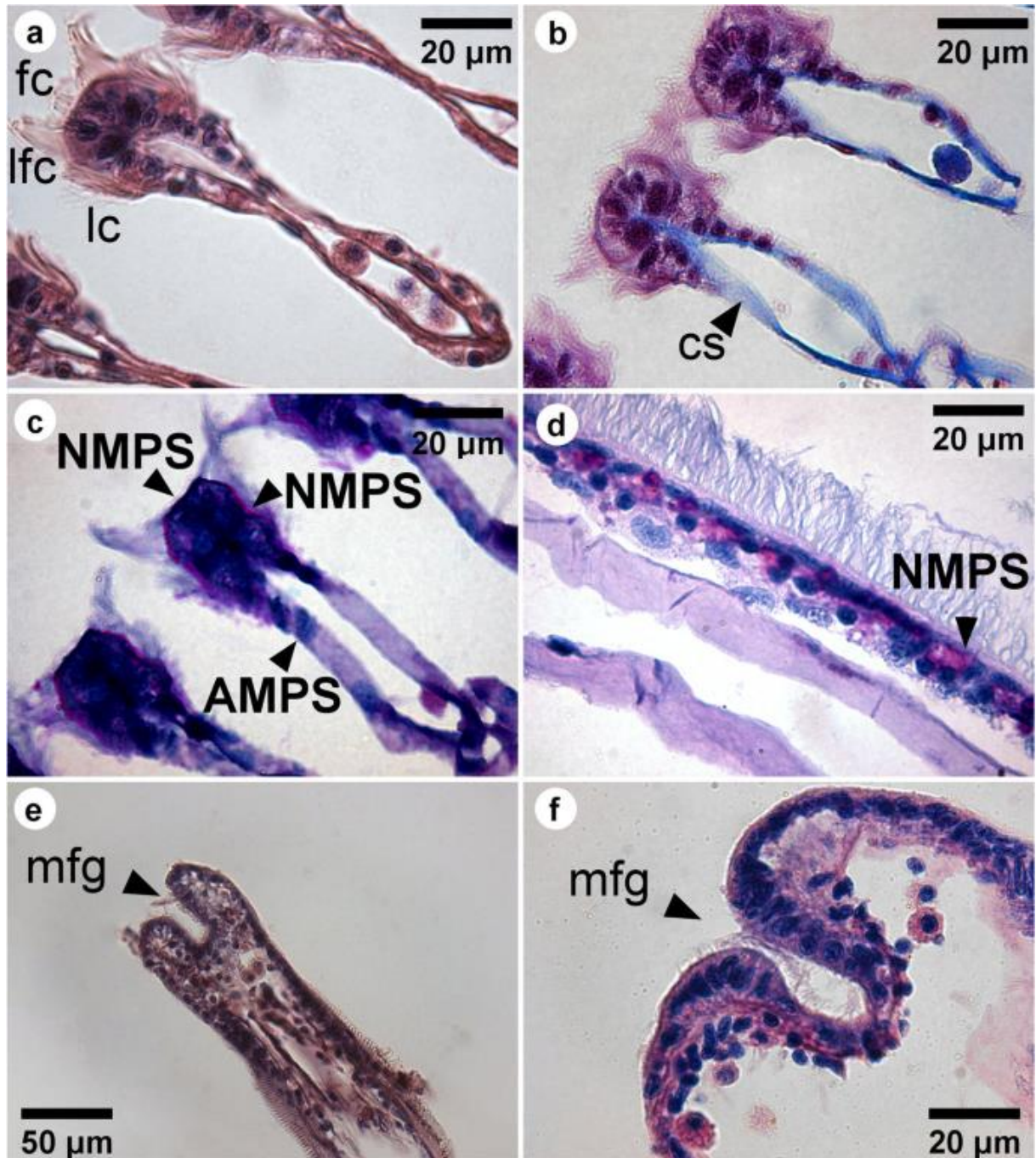


Figure 4 LM images showing the transverse (a, b, c) and coronal (c, d) sections of a gill filament of *L. fortunei*. Filaments stained with hematoxylin and eosin are shown in the images (a, e). The filaments stained with Alcian Blue/PAS shown in images (c, d, f), and stained with Masson's trichrome in image (b). Neutral mucopolysaccharides (NMPS) are coloured in pink and acid mucopolysaccharides (AMPS) are coloured in blue. Lateral cilia [lc], laterofrontal cirri [lfc], frontal cilia [fc], marginal food groove [mfg], and collagenous structure [cs] are indicated.

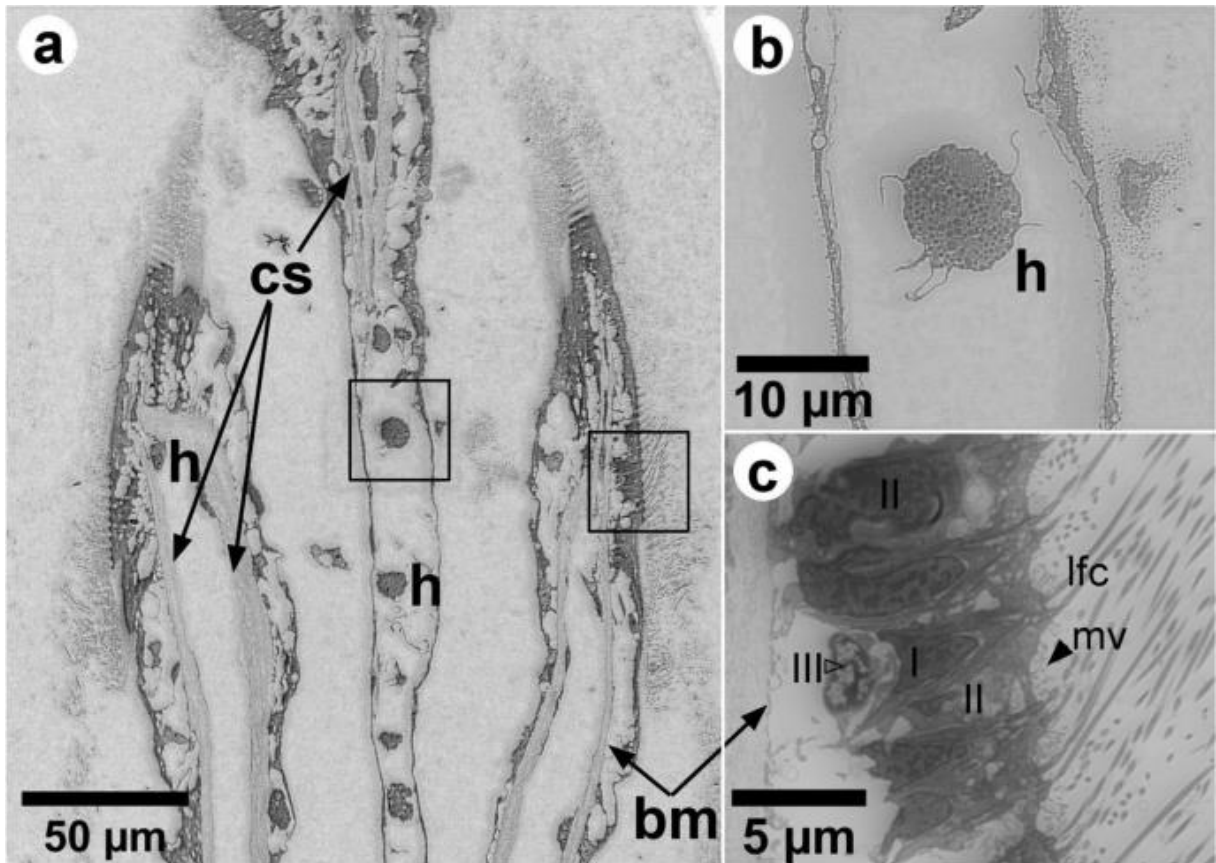


Figure 5 (a) Backscattered electron SEM images (with inverse contrast) of a thin section longitudinal to the gill filament close to the marginal food groove (at the top, not visible). The collagenous structure [cs] supporting the hemolymph vessel of the epithelium, the smooth basal membrane [bm], and hemocytes [h] are shown. (b, c) Higher magnification images of the squares shown in (a). A lobed hemocyte in the central hemolymph shown in (b). Large vacuoles [vc], cs and bm are shown in (c). Three types of cells are indicated, types I and II with a dark nuclei, and the type III with a bright nucleus. The filled arrowheads indicate the microvilli on the apex of cells of type II. The lfc that arise from the cells of type I are also shown.

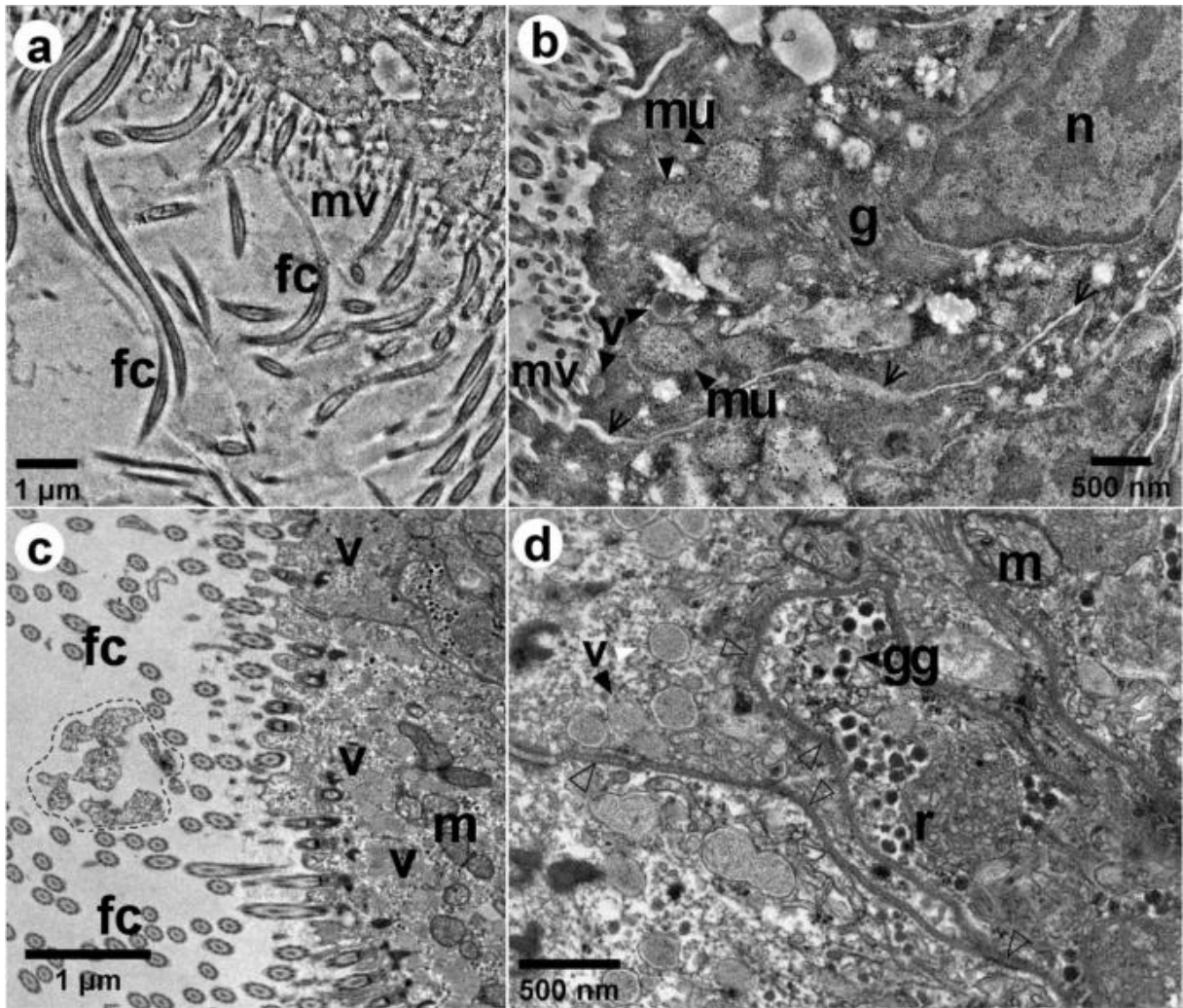


Figure 6 Bright-field TEM images of the epithelial cells of *L. fortunei*, showing coronal sections of a gill filament. In image (a), many frontal cilia [fc] are observed longitudinal to the gill filament, and in image (c) the fc are observed in cross-section. (b, d) Epithelial cells at higher magnification, displaying the nucleus [n], mitochondria [m], Golgi complex [g], vesicles [v], smooth reticulum [r], and glycogen granules [gg]. The region highlighted in image (c) shows possibly mucus in between the fc. The filled arrowheads in images (b, d) point out some vesicles, mitochondria, and glycogen granules. The open arrowheads in (b) indicate apparent non-junctional regions of the cell membranes with a slightly increased space. The open arrowheads in (d) indicate the septate junctions.

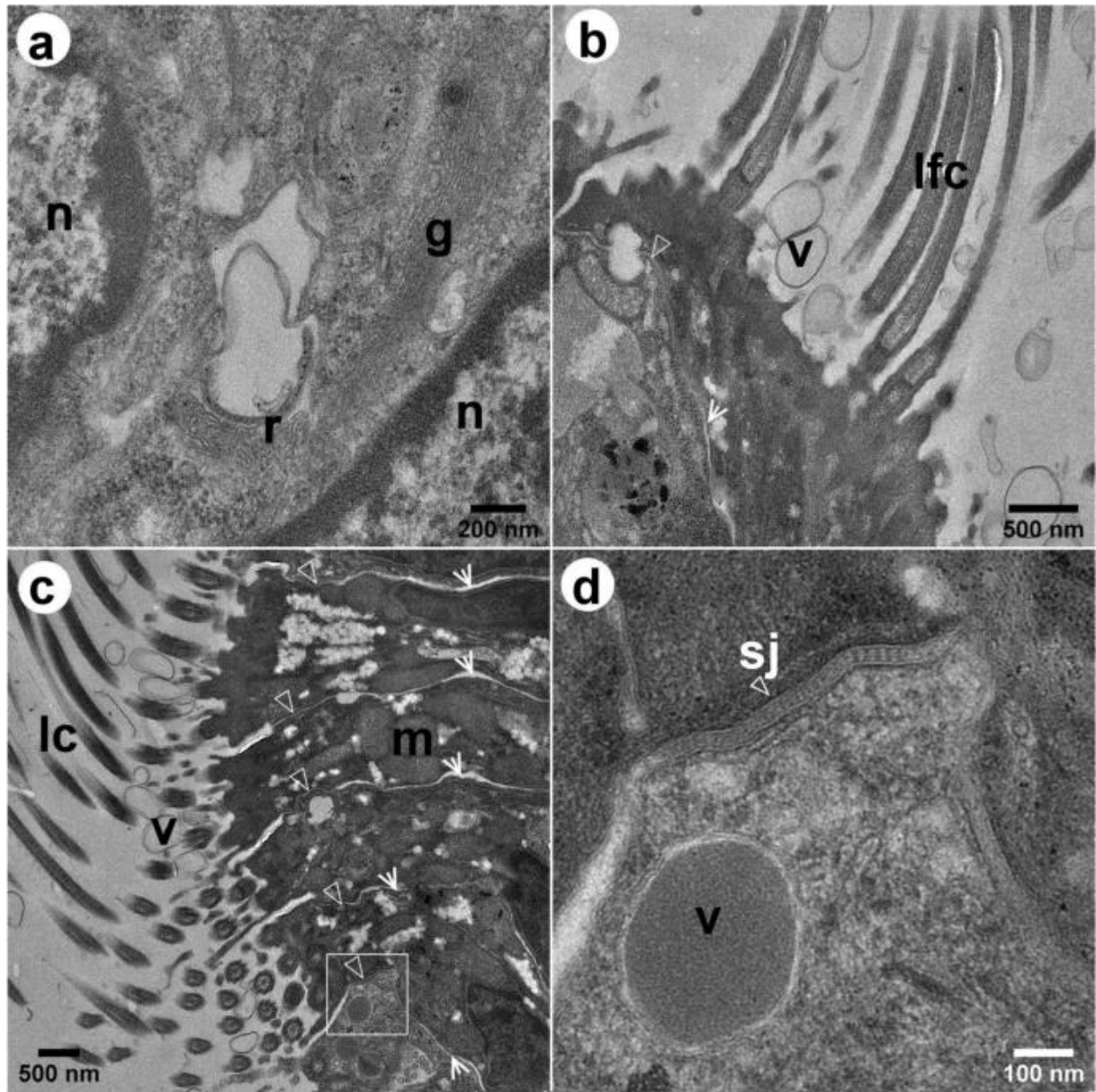
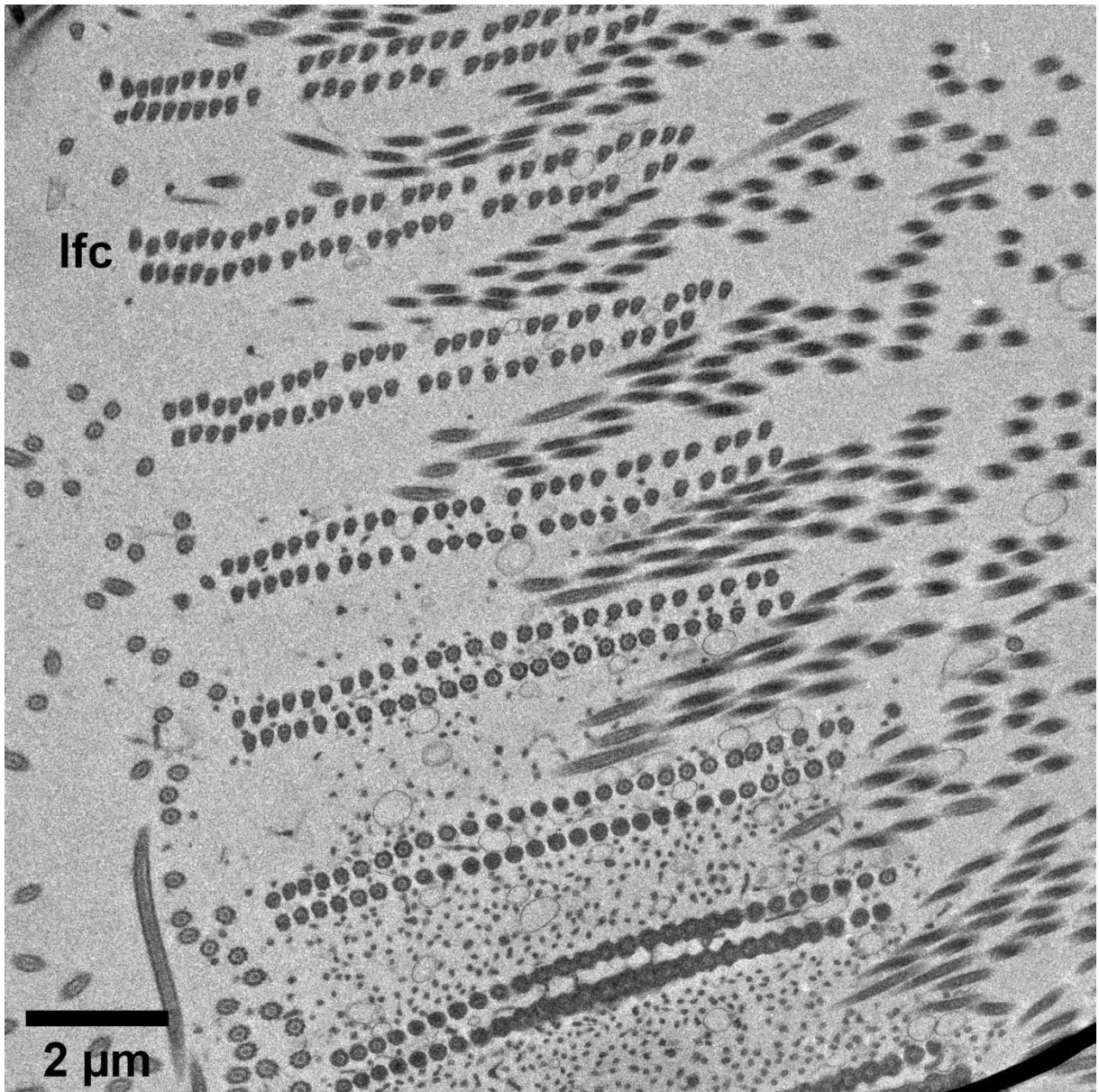
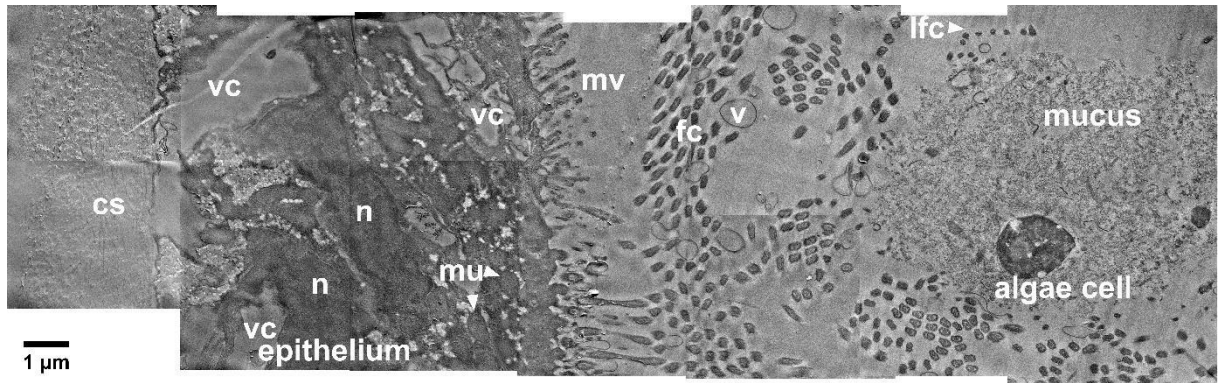


Figure 7 Bright-field TEM images of the epithelial cells of *L. fortunei*, showing transversal sections of the gill filament. (a) Epithelial cells of the frontal tract, displaying the nucleus [n], Golgi complex [g] and smooth reticulum [r]. (b) Cells at the margin of the frontal tract showing the laterofrontal cirri [lfc] and spherical vesicles [v] above the epithelium. (c) Cells of the lateral tract that bears the lateral cilia [lc]. Spherical vesicles are also present in between the lc. (d) Higher magnification image of the square in (c) showing vesicle possibly containing mucus, and the septate junction in detail [sj]. The open arrowheads in images (b, c) indicate septate junctions. The outlined arrowheads point out non-junctional regions of the cell membranes with increased space

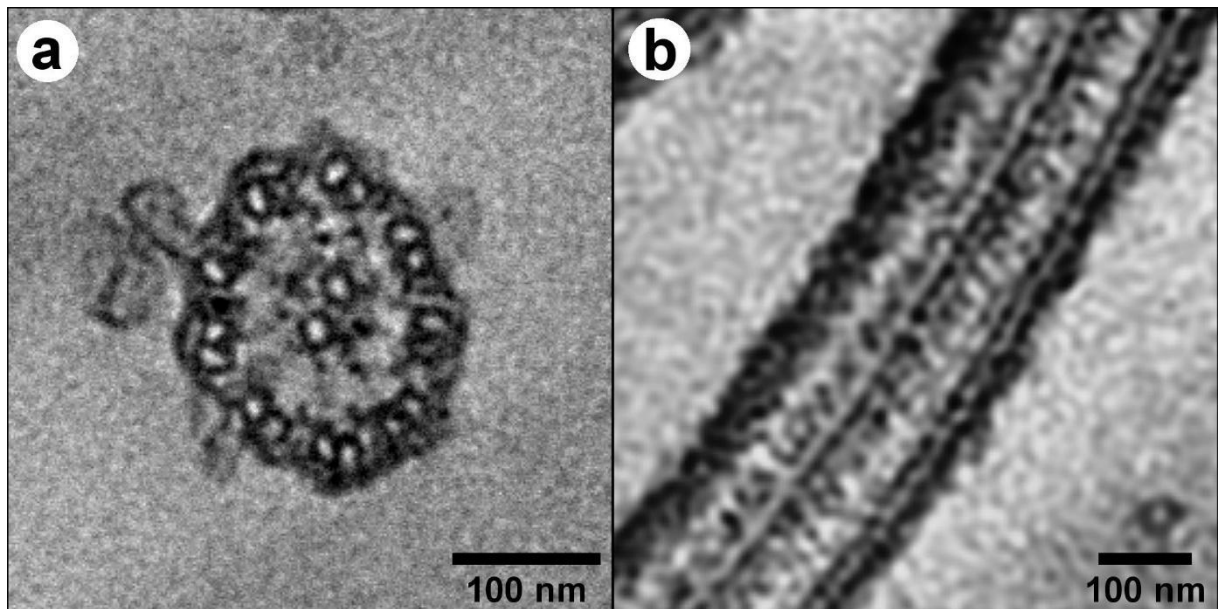
3.10 SUPPLEMENTARY INFORMATION



Additional file 1 TEM bright field image showing coronal section of a filament of *L. fortunei*'s gill. The laterofrontal cirri [lfc] are shown in cross-section view.



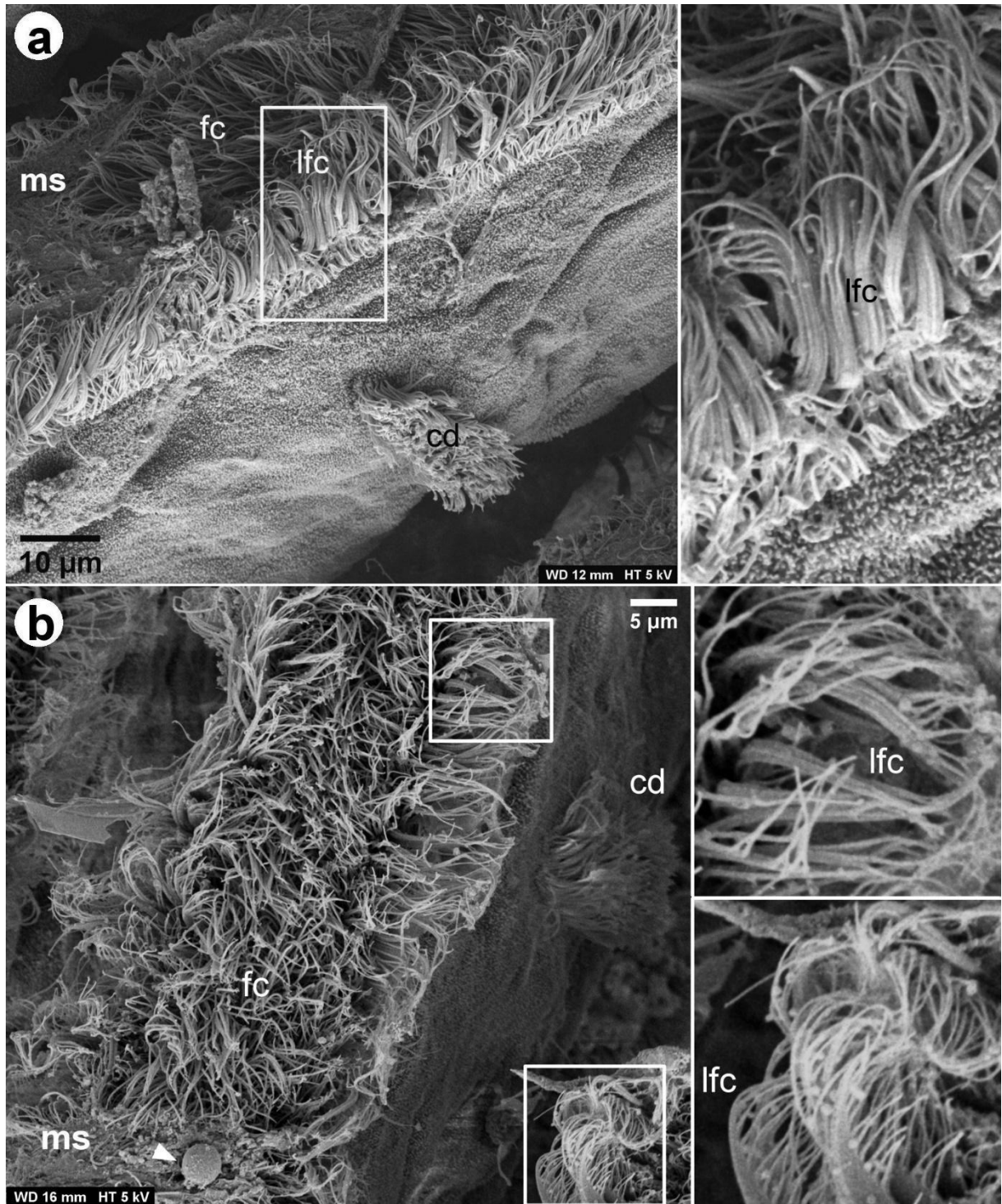
Additional file 2 Montage of TEM bright field images showing longitudinal view of the whole gill epithelium. Legend: cs – collagenous supporting structure, n – nucleus, vc – vacuoles, mu – mucin, mv – microvilli, lfc –laterofrontal cirrus, fc – frontal cilia, v – vesicle.



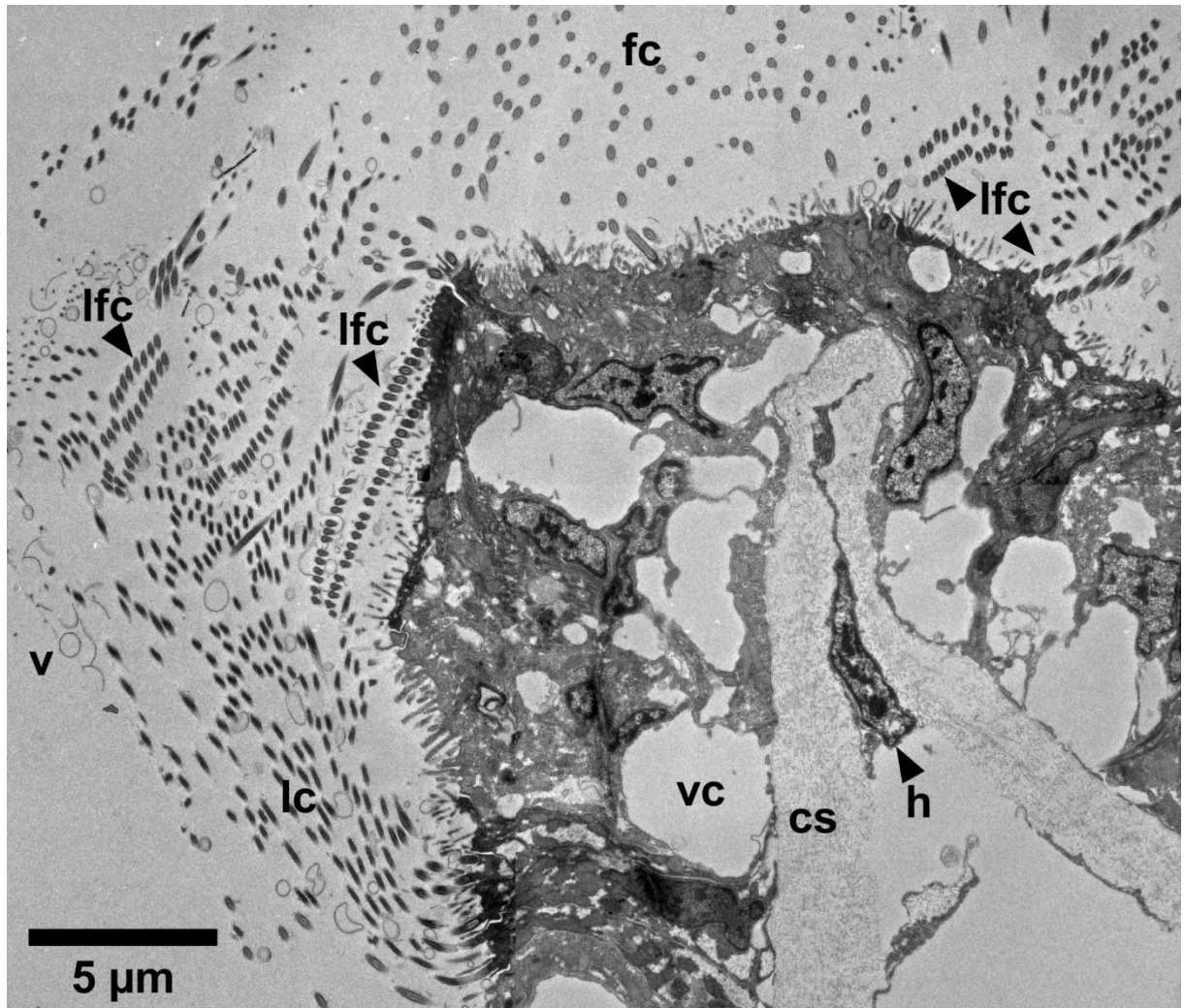
Additional file 3 TEM bright field images showing the detail microtubule cytoskeleton of laterofrontal cirri in cross-section (a) and longitudinal (b) views.



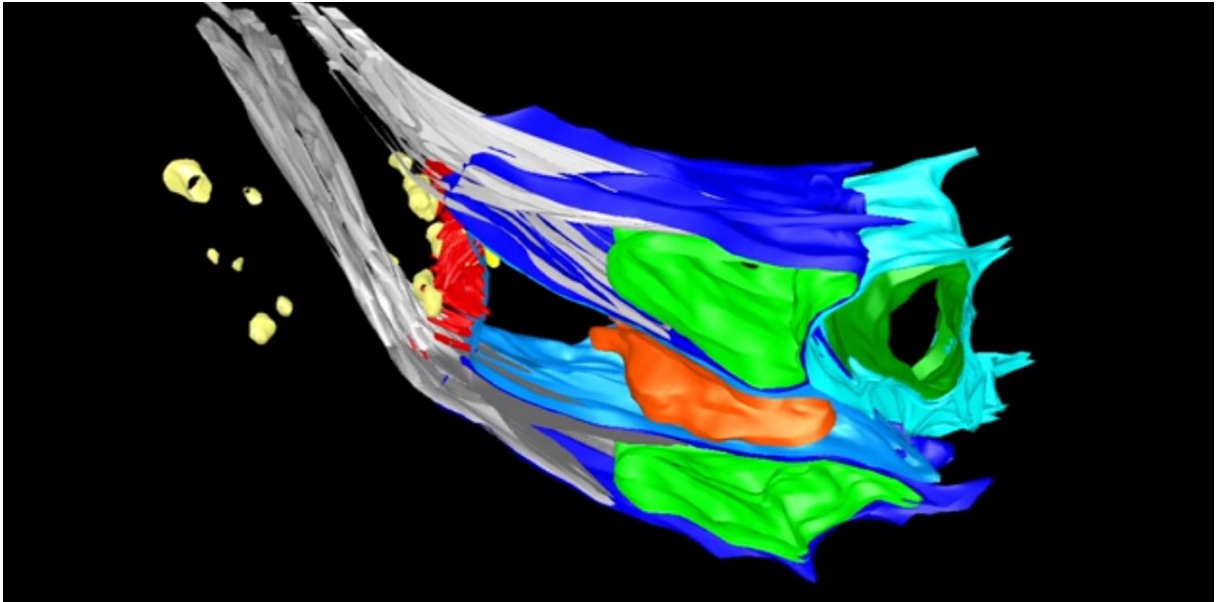
Additional file 4 Transmitted light microscopy of the plastic embedded block of the mussel gill in Volta Grande (VR) specimen.



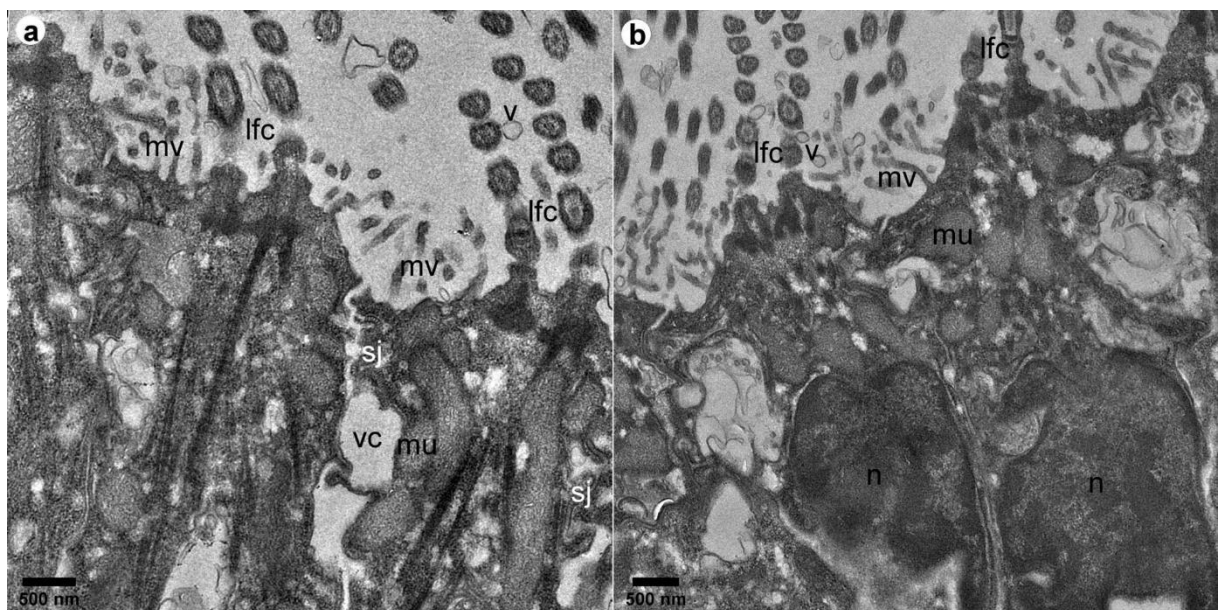
Additional file 5 SEM images of the frontal and lateral tract of gillfilament. The white arrowhead points a 4-5 µm particle on the frontal tract. Legend: ms – mucus string, fc – frontal cilia, lfc – laterofrontal cirri, cd – ciliary discs.



Additional file 6 Montage of bright-field TEM images of a thin section transversally to a gill filament of *L. fortunei*, showing its frontal portion. Lateral cilia [lc], laterofrontal cirri [lfc], and frontal cilia [fc] are observed in cross-section view. Spherical vesicles [v], vacuoles [vc], the collagenous structure [cs] of the hemolymph, and a hemocytes [h] are indicated.



Additional file 7 Threedimensional reconstruction of a portion of the *L. fortunei* gill epithelium showing three different types of cells. Cell I show a colored green nucleus and bear the laterofrontal cirri (in light gray). Cell II shows a colored orange nucleus. It possesses microvilli (in red) and is positioned in between cell I. Cell III shows a colored dark green and is located at basal region of the epithelium. Spherical vesicles are located inside cell II (in yellow) and outside (in beige). The reconstruction was carried out by serial-sectioning-array BSE-SEM images and using the Free-D software: Andrey P., Maurin Y. (2005). *J Neurosci Methods*. 145(1-2):233-44. doi:10.1016/j.jneumeth.2005.01.006.



Additional file 8 Bright-field TEM images showing coronal thin sections of the gill epithelium of *L. fortunei*. The laterofrontal cirri [lfc] are shown in cross-section view. Mucins [mu] and vacuoles [vc] are observed in the cells that possess microvilli [mv]. Spherical vesicles [v] are present close to the lfc and septate junctions [sj] and nuclei [n] are indicated.

Measurements of the gills structure variables (mean \pm standard deviation).

<u>Specimen</u>	<u>Filament</u> <u>width</u> <u>(μm)</u>	<u>Inter-</u> <u>Filamentary</u> <u>space</u> <u>(μm)</u>	<u>Filament</u> <u>linear density</u> <u>(N / μm)</u>	<u>Cilia</u> <u>length</u> <u>(μm)</u>	<u>Cilia</u> <u>diameter</u> <u>(μm)</u>	<u>Cilia linear</u> <u>density</u> <u>(N / μm)</u>
VG	*17.4 \pm 1.9	*17.3 \pm 2.4	*19.5 \pm 1.7	15.1 \pm 1.1	246 \pm 11	18.4
PR	10.4 \pm 1.5	20.5 \pm 0.7	40.5 \pm 0.8	10.7 \pm 1.1	247 \pm 10	15.7

* Measurements performed with transmission light microscopy images

Additional file 9 Measurements of the gills structure variables (mean \pm standard deviation) of the Volta Grade (VG) and Paranaíba River (PR) specimens. Errors were estimated from measurements performed in different parts of the image.

4. CAPÍTULO 2

**MORPHOLOGICAL AND MOLECULAR CHANGES OF *LIMNOPERNA FORTUNEI*
GILLS EXPOSED TO BIOCIDES SODIUM DICHLOROISACYANURATE (NADCC)
AND MXD-100 IN DIFFERENT PERIODS**

Morphological and molecular changes of *Limnoperna fortunei* gills exposed to biocides Sodium Dichloroisocyanurate (NaDCC) and MXD-100 in different periods

Amanda Maria Siqueira Moreira^{12†}, Rayan Silva de Paula¹², Erico Tadeu Fraga Freitas³, Mariana de Paula¹², Júlia Meireles Nogueira², Newton Ulhoa¹, André Luiz Martins Reis⁵, Miriam Velter², Afonso Pelli¹, Paulo Camargo¹, Antônio Valadão Cardoso¹⁴, Erika Cristina Jorge²

1 Centro de Bioengenharia de Espécies Invasoras de Hidrelétricas (CBEIH), Belo Horizonte, MG, 31035-536, Brazil.

2 Universidade Federal de Minas Gerais (UFMG), Instituto de Ciências Biológicas, Belo Horizonte, MG, 31270-901, Brazil.

3 Universidade Federal de Minas Gerais (UFMG), Centro de Microscopia, Belo Horizonte, MG, 31270-901, Brazil.

4 Universidade do Estado de Minas Gerais (UEMG), Escola de Design, Belo Horizonte, MG, 30140-091, Brazil.

5 University of New South Wales (UNSW), Sydney, NSW, Australia.

†Corresponding Author: A. Moreira amandasmoreira@outlook.com

4.1 ABSTRACT

Limnoperna fortunei, golden mussel, is a bivalve mollusk native to Asia and considered an invader in South America. This species is responsible for ecological and economic damages due to its voluminous fouling characteristic. Chemical biocides have been proposed to potentially control fouling mussels. Among them, the MXD-100 biocide, composed of tannins and quaternary ammonias, and the sodium dichloroisocyanurate (NaDCC), an oxidizing organic compound, are often used to control golden mussel infestation in hydraulic systems. The present study was aimed to investigate the action effects of different periods of MXD-100 and NaDCC on the gills of *L. fortunei* by morphological and molecular analyses. They were exposed to NaDCC (1.5mg/L) and MXD-100 (0.56 mg/L) under controlled laboratory conditions for 24, 48 and 72h. The gill's ciliary epithelium was assessed by morphological (light microscopy, transmission and scanning electron microscopies TEM, SEM) and molecular analyses (*Superoxide dismutase - SOD*, *Catalase - CAT*, *Cytochrome P450 - CYP*, and *Heat Shock Protein 70 - HSP70* activities). The results showed that NaDCC promoted progressive morphological changes during the analyzed periods and an upregulation of *SOD* and *HSP70* expression during 24 hours-exposition. The MXD-100 led to severe morphological changes since the first period of exposure, besides an upregulation of *SOD*, *CAT*, *HSP70* and *CYP* expression during 24 hours. In contrast, there was a downregulation of *CAT* transcription during 48 hours of exposure. This study suggests that, in static conditions, NaDCC (1.5 mg/L) has lethal damage after 72 hours of exposure, and to achieve the control of species its exposure need to be continuously. While the MXD-100 (5.6 mg/L) treatment presented several effects during the first 24 hours, showing an acute toxicity in a shorter period of time.

Keys words: biocides, gills epithelium, golden mussel, histology, stress biomarkers

4.2 INTRODUCTION

Limnoperna fortunei (Dunker, 1857), known as golden mussel, is a small freshwater bivalve (subclass Pteriomorpha, order Mytiloida, family Mytilidae) native to the Pearl River basin in China (XU, 2015). Due to its high abundance and geographic dispersion, it is considered an important invasive species (DA COSTA FERNANDES et al., 2012), quickly expanding in South America along navigable waterways (DARRIGRAM; PASTORINO, 1993; BRUGNOLI et al., 2005; BOLTOVSKOY et al., 2006; OLIVEIRA et al., 2015). *Limnoperna fortunei* has a high acclimatization capacity and aggregation behavior on hard surfaces, generating macrofouling that causes environmental and economical issues (SILVA et al., 2016; ADELINO et al., 2021).

Hydroelectric power plants have often been affected by the macrofouling process of the golden mussel. Alterations such as obstructions in pipes and clogging of water collection pumps involve high costs with system shutdowns (MANSUR et al., 2003; DARRIGRAM; DAMBORENEA, 2005; da SILVA BERTÃO et al., 2021). To reduce the infestation of this species in industrial facilities, several population control measures are used. Industry used to prefer chemical control options because treatment can be applied throughout the entire facility from a single dosing point (ALDRIDGE et al., 2006). Usually classified as oxidising and non-oxidising biocides, these chemical compounds are commonly used in an attempt to control biofouling (CLOETE et al., 1998). Several compounds have been reported as biocides, including potassium chloride (WALLER et al., 1993; COSTA et al., 2008), sodium hydroxide (BOWMAN; BAILEY, 1998; MONTRESOR et al., 2013), chlorine based compounds (CATALDO et al., 2003), quaternary ammonia compounds (MONTRESOR et al., 2013; DARRIGRAM et al., 2007), and microencapsulated compounds (CALAZANS et al., 2013; TANG; ALDRIDGE, 2019).

The sodium dichloroisocyanurate (NaDCC) is an organic chlorine-based oxidant, presented in granular or pellet form (VIDAL, 2019), widely used in the control of freshwater mollusks due to its relatively low cost and ease of handling (CATALDO et al., 2003; VENKATNARAYANAN et al., 2021). Studies with *L. fortunei* (CATALDO et al., 2003), *Dreissena polymorpha* (Pallas, 1771) (RAJAGOPAL et al., 2002) and *Perna viridis* (Linnaeus, 1758) (VENKATNARAYANAN et al., 2021) show the effectiveness of chlorination on mortality in low concentrations. The MXD-100 is a Brazilian commercial non-oxidizing antifouling biocide with active compounds based on extracts of tannins and quaternary

ammonia (NETTO, 2012; VIDAL, 2019). These substances were developed as control agents for bacteria or algae and their use extended to mollusks (molluscicides). Efficient results of MXD-100 were seen in larvae (DARRIGRAN et al., 2007) and adults (MONTRESOR et al., 2013) of *L. fortunei*. Research understanding the effectiveness of these biocides on mussel morphophysiology is essential as an important part of combating biofouling.

The gills of bivalves have a large surface area for absorption of substances and are in direct contact with the aquatic environment and consequently with compounds dissolved in it. (PAL et al., 2012; VELMURUGAN et al., 2018; HAMZA, 2019). As part of the Bivalvia class, *L. fortunei* has two valves articulated around the body, a single foot involving the visceral mass, and two pairs of gills (Ctenidae) (BOGAN, 2007). A recent work of our group characterized ultrastructurally the gill epithelium of the *L. fortunei* gills, showing a high organization of these structures (FREITAS et al., 2022). On the surface, the epithelium is composed of ciliated cells, non-ciliated absorptive cells and mucus-producing cells (NOGAROL et al., 2012), mucus facilitates the capture and transport of particles in the branchial filaments (ROSA et al., 2018; FOSTER-SMITH, 1975). In this way, gills fulfill the roles of respiration, capturing, and transporting particles (MORTON, 2015).

Observations of morphological and molecular alterations play an important role in understanding the mechanism of action of population control methods for this species. Genes related to environmental stress regulation, such as *Superoxide dismutase (SOD)*, *Catalase (CAT)*, *Cytochrome P450 (CYP)* and *Heat Shock Protein 70 (HSP70)*, have been reported as cellular defense biomarkers in *L. fortunei*. Thus, the exposure of these organisms to stressors can affect the pattern of these gene expressions (ULIANO-SILVA et al., 2014; GIRARDELLO et al., 2016).

In view of the impacts caused by the invasion of the golden mussel and the lack of precise information about the mechanisms of biocides' action, this work aimed to understand the metabolic responses of the *L. fortunei* gill's against exposure of the chemical compounds NaDCC and MXD-100 in different periods, using morphological and molecular analysis. These data will allow us to determine, from pre-established concentrations, the necessary time of exposure to biocides that are efficient for the control of biofouling.

4.3 MATERIALS AND METHODS

Mussel management

Adult specimens of *L. fortunei* were collected from colonies adhered to natural substrates in the reservoir of the Volta Grande (VG), Minas Gerais, Brazil (S 20° 05 '33"; W 48° 06' 18"). They were packed in cloth bags and transported to the laboratory at the *Centro de Bioengenharia de Espécies Invasoras de Hidrelétricas* (CBEIH). Nearly 170 animals were acclimated in aquariums with 36 L capacity containing artesian water, pH 7.7, dissolved oxygen 6.8 mg L⁻¹ and turbidity (NTU) 1.68, at constant aeration, temperature of 18 to 20 °C to minimize stress and constant feeding. After acclimation, the mollusks were kept under the same conditions and temperature of 22 ± 1 °C until the day of the assays. The authorization for activities with scientific purpose is registered in the SISBIO (Sistema de Autorização e Informação em Biodiversidade) with the access code 72222-2.

Exposure to biocides

Groups of 7 individuals each, approximately 1 to 2 cm in length, were randomly distributed in 24 glass jars, each one containing 1 L of dechlorinated water with constant aeration. Two short-term and independent bioassays were conducted evaluating the compounds sodium dichloroisocyanurate 60% (Hidrodomi do Brasil Industria de Domissaneantes LTDA) (NaDCC) (bioassay 1) and MXD-100 (Maxclean Ambiental e Química SA, Brazil) (bioassay 2) (fig.1). Each bioassay consisted of three groups with different exposure times (24, 48 and 72 hours) and each group had a control group with dechlorinated water only. All assays were conducted in triplicates. The animals in bioassay 1 were exposed to concentrations of NaDCC (1.5 mg/L free available chlorine), during two hours per day, and in bioassay 2 were exposed to concentrations of MXD-100 (0.56 mg/L) for 10 minutes every 8 hours, totaling 30 minutes daily. The exposure times and concentrations were chosen according to normative instructions for use by the Instituto Brasileiro do Meio Ambiente e dos Recursos Naturais Renováveis (IBAMA), nº 17¹ and nº 18², of October 21, 2015 and which are exclusively approved and frequently used in treatments in hydroelectric plants. After exposure, the animals were collected, sacrificed and preserved. Water quality parameters (temperature, pH, oxygenation,

¹ Availabe at <http://www.ibama.gov.br/sophia/cnia/legislacao/IBAMA/IN0017-21102015.pdf>

² Availabe at <http://www.ibama.gov.br/sophia/cnia/legislacao/IBAMA/IN0018-21102015.pdf>

ORP-oxidation-reduction potential, conductivity, turbidity, salinity, and total solids) were measured twice a day during the experiment.

Histological analysis

Gills from 3 animals from each glass jars (9 individuals per exposed group and 3 per control group) were immersed in Bouin's fixative for 24 hours. Afterward, they were dehydrated in a progressive series of ethanol, cleared in xylene, and then embedded in paraffin. The transverse histological sections (5 µm) were dewaxed in xylene, hydrated in graded ethanol, later stained accordingly: sections were stained with hematoxylin-eosin method for structural analysis; periodic acid Schiff (PAS) method combined with Alcian Blue (AB) in pH 2.5 to detection of mucins. Digital image capture was performed with the Leica DM4500 microscope.

Morphometry

The thickness of the gill epithelium was measured by transverse histological sections in 50 gills filaments per individual (9 individuals per exposed group and 3 per control group). The morphometric analyses was performed using the ImageJ® (Image-Pro Plus® 7.01; National Institutes Of Health, Bethesda, Maryland, USA) software.

Mucous Cell Analysis

To monitor the response of exposure to biocides on the amount of polysaccharides present in cells of the gill epithelium was counted, using ImageJ® software, the number of mucous cells in 50 gill filaments per individual, as described by David et al., (2009).

Scanning electron microscopy (SEM) preparations

For electron microscopy analysis, one golden mussel per glass jar (one control and three tests per treatment) was used. The gills of this mussel were dissected, and each one used for an electron microscopy technique (transmission and scanning). Thus the observation of gill surface structures, fragments of the gill was placed into phosphate buffer solution (PBS), then placed in solutions of osmium tetroxide, tannic acid, phosphate buffer and again in osmium tetroxide, respectively. After washing in distilled water, the samples were dehydrated and consequently dried with CO₂. Finally, the specimens were coated with gold for morphological analysis under

a scanning microscope FEI Quanta 200. The sample preparation and their analysis were performed at the Centro de Microscopia at the Universidade Federal de Minas Gerais (UFMG).

Transmission electron microscopy (TEM) preparations

The fragments of the gills were placed into phosphate buffer solution (PBS), the samples were applied, respectively, in osmium tetroxide solutions, deionized water and uranyl acetate. Consequently, they were dehydrated in alcoholic solution and replaced by acetone. The inclusion was performed with resin, and after sectioning into 60 nm fragments, the tissues were then contrasted with uranyl acetate and lead citrate. The sample preparation and their analysis were performed at the Centro de Microscopia at the Universidade Federal de Minas Gerais (UFMG), using the FEI Tecnai Spirit BioTwin microscope.

Molecular analysis

Primer Design

We used the available reference genome and gene annotation of *L. fortunei* (PRJNA330677) to recover the nucleotide sequence of the defense genes described by Uliano-Silva et al. (2014). Firstly, to identify the genes of interest among the predicted genes, we performed a similarity search using blastp against the Uniprot database. Then, we searched for the product name of our genes of interest in the blastp results, only selecting hits with over 70% identity and E-value lower than 0.001. To further confirm the identity of the selected genes, we performed an additional similarity search with blastp, but against the NCBI non-redundant protein database, only retaining genes for which known homologs were found in other mussel species. Additionally, we also mapped the defense gene transcripts reported by Uliano-Silva et al. (2014) into the genome with minimap2 (using the splice preset). Then, we retained only mapped transcripts with a MAPQ equal to 60 that overlapped the genome coordinates of predicted genes present in the gene annotation. Again, to confirm that the identity of the overlapped predicted genes matched the genes reported by Uliano-Silva et al. (2014), we performed a blastp search against the NCBI non-redundant protein database, considering only genes related to the transcriptome study or other mussel species. Finally, with the genome coordinates of all the genes of interest (also including GAPDH as a gene that should show stable expression in the samples - reference), we recovered the nucleotide sequence of the CDS for

the predicted transcript of each gene using bedtools getfasta (with the -split and -s parameters). Those nucleotide sequences were then used to design primers in Primer3Plus software.³ Table 1 shows the primer pairs used to evaluate gene expression.

Gene expression

Three animals per glass jar (nine golden mussels per exposed group and 3 per control group) were submitted to total RNA extraction according to instructions from the TRI Reagent[®] (Sigma, St. Louis, MO) manufacturer. 1,5 µg of total RNA was converted to cDNA following the manufacturer's instructions with the RevertAid[™] H. Minus First Strand cDNA Synthesis kit (Thermo Scientific, Waltham, MA). The RT-qPCR mix contained 5 µL of iTaq[™] Universal SYBR[®] Green Supermix (Bio-Rad, Hercules, CA), 0.4 µM of each of primers, 1 µL cDNA diluted (1:10 in water nuclease-free), and final volume adjustment to 10 µL with water nuclease-free. The reactions occurred at 50 °C for 2 min, 95 °C for 2 min, and 45 cycles of 94 °C for 15 s, 60 °C for 15 s and 72 °C for 20 s and extra extension for 72 °C for 5 min. The dissociation step to assess the specific melting temperature for each set of primers was carried out at the end of the amplification.

Statistical analysis

To test how the number of mucous cells and the thickness of the epithelium were influenced by the presence of MXD-100 and NaDCC, over time and between groups, generalized linear models (GLM, following the Crawley, 2012 protocol) were built using the R platform⁴. Differential gene expression analysis was performed using the REST[®] 2009 software (PFAFFL et al., 2002).

³ <https://www.bioinformatics.nl/cgi-bin/primer3plus/primer3plus.cgi>

⁴ R Development Core Team 2015

4.4 RESULTS

Changes from exposure to sodium dichloroisocyanurate (NaDCC)

Individuals exposed to NaDCC showed filament degradation and ciliary deformation progressively from mild to severe, during the three exposure periods - 24 hours (fig.2 D-F), 48 hours (fig.2 G-I), 72 hours (fig.2 J-L). The cilia were loose in the non-ciliated region of the filaments. No changes were observed in the gill filaments in individuals in the control group (fig.2 A-C).

The increase in the thickness of the epithelium was observed between the groups ($p < 0.001$, $F = 415.42$, $Df = 1$) and in the period of 24 hours, in relation to 48 hours ($p < 0.001$, $F = 172.18$, $Df = 2$) (fig.3). In addition, when compared to the control (fig.4 A), histological sections showed lifting of the epithelium, during the periods of 24 and 48 hours of exposure (fig.4 B, C), and epithelial desquamation from the second exposure period (48 hours) (fig.4 C, D).

There was an increase in the number of mucus-producing cells in animals exposed to NaDCC for 24 hours ($p < 0.001$, residual deviance = 114.5, $Df = 1$) (fig.5 A), which was not observed in 48 hours (fig.5 B, C). In 72 hours, the number of cells could not be counted due the high mortality of animals in this period. It was also possible to observe a large accumulation of mucus on the front surface of the filaments in individuals exposed to all periods (fig.2 E, H, K).

In ultra-morphological aspect, during exposure to all treatments times, gill epithelial cells showed autophagosomes in the cytoplasm (fig.6 B, C). The exposure for 48 and 72h hours showed cytoplasmic dilatations (fig.6 C, D). The nuclei of the cells had clusters of chromatin and a clear appearance only in 72h (fig.6 D).

Treatment with NaDCC was able to upregulate *SOD* (~20,7 foldchange) and *HSP70* (26,8 foldchange) expressions during 24 hours exposure, compared to the control (fig.7 A). There was no statistical difference at 48 (fig.7 B) and 72 hours (fig.7 C) of exposure for these transcripts. The *CYP* gene did not change its expression in any of the NaDCC exposure treatments, and *CAT* did not amplify during exposure for 72 hours (fig.7 C).

Changes from exposure to MXD-100

Individuals exposed to MXD-100 presented filaments in the process of deformation, in a severe stage, since the first period of exposure (24 hours) (fig.8 D, G, J), while those in the control group showed no morphological changes (fig.8 A-C). Severely ciliary loss was also identified from the shortest time of exposure (fig.8 E, H, K). There was a significant effect on the thickness of the epithelium between groups ($p<0.001$, $F=77.59$, $Df=1$) and between time periods ($p<0.001$, $F=107.21$, $Df=1$). The increase in the thickness was observed in 24 hours, but there was a decrease in 48 hours. It was not possible to observe it in 72 hours, because all individuals died (fig. 9).

In histological sections, a moderate to severe lifting of the epithelium was observed during periods of 24 and 48 hours of exposure (fig.10 B, C, D). In relation to epithelial desquamation, it was moderate for the first exposure time (24 hours), and severe for the period of 72 hours (fig.10 B, C, D). A hyperplastic increase could be seen during all three exposure periods (24, 48, 72 hours) to MXD-100, mainly in epithelial cells in the frontal region of the filaments (fig.10 B, C, D). No alterations could be observed in the control group (fig.10 A).

An accumulation of mucus on the front surface of the filaments was also identified in individuals at all periods of exposure to MXD-100 (fig.8 F, L), but no statistical difference in the number of mucus-producing epithelial cells could be observed between 24 and 48h groups. This number could not be assessed at the 72h group as the cells were no longer present.

The internal cellular organization of the groups exposed to MXD-100 for 24 and 48 hours showed translucent cytoplasm with dilatations, lamellar bodies and few organelles (fig.11 B, C). The nuclei had a clear appearance with a chromatin cluster and, only in 48 hours, the nuclear envelope was damaged (fig.11 C). In animals exposed to MXD-100 for 72 hours, the cells become scarcer, looser, with inapparent cytoplasm and a high degree of degeneration (fig.11 D).

Changes in gene expression were observed in animals exposed to MXD-100 from the shortest period of exposure. *CYP*, *SOD*, *CAT*, and *HSP70* were upregulated during the 24 hours period, compared to the control (fig.12 A). *CAT* expression was downregulated during the 48 hours period of exposure, compared to control (fig.12 B). The 72 hours period of exposure to MXD-100 did not present any changes in all markers measured (fig.12 C).

4.5 DISCUSSION

The infestation of the golden mussel in South American waters has caused many economic impacts due to the macrofouling (DARRIGRAM et al., 2004; OLIVEIRA et al., 2015). This issue is faced with the use of chemical treatments to mitigate invasive organisms in aquatic systems (DARRIGRAM et al., 2007; TANG; ALDRIDGE, 2019). The gills are one of the first target organs for several xenobiotic compounds due to their direct contact with the contaminants in water (PAL et al., 2012). In this study, the gills of *L. fortunei* were evaluated after exposure to two of the commonly used biocides at different times.

Morphological knowledge provides information about the health status of the organism and an understanding of the action of population control methods (MANSUR et al., 2012). Thus, mussel biology, including the morphology of *L. fortunei* foot, the shell microstructure, the ultra-characterization of the ciliary epithelium of the gills, and its repertoire of survival strategies have been the subject of several studies (COSTA et al., 2013; NAKAMURA et al., 2014; ANDRADE et al., 2015; FREITAS et al., 2022). Our results showed constant changes in the gill epithelium of both treatments (NaDCC and MXD-100), reinforcing their vulnerability (DE OLIVEIRA RIBEIRO et al., 2002) besides to emphasize how phenotypic plasticity is an important mechanism for adaptation to shifts in environmental conditions (PAOLUCCI et al., 2014).

Furthermore, differences in gene expression can provide information on specific cellular responses in mollusks (WOO et al., 2013; WANG et al., 2020). Several biochemical markers are used to evaluate the toxicity of bivalves. These biomarkers include parameters related to the oxidation of biomolecules, changes in the levels of antioxidants, detoxification and general metabolic enzymes (IUMMATO et al., 2018).

NaDCC has a molluscicidal action based on the oxidation of organic matter, which confers toxic and lethal effects on the target organisms (PENAFORTE, 2014). When in contact with water, the NaDCC releases free available chlorine in the form of hypochlorous acid (HOCl) (FERNANDES et al., 2012; SEO; JO, 2021). Beyond that, isocyanurates compounds are cyanuric acid, the carrier that allows the chlorine to be contained in a solid, stable, and dry form (SEO; JO, 2021). It has been observed that chlorine induces oxidative stress in cells by generating reactive oxygen species (ROS), which can damage cell membranes, proteins and nucleic acids (CHAVAN et al., 2016). Consistent with this, our results showed that NaDCC in 24 hours led to an upregulation of the expression of superoxide dismutase (*SOD*), compared to

the control treatment. *SOD* are universal enzymes of organisms that live in the presence of oxygen (WANG et al., 2018). They decrease ROS levels in oxidative stress by reducing superoxide ion radical to hydrogen peroxide (GIRARDELLO et al., 2016). In addition, during 24 hours of exposure, there was also an upregulation of The Heat Shock Protein 70 (*HSP70*) expression, compared to the control treatment. *HSP70* acts in cellular protection against harmful conditions by binding and refolding damaged proteins, playing an important role in the response to cellular stress (PAPO et al., 2014; MACÊDO et al., 2020). These results possibly show that NaDCC induces an acute cellular response to the generated oxidative stress.

In the same period, the thickness of the epithelial and the number of mucous cells were higher, probably because the gills respond to the first contact to the biocide, trying to avoid the entry of substances through passive diffusion in the tissue, forming inert compounds that can be excreted as pseudofeces (BOUALLEGUI et al., 2017).

During the 72 hours, no expression of the *CAT* gene was observed. *SOD* and *CAT* are antioxidant enzymes that operate in the same pathway, acting in the defense against oxidative stress by reactive oxygen species (ROS). While *SOD* accelerates the reaction between the superoxide and hydrogen peroxide, the *CAT* eliminates hydrogen peroxide in cells (KANKAANPAA et al., 2007). Thus, the *SOD/CAT* pathway may have been blocked in 72-hours exposition, stopping the expression of the *CAT* gene.

Other morphological changes occurred gradually during the three exposure periods, the ciliary damage possibly occurred by direct contact with the chemical (CHEUNG; SHIN, 2005), and lifting and desquamation of the epithelium occurred as a form of gill defense mechanisms against frequent exposure to toxic agents (MACÊDO et al., 2020).

Cytoplasmic and cellular damage appeared gradually during exposures, including autophagolysosomes that can also be observed in the three periods, being a conserved cytoprotective mechanism and activated by environmental stimuli (CARELLA et al., 2015). Thus, from the changes observed here related to protection mechanisms - molecular (increased *SOD* and *HSP70*), morphological (increased mucus production and epithelial thickness), and ultramorphological (presence of autophagosomes) changes - it seems that up to the 48 hours the alterations may be reversible, while only in the 72 hours there were serious cellular alterations related to the cell death process (epithelial desquamation, nuclei with clusters of chromatin and a clear appearance). In other words, in 72 hours, the cellular adaptive response can no longer accommodate the stressor (CARELLA et al., 2015). These data are consistent with previous studies that observed that chlorination at low doses is effective for mussels when

it occurs continuously, because, in a short period, mussels can physiologically recover themselves (CHAVAN et al., 2016; VENKATNARAYANAN et al., 2021). It probably happens since the animals, when in contact with the biocide, close the shell delaying the effect of the compound.

Regarding the MXD-100, it is relatively inert to the internal infrastructure of industrial water systems, effective in low concentrations, quickly inactivated and easy to handle (MARONAS; DAMBORENEA, 2009; MACKIE; CLAUDI, 2009). They are a combination of tannins and quaternary ammonium (QAC) that binds to the negatively charged surface of mollusk membranes, causing membrane rupture and intracellular constituent leakage (CLOETE et al., 1998; MARONAS; DAMBORENEA, 2009; ZHANG et al., 2015). Compatible with this information, a study showed that tannin formulations have acute toxicity for golden mussels (PEREYRA et al., 2011).

In our experiments, the animals exposed to MXD-100 for 24 hours showed an upregulation of the expression of *SOD*, *CAT*, *CYP*, and *HSP70* gene markers, compared to the control treatment. The cells have antioxidant systems which limit the effects of the ROS, and these systems are composed of molecules and enzymes such as *SOD* e *CAT* (MANDUZIO et al., 2005; WOJTAL-FRANKIEWICZ et al., 2017). The upregulation of the expression of these genes plus the upregulation of *HSP70* showed a cellular stress response. Further, an upregulation in *CYP* expression was observed after 24 hours of exposure, once the Cytochrome P450 enzymes (*CYP*) are responsible for the oxidative metabolism of endogenous and xenobiotic compounds, playing a significant role in the biosynthesis of endogenous compounds and the biotransformation of xenobiotics (ZANGAR et al., 2004; REWITZ et al., 2006; SIEBERT et al., 2017). Thus, in addition to the cellular response to oxidative stress, there was also activation of xenobiotic biotransformation and detoxification processes in an attempt to eliminate MXD-100 in golden mussel gills.

After 48 hours, there was no change in *SOD* gene expression levels. However, there was a downregulation of the expression of *CAT* transcripts, compared to the control. This downregulation probably occurred because there was no action of *SOD* on the transformation of superoxide into hydrogen peroxide to be eliminated by *CAT*. In other words, 24-hours exposure may increase enzymatic activity, but 48-hours of exposure can inhibit enzymatic activity caused by oxidative stress, reducing defense mechanisms (GURKAN; GURKAN, 2021).

Cell damage related to cell death was observed during exposure to MXD-100, such as translucent cytoplasm, nuclear damage, and lamellar bodies. It may happen because reactive oxygen species are genotoxic (CHÂTEL et al., 2011) and can activate apoptosis pathways (CARELLA et al., 2015; BOUALLEGUI et al., 2017). Apoptosis is a type of programmed cell death that produces changes in cell morphology and biochemical processes and may occur in response to cell damage caused by toxic agents (ROMERO; FIGUERAS, 2015). The lamellar bodies observed here are formed by layers of concentric membranes produced during the autophagic process (HARIRI et al., 1999; MARISHITA et al., 2020), being indicative of the activation of the apoptotic pathway.

The structural architecture of the gills epithelium was also altered due to the acute toxicity of MXD-100. The increase in epithelial thickness was seen only for 24 hours as a means of protection, trying to isolate the organism from the environment (PANDEY et al., 2008). However, it is possible that the number of mucous cells increased before 24 hours due to the high toxicity of the compound. The decrease in the thickness of the epithelium in 48 hours might have occurred due to the high cytotoxicity of MXD-100, which led to rapid cell death. Other changes (desquamation, epithelial lifting, hyperplasia) remained severe at all times, as a way of trying to decrease the respiratory surface to inhibit the absorption of compounds and an increase in diffusion distance (VELMURUGAN et al., 2018). These acute changes caused by MXD-100 from 24 hours of exposure may have occurred because the mussel cannot detect this biocide as a harmful compound and the closing response is not provoked (SPRECHER; GETSINGER, 2000).

Changes in the environment trigger changes in cellular response, thus the timing and success of these changes ultimately determine cell survival and acclimation or cell death (FABBRI et al., 2008). According to the results obtained in this study, the NaDCC (1.5 mg/L) shows lethal damage after 72 hours of exposure, with gill cells showing reversible changes up to 48 hours, while MXD-100 (0.56 mg/L) showed severe and irreversible gill changes after 24 hours of exposure. Thereby, ultramorphological and molecular analyses of gills might be efficient to identify the toxicity of chemical biocides in golden mussels.

4.6 CONCLUSIONS

The “ideal biocide” would be capable of effective mitigation against the invasion of *L. Fortunei* in aquatic systems, with no costs to the environment. However, this antifouling compound has not yet been obtained, requiring investigations aiming to minimize its environmental impacts (MARONAS; DAMBORENEA, 2009). Our results showed that the MXD-100 had acute toxicity in a shorter time, while NaDCC possibly needs continuous exposure to achieve the control of the species. The differences between these data and those presented in the literature might be a consequence of the use of static bioassay.

Further studies evaluating the dose-response effect on the gills should be considered, as well as a more prolonged action study, with a chronic effect. In addition to the gills, other tissues of *L. fortunei* should be evaluated against the treatment with biocides.

4.7 ACKNOWLEDGMENTS

We thank Maxclean Ambiental e Quimica S/A for the availability of biocide. This work was supported by the Companhia Energética de Minas Gerais (Cemig) GT/ANEEL R&Ds GT-0604. The authors are grateful for the support given by Núbia Oliveira and Kelly Carneiro at the CBEIH laboratory, by Nataly Mendes Neves at the Biotério Nico Nieser (UFTM), and by the Center of Microscopy at UFMG.

DISCLOSURE STATEMENT

No potential conflict of interest was reported by the author(s).

FUNDING

This work was supported by the Companhia Energética de Minas Gerais (CEMIG) R&Ds ANEEL GT-0604.

4.8 REFERENCES

- ADELINO, José et al. The economic costs of biological invasions in Brazil: a first assessment. **NeoBiota**, v. 67, p. 349-374, 2021.
- ALDRIDGE, David C.; ELLIOTT, Paul; MOGGRIDGE, Geoff D. Microencapsulated BioBullets for the control of biofouling zebra mussels. **Environmental science & technology**, v. 40, n. 3, p. 975-979, 2006.
- ANDRADE, Gabriela Rabelo et al. Functional Surface of the golden mussel's foot: morphology, structures and the role of cilia on underwater adhesion. **Materials Science and Engineering**, v. 54, p. 32-42, 2015.
- BOGAN, Arthur E. Global diversity of freshwater mussels (Mollusca, Bivalvia) in freshwater. In: **Freshwater animal diversity assessment**. Springer, Dordrecht, p. 139-147, 2007.
- BOLTOVSKOY, Demetrio et al. Dispersion and ecological impact of the invasive freshwater bivalve *Limnoperna fortunei* in the Río de la Plata watershed and beyond. **Biological Invasions**, v. 8, n. 4, p. 947-963, 2006.
- BOUALLEGUI, Younes et al. Histopathology and analyses of inflammation intensity in the gills of mussels exposed to silver nanoparticles: role of nanoparticle size, exposure time, and uptake pathways. **Toxicology mechanisms and methods**, v. 27, n. 8, p. 582-591, 2017.
- BOWMAN, Michelle F.; BAILEY, R. C. Upper pH tolerance limit of the zebra mussel (*Dreissena polymorpha*). **Canadian Journal of Zoology**, v. 76, n. 11, p. 2119-2123, 1998.
- BRUGNOLI, Ernesto et al. Golden mussel *Limnoperna fortunei* (Bivalvia: Mytilidae) distribution in the main hydrographical basins of Uruguay: update and predictions. **Anais da Academia Brasileira de Ciências**, v. 77, n. 2, p. 235-244, 2005.

CALAZANS, Sávio Henrique C. et al. Assessment of toxicity of dissolved and microencapsulated biocides for control of the Golden Mussel *Limnoperna fortunei*. **Marine environmental research**, v. 91, p. 104-108, 2013.

CARELLA, F. et al. Comparative pathology in bivalves: A etiological agents and disease processes. **Journal of invertebrate pathology**, v. 131, p. 107-120, 2015.

CATALDO, Daniel; BOLTOVSKOY, Demetrio; POSE, Monica. Toxicity of chlorine and three nonoxidizing molluscicides to the pest mussel *Limnoperna fortunei*. **Journal-American Water Works Association**, v. 95, n. 1, p. 66-78, 2003.

CHÂTEL, A. et al. Induction of apoptosis in mussel *Mytilus galloprovincialis* gills by model cytotoxic agents. **Ecotoxicology**, v. 20, n. 8, p. 2030-2041, 2011.

CHAVAN, Pooja et al. Chlorination-induced genotoxicity in the mussel *Perna viridis*: assessment by single cell gel electrophoresis (comet) assay. **Ecotoxicology and Environmental Safety**, v. 130, p. 295-302, 2016.

CHEUNG, S. G.; SHIN, P. K. S. Size effects of suspended particles on gill damage in green-lipped mussel *Perna viridis*. **Marine pollution bulletin**, v. 51, n. 8-12, p. 801-810, 2005.

CLOETE, Thomas Eugene; JACOBS, Liesel; BRÖZEL, Volker Siegfried. The chemical control of biofouling in industrial water systems. **Biodegradation**, v. 9, n. 1, p. 23-37, 1998.

COSTA, R.; ALDRIDGE, D. C.; MOGGRIDGE, G. D. Seasonal variation of zebra mussel susceptibility to molluscicidal agents. **Journal of Applied Ecology**, v. 45, n. 6, p. 1712-1721, 2008.

COSTA, Pedro M. et al. Development of histopathological indices in a commercial marine bivalve (*Ruditapes decussatus*) to determine environmental quality. **Aquatic toxicology**, v. 126, p. 442-454, 2013.

CRAWLEY, Michael J. **The R book**. John Wiley & Sons, 2012.

DA SILVA BERTÃO, Ana Paula et al. Ecological interactions between invasive and native fouling species in the reservoir of a hydroelectric plant. **Hydrobiologia**, v. 848, n. 21, p. 5169-5185, 2021.

DARRIGRAN, Gustavo Alberto; MAROÑAS, Miriam Edith; COLAUTTI, Darío César. Air exposure as a control mechanism for the golden mussel, *Limnoperna fortunei*, (Bivalvia: Mytilidae). **Journal of Freshwater Ecology**, v. 19, n. 3, p. 461-464, 2004.

DARRIGRAN, Gustavo A.; COLAUTTI, Darío C.; MAROÑAS, Miriam E. A potential biocide for control of the golden mussel, *Limnoperna fortunei*. 2007.

DARRIGRAN, Gustavo Alberto; DAMBORENEA, Maria Cristina. A South American bioinvasion case history: *Limnoperna fortunei* (Dunker, 1857), the golden mussel. 2005.

DARRIGRAN, GUSTAVO; PASTORINO, GUIDO. Bivalvos invasores en el Río de la Plata, Argentina. **Comunicaciones de la Sociedad Malacológica del Uruguay**, v. 7, n. 64-65, p. 309-313, 1993.

DAVID, José Augusto de Oliveira; FONTANETTI, Carmem S. The Role of Mucus in *Mytella falcata* (Orbigny 1842) gills from polluted environments. **Water, air, and soil pollution**, v. 203, n. 1, p. 261-266, 2009.

DE OLIVEIRA RIBEIRO, Ciro Alberto et al. Histopathological evidence of inorganic mercury and methyl mercury toxicity in the arctic charr (*Salvelinus alpinus*). **Environmental research**, v. 90, n. 3, p. 217-225, 2002.

FABBRI, E.; VALBONESI, P.; FRANZELLITTI, S. HSP expression in bivalves. **Invertebrate survival journal**, v. 5, n. 2, p. 135-161, 2008.

FERNANDES, L. V. de G. et al. Formas de Cloro. CAMPOS, SHC, FERNANDES, FDC, **Moluscos límnicos invasores no Brasil: biologia, prevenção e controle. Porto Alegre: Redesp**, p. 303-306, 2012.

FERNANDES, F. da C. et al. Abordagem conceitual dos moluscos invasores nos ecossistemas límnicos brasileiros. MANSUR, MCD, SANTOS, CP, PEREIRA, D., PAZ, ICP, ZURITA, MLL, RODRIGUEZ, MTR, NEHRKE, MV & BERGONCI, PEA **Moluscos límnicos invasores no Brasil: biologia, prevençaoe controle. Porto Alegre: Redesp**, p. 19-23, 2012.

FOSTER-SMITH, R. L. The function of the pallial organs of bivalves in controlling ingestion. **Journal of Molluscan Studies**, v. 44, n. 1, p. 83-99, 1978.

FREITAS, Erico Tadeu Fraga et al. Ultrastructure of the gill ciliary epithelium of *Limnoperna fortunei* (Dunker 1857), the invasive golden mussel. **BMC Zoology**, v. 7, n. 1, p. 1-14, 2022.

GIRARDELLO, Francine et al. Antioxidant defences and haemocyte internalization in *Limnoperna fortunei* exposed to TiO₂ nanoparticles. **Aquatic Toxicology**, v. 176, p. 190-196, 2016.

GIRARDELLO, Francine et al. Titanium dioxide nanoparticles induce genotoxicity but not mutagenicity in golden mussel *Limnoperna fortunei*. **Aquatic Toxicology**, v. 170, p. 223-228, 2016.

GÜRKAN, Selin; GÜRKAN, Mert. Toxicity of gamma aluminium oxide nanoparticles in the Mediterranean mussel (*Mytilus galloprovincialis*): histopathological alterations and antioxidant responses in the gill and digestive gland. **Biomarkers**, v. 26, n. 3, p. 248-259, 2021.

HAMZA, Dalia S. Morphological Effects of Pollution on Gill of Common Clam, *Tapes decussatus* Linnaeus, 1758 (Bivalvia: Veneridae). **Egyptian Academic Journal of Biological Sciences, B. Zoology**, v. 11, n. 3, p. 169-179, 2019.

HARIRI, Mehrdad et al. Biogenesis of multilamellar bodies via autophagy. **Molecular Biology of the Cell**, v. 11, n. 1, p. 255-268, 2000.

IUMMATO, María Mercedes et al. Biochemical responses of the golden mussel *Limnoperna fortunei* under dietary glyphosate exposure. **Ecotoxicology and environmental safety**, v. 163, p. 69-75, 2018.

KANKAANPÄÄ, Harri et al. Accumulation and depuration of cyanobacterial toxin nodularin and biomarker responses in the mussel *Mytilus edulis*. **Chemosphere**, v. 68, n. 7, p. 1210-1217, 2007.

MACÊDO, Anderson Kelvin Saraiva et al. Histological and molecular changes in gill and liver of fish (*Astyanax lacustris* Lütken, 1875) exposed to water from the Doce basin after the rupture of a mining tailings dam in Mariana, MG, Brazil. **Science of the Total Environment**, v. 735, p. 139505, 2020.

MACKIE, Gerald L.; CLAUDI, Renata. **Monitoring and control of macrofouling mollusks in fresh water systems**. CRC Press, 2009.

MANDUZIO, Hélène et al. The point about oxidative stress in molluscs. **Invertebrate Survival Journal**, v. 2, n. 2, p. 91-104, 2005.

MANSUR, Maria Cristina Dreher et al. Primeiros dados quali-quantitativos do mexilhão-dourado, *Limnoperna fortunei* (Dunker), no Delta do Jacuí, no Lago Guaíba e na Laguna dos Patos, Rio Grande do Sul, Brasil e alguns aspectos de sua invasão no novo ambiente. **Rev. Bras. Zool.**, Curitiba, v. 20, n. 1, p. 75-84, mar. 2003.

MANSUR, M. C. D. Bivalves invasores límnicos: morfologia comparada de *Limnoperna fortunei* e espécies de *Corbicula spp.* **Moluscos Limnicos Invasores no Brasil: Biologia, Prevenção, Controle**. Redes Editora, Porto Alegre, p. 61-74, 2012.

MAROÑAS, Miriam Edith; DAMBORENEA, Maria Cristina. Efeito de biocidas e tolerância à exposição ao ar. Em: **Introdução a Biologia das Invasões: O Mexilhão Dourado na América do Sul: biologia, dispersão, impacto, prevenção e controle**, p. 169-183, 2009.

MONTRESOR, Lângia C. et al. Short-term toxicity of ammonia, sodium Hydroxide and a commercial biocide to golden mussel *Limnoperna fortunei* (Dunker, 1857). **Ecotoxicology and environmental safety**, v. 92, p. 150-154, 2013.

MORISHITA, Hideaki et al. Autophagy is required for maturation of surfactant-containing lamellar bodies in the lung and swim bladder. **Cell reports**, v. 33, n. 10, p. 108477, 2020.

MORTON, Brian. The biology and anatomy of *Limnoperna fortunei*, a significant freshwater bioinvader: blueprints for success. In: ***Limnoperna fortunei***. Springer, Cham, 2015. p. 3-41.

NOGAROL, Larissa Rosa et al. Morphological and histochemical characterization of gill filaments of the brazilian endemic bivalve *Diplodon expansus* (Küster, 1856)(Mollusca, Bivalvia, Hyriidae). **Microscopy and Microanalysis**, v. 18, n. 6, p. 1450-1458, 2012.

NAKAMURA FILHO, Arnaldo et al. Polymorphism of CaCO₃ and microstructure of the shell of a Brazilian invasive mollusc (*Limnoperna fortunei*). **Materials Research**, v. 17, p. 15-22, 2014.

NETTO, Otto Samuel Mäder. Controle da incrustação de organismos invasores em materiais de sistemas de resfriamento de usinas hidrelétricas. 2012.

OLIVEIRA, Marcia D. et al. Colonization and spread of *Limnoperna fortunei* in South America. In: ***Limnoperna fortunei***. Springer, Cham, p. 333-355, 2015.

PAL, Sandipan et al. Histopathological alterations in gill, liver and kidney of common carp exposed to chlorpyrifos. **Journal of Environmental Science and Health, Part B**, v. 47, n. 3, p. 180-195, 2012.

PANDEY, Suwarna et al. Effects of exposure to multiple trace metals on biochemical, histological and ultrastructural features of gills of a freshwater fish, *Channa punctata* Bloch. **Chemico-biological interactions**, v. 174, n. 3, p. 183-192, 2008.

PAOLUCCI, Esteban M. et al. Morphological and genetic variability in an alien invasive mussel across an environmental gradient in South America. **Limnology and Oceanography**, v. 59, n. 2, p. 400-412, 2014.

PAPO, Michele Boscolo et al. Histopathology and stress biomarkers in the clam *Venerupis philippinarum* from the Venice Lagoon (Italy). **Fish & shellfish immunology**, v. 39, n. 1, p. 42-50, 2014.

PENAFORTE, Leonardo Ruas. Invasão do Mexilhão Dourado, *Limnoperna fortunei* (Dunker, 1857): impactos, métodos de controle e estratégias de gestão adotadas. 2014.

PEREYRA, Patricio Javier; BULUS ROSSINI, Gustavo Daniel; DARRIGRAN, Gustavo Alberto. Toxicity of three comercial tannins to the nuisance invasive species *Limnoperna fortunei* (Dunker, 1857): implications for control. 2011.

PFAFFL, Michael W.; HORGAN, Graham W.; DEMPFLER, Leo. Relative expression software tool (REST©) for group-wise comparison and statistical analysis of relative expression results in real-time PCR. **Nucleic acids research**, v. 30, n. 9, p. e36-e36, 2002.

RAJAGOPAL, Sanjeevi; VAN DER VELDE, Gerard; JENNER, Henk A. Effects of low-level chlorination on zebra mussel, *Dreissena polymorpha*. **Water Research**, v. 36, n. 12, p. 3029-3034, 2002.

REWITZ, Kim F. et al. Marine invertebrate cytochrome P450: emerging insights from vertebrate and insect analogies. **Comparative Biochemistry and Physiology Part C: Toxicology & Pharmacology**, v. 143, n. 4, p. 363-381, 2006.

ROMERO, A.; NOVOA, B.; FIGUERAS, A. The complexity of apoptotic cell death in mollusks: an update. **Fish & shellfish immunology**, v. 46, n. 1, p. 79-87, 2015.

ROSA, Maria; WARD, J. Evan; SHUMWAY, Sandra E. Selective capture and ingestion of particles by suspension-feeding bivalve molluscs: a review. **Journal of Shellfish Research**, v. 37, n. 4, p. 727-746, 2018.

SEO, DongSeok; JO, JiMin. Humidifier disinfectant, sodium dichloroisocyanurate (NaDCC): assessment of respiratory effects to protect workers' health. **Scientific Reports**, v. 11, n. 1, p. 1-14, 2021.

SIEBERT, Marília Nardelli et al. Candidate cytochrome P450 genes for ethoxyresorufin O-deethylase activity in oyster *Crassostrea gigas*. **Aquatic Toxicology**, v. 189, p. 142-149, 2017.

SILVA, F. A. et al. Mexilhão-Dourado no Brasil: Detecção de um perigoso invasor. **Ciência Hoje**, v. 57, p. 38-42, 2016.

SPRECHER, Susan L.; GETSINGER, Kurt D. **Zebra mussel chemical control guide**. p. -14, 2000.

TANG, Feng; ALDRIDGE, David C. Microcapsulated biocides for the targeted control of invasive bivalves. **Scientific Reports**, v. 9, n. 1, p. 1-10, 2019.

ULIANO-SILVA, Marcela et al. Gene discovery through transcriptome sequencing for the invasive mussel *Limnoperna fortunei*. **PLoS One**, v. 9, n. 7, p. e102973, 2014.

VELMURUGAN, Babu et al. Cytological and histological effects of pesticide chlorpyrifos in the gills of *Anabas testudineus*. **Drug and Chemical Toxicology**, v. 43, n. 4, p. 409-414, 2018.

VENKATNARAYANAN, Srinivas et al. Response of green mussels (*Perna viridis*) subjected to chlorination: investigations by valve movement monitoring. **Environmental Monitoring and Assessment**, v. 193, n. 4, p. 1-12, 2021.

VIDAL, Fabrício Salvador. Uso de métodos químicos como ferramenta de prevenção e controle do mexilhão-dourado *Limnoperna fortunei* (DUNKER, 1857). 2019.

WALLER, Diane L. et al. Toxicity of candidate molluscicides to zebra mussels (*Dreissena polymorpha*) and selected nontarget organisms. **Journal of Great Lakes Research**, v. 19, n. 4, p. 695-702, 1993.

WANG, Ying et al. Superoxide dismutases: Dual roles in controlling ROS damage and regulating ROS signaling. **Journal of Cell Biology**, v. 217, n. 6, p. 1915-1928, 2018.

WANG, Gongsu; ZHANG, Chengkai; HUANG, Bo. Transcriptome analysis and histopathological observations of *Geloina erosa* gills upon Cr (VI) exposure. **Comparative Biochemistry and Physiology Part C: Toxicology & Pharmacology**, v. 231, p. 108706, 2020.

WOJTAL-FRANKIEWICZ, Adrianna et al. The role of environmental factors in the induction of oxidative stress in zebra mussel (*Dreissena polymorpha*). **Aquatic Ecology**, v. 51, n. 2, p. 289-306, 2017.

WOO, Seonock et al. Expressions of oxidative stress-related genes and antioxidant enzyme activities in *Mytilus galloprovincialis* (Bivalvia, Mollusca) exposed to hypoxia. **Zoological Studies**, v. 52, n. 1, p. 1-8, 2013.

XU, Mengzhen. Distribution and spread of *Limnoperna fortunei* in China. In: **Limnoperna fortunei**. Springer, Cham, p. 313-320, 2015.

ZANGAR, Richard C.; DAVYDOV, Dmitri R.; VERMA, Seema. Mechanisms that regulate production of reactive oxygen species by cytochrome P450. **Toxicology and applied pharmacology**, v. 199, n. 3, p. 316-331, 2004.

ZHANG, Chang et al. Quaternary ammonium compounds (QACs): a review on occurrence, fate and toxicity in the environment. **Science of the Total Environment**, v. 518, p. 352-362, 2015.

4.9 LIST OF ABBREVIATION

AB-PAS – Alcian blue and periodic acid Schiff

CAT - Catalase enzyme

CBEIH - Centro de Bioengenharia de Espécies Invasoras de Hidrelétricas

Cd – Ciliary discs

CYP - Cytochrome P450 enzyme

Fc – Frontal cilia

HSP70 - Heat Shock Protein 70

IBAMA - Instituto Brasileiro do Meio Ambiente e dos Recursos Naturais Renováveis

Lc – Lateral cilia

Lfc – Laterofrontal cirri

LM – Light Microscopy

MXD-100 - Produto comercial da empresa Maxclean

Nadcc - Sodium dichloroisocyanurate

PBS – Phosphate buffer solution

QACS - Quaternary ammonium compounds

ROS - Reactive oxygen species

SEM – Scanning Electron Microscopy

SISBIO - Sistema de Autorização e Informação em Biodiversidade

SOD - Superoxide dismutase enzyme

TEM – Transmission Electron Microscopy

VG - Volta Grande

4.10 FUGURE LEGENDS

Fig. 1 Scheme representing the methodology of bioassays 1 (Sodium Dichloroisocyanate) (a) and 2 (MXD-100) (b). (c) number of animals in jar per analysis.

Fig. 2 SEM images of the *L. fortunei* gills. (a-c) Control group and (d-l) groups exposed to NaDCC. (a) Ciliated gill with inner [id] and outer demibrach [od]. (b) Dorsal view of gill lamellae showing the frontal region of the filaments with frontal cilia [fc] and laterofrontal cirri [lfc]. (c) View in perspective of a set of filaments, showing frontal cilia [fc] and laterofrontal cirri [lfc]. (d-f) Group exposed for 24 hours. (g-i) Group exposed for 48 hours. (j-l) Group exposed for 72 hours. Mucus [white arrow], loose cilia [arrow head].

Fig. 3 Mean and standard deviation of thickness of the epithelium in 50 branchial filaments exposed to different times of sodium dichloroisocyanurate (24, 48 and 72 hours). Significant differences between exposed groups were represented by, * $p < 0.01$.

Fig. 4 LM images showing the transverse sections of a gill filament of *L. fortunei* exposed to NaDCC. (a) Group control. (b) Group exposed for 24 hours. (c) Group exposed for 48 hours. (d) Group exposed for 72 hours. Cilia [c], hemolymphatic vessel [hv], epithelium lifting [*], epithelial desquamation [arrow head].

Fig. 5 Mean and standard deviation of the number of mucous cells present in 50 branchial filaments to NaDCC exposed (24 and 48 hours) (a). Significant differences between exposure groups were represented by * $p < 0.01$. Group exposed for 72 hours showed almost 100% of mortality. (b-c) LM images showing the transverse sections of a gill filament of *L. fortunei* stained with Alcian Blue/PAS. (a) Group exposed for 24 hours. (b) Group exposed for 48 hours. Mucus-producing cells [arrow].

Fig. 6 Bright-field TEM images of the epithelial cells of *L. fortunei* exposed to NaDCC. (a) Control group. (b) Group exposed for 24 hours. (c) Group exposed for 48 hours. (d) Group exposed for 72 hours. Autophagosome [a], nuclei [n], cytoplasmic dilatations [arrow head].

Fig. 7 Activity of defence enzymes (CYP, SOD, CAT, HSP70) in the *L. fortunei* gills exposed to NaDCC for 24 hours, 48 hours and 72 hours. [*] Significant differences (p 0.05).

Fig. 8 SEM images of the *L. fortunei* gills. (a-c) Control group and (d-l) groups exposed to MXD-100. (a) Ciliated gill with inner [id] and outer demibrach [od]. (b) Dorsal view of gill lamellae showing the frontal region of the filaments, frontal cilia [fc] and laterofrontal cirri [lfc]. (c) View in perspective of a set of filaments, showing frontal cilia [fc] and laterofrontal cirri [lfc]. (d–f) Group exposed for 24 hours. (g–i) Group exposed for 48 hours. (j–l) Group exposed for 72 hours. Mucus [white arrow], loose cilia [arrow head].

Fig. 9 Mean and standard deviation of thickness of the epithelium in 50 branchial filaments exposed to different times of MXD-100 (24 and 48 hours). All individuals died in 72-hour exposition. Significant differences between exposure groups were represented by * p < 0.01.

Fig. 10 LM images showing the transverse sections of a gill filament of *L. fortunei* exposed to MXD-100. (a) Group control. (b) Group exposed for 24 hours. (c) Group exposed for 48 hours. (d) Group exposed for 72 hours. Cilia [c], hemolymphatic vessel [hv], hyperplasia [arrow], epithelial desquamation [arrow head], epithelium lifting [*].

Fig. 11 Bright-field TEM images of the epithelial cells of *L. fortunei* with MXD-100. (a) Control group. (b) Group exposed for 24 hours. (c) Group exposed for 48 hours. (d) Group exposed for 72 hours. Lamellar bodies [lb], nuclei [n], cytoplasmic dilatations [arrow head].

Fig. 12 Expression of defense enzymes (CYP, SOD, CAT, HSP70) in the *L. fortunei* gills exposed to MXD-100 for 24 hours, 48 hours and 72 hours. [*] Significant differences p < 0.05.

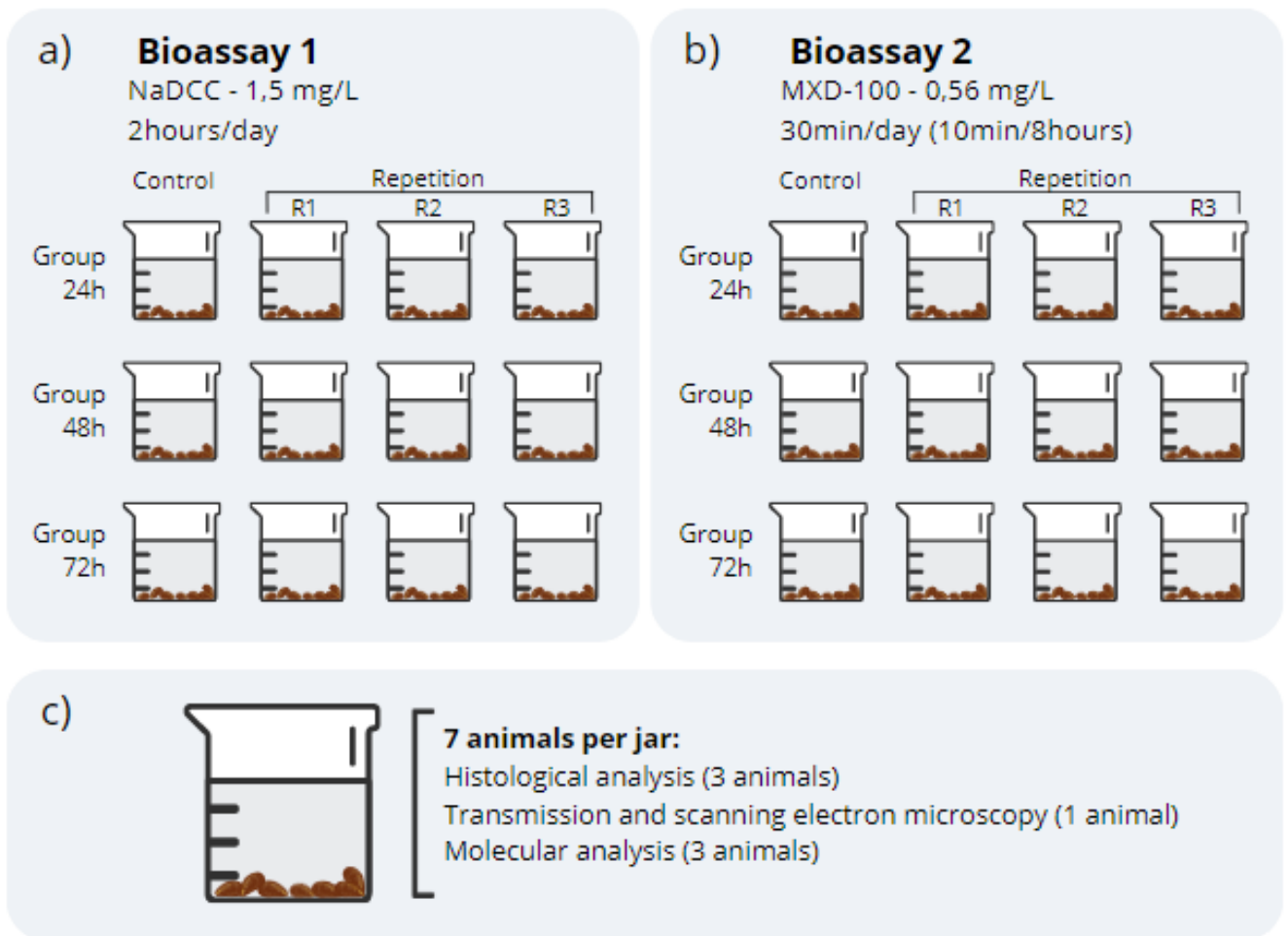


Figure 1 Scheme representing the methodology of bioassays 1 (Sodium Dichloroisocyanate) (a) and 2 (MXD-100) (b). (c) number of animals in jar per analysis.

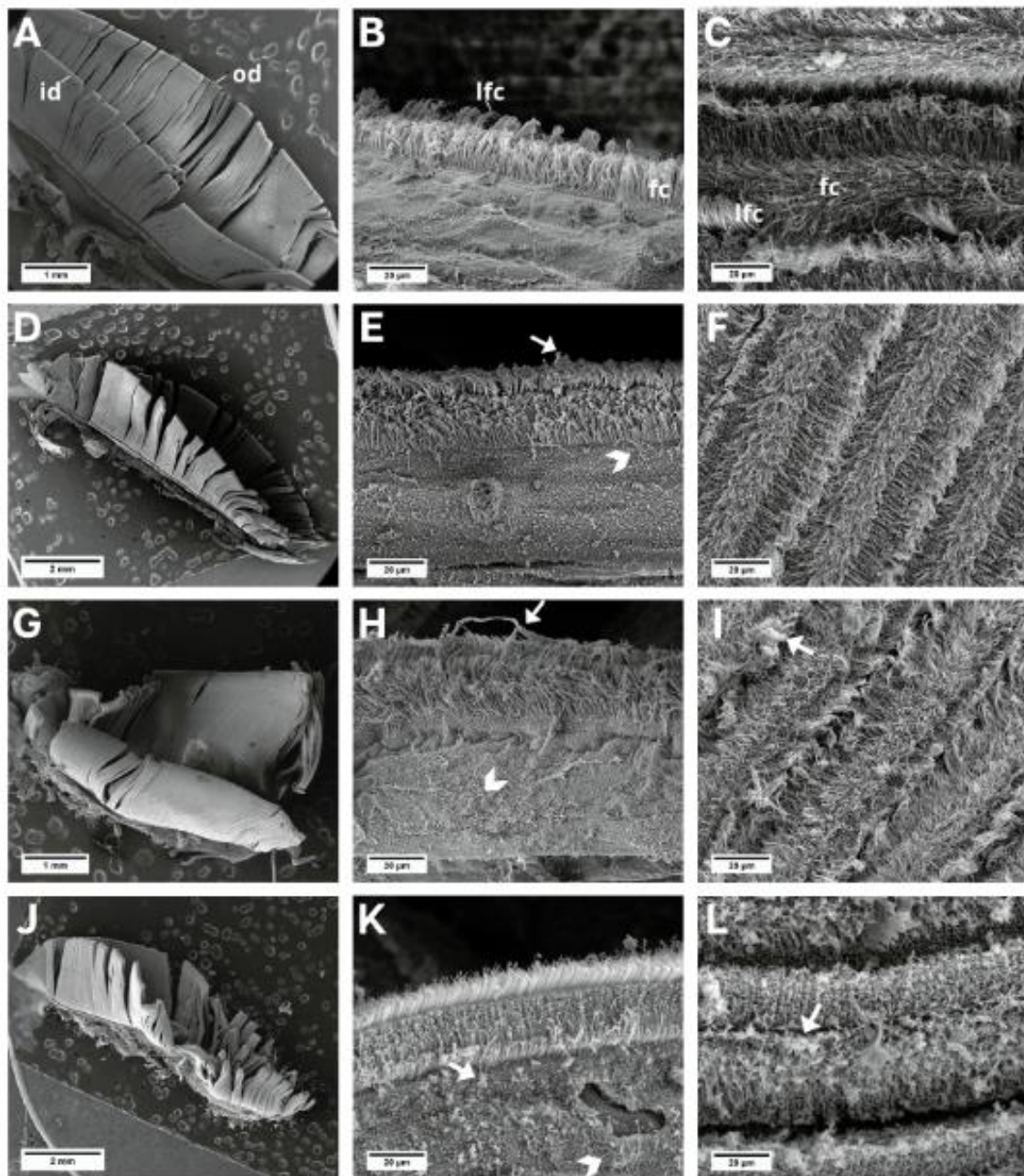


Figure 2 SEM images of the *L. fortunei* gills. (a-c) Group control and (d-l) groups exposed to NaDCC. (a) Ciliated gill with inner [id] and outer demibrach [od]. (b) Dorsal view of gill lamellae showing the frontal region of the filaments with frontal cilia [fc] and laterofrontal cirri [lfc]. (c) View in perspective of a set of filaments, showing frontal cilia [fc] and laterofrontal cirri [lfc]. (d-f) Group exposed for 24 hours. (g-i) Group exposed for 48 hours. (j-l) Group exposed for 72 hours. Mucus [white arrow], loose cilia [arrow head].

Thickness of the epithelium

NaDCC

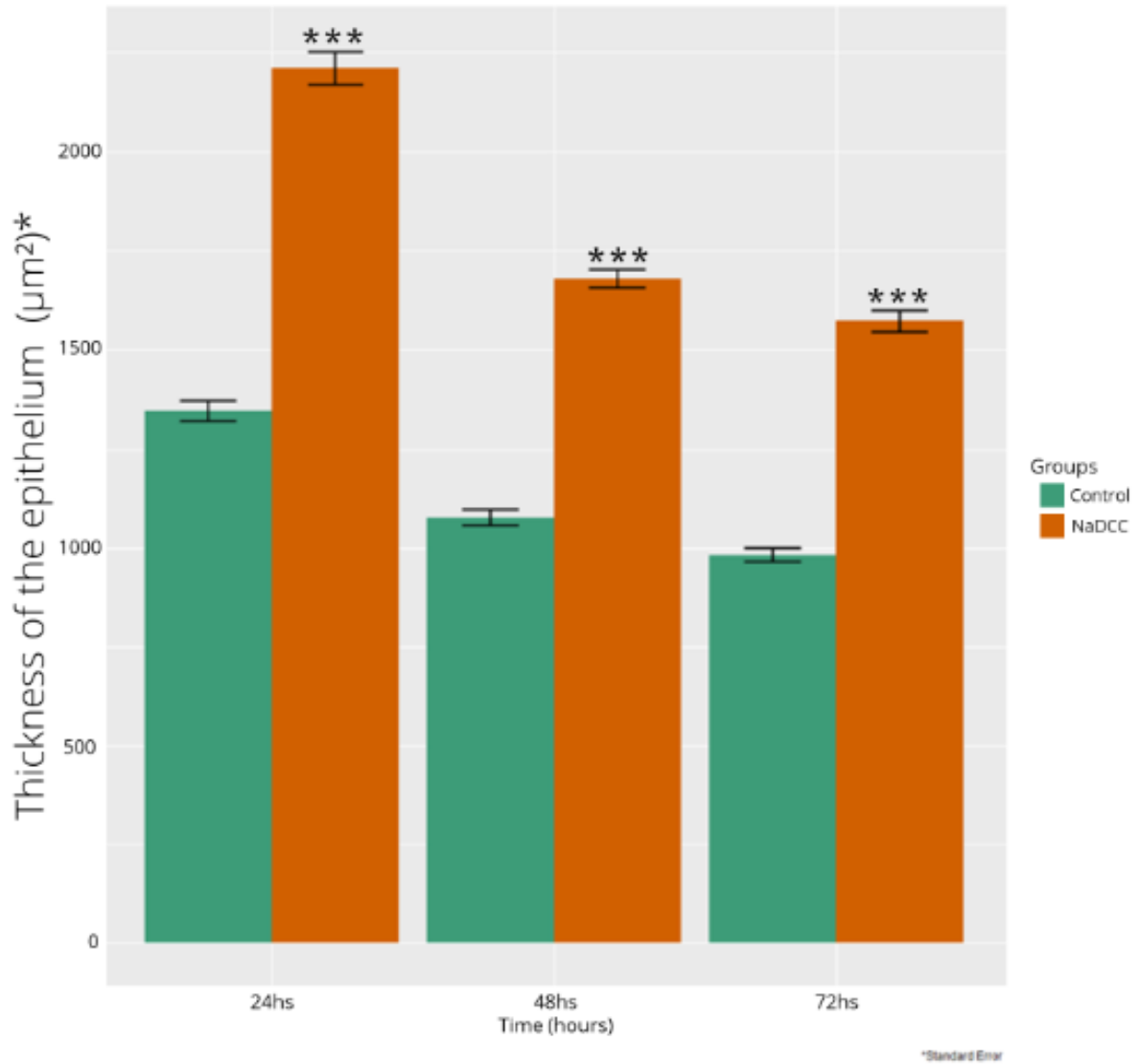


Figure 3 Mean and standard deviation of thickness of the epithelium in 50 branchial filaments exposed to different times of Sodium Dichloroisocyanurate (24, 48 and 72 hours). Significant differences between exposure groups were represented by, p 0.01.

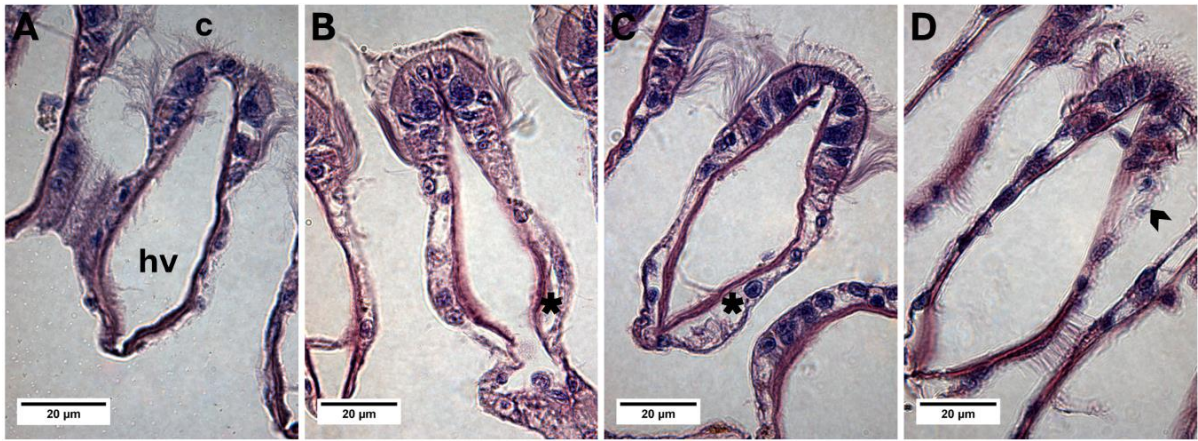


Figure 4 LM images showing the transverse sections of a gill filament of *L. fortunei* exposed to NaDCC. (a) Group control. (b) Group exposed for 24 hours. (c) Group exposed for 48 hours. (d) Group exposed for 72 hours. Cilia [c], hemolympatic vessel [hv], epithelium lifting [*], epithelial desquamation [arrow head].

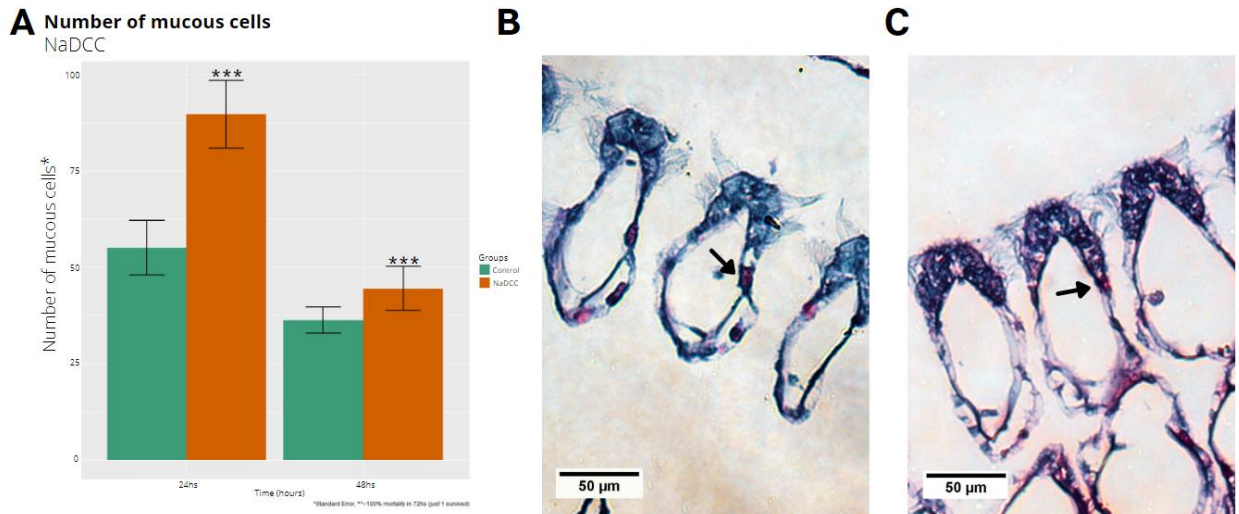


Figure 5 Mean and standard deviation of the number of mucous cells present in 50 branchial filaments to NaDCC exposed (24 and 48 hours) (a). Significant differences between exposure groups were represented by, $p < 0.01$. 72 hours group showed almost 100% of mortality. (b-c) LM images showing the transverse sections of a gill filament of *L. fortunei* stained with Alcian Blue/PAS. (a) Group exposed for 24 hours. (b) Group exposed for 48 hours. Mucus-producing cells [arrow].

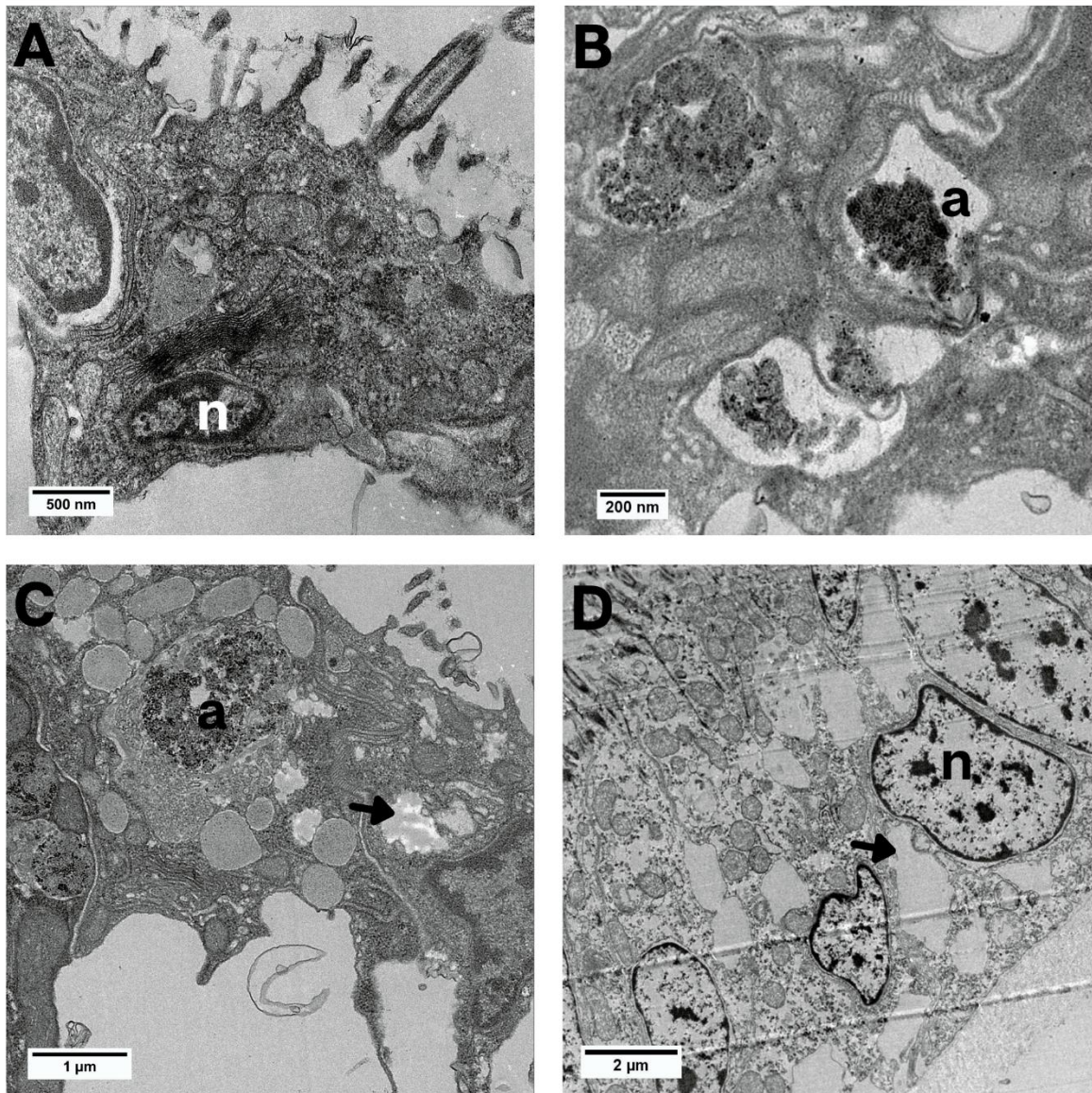


Figure 6 Bright-field TEM images of the epithelial cells of *L. fortunei* exposed to NaDCC. (a) Control group. (b) Group exposed for 24 hours. (c) Group exposed for 48 hours. (d) Group exposed for 72 hours. Autophagosome [a], nuclei [n], cytoplasmic dilatations [arrow head].

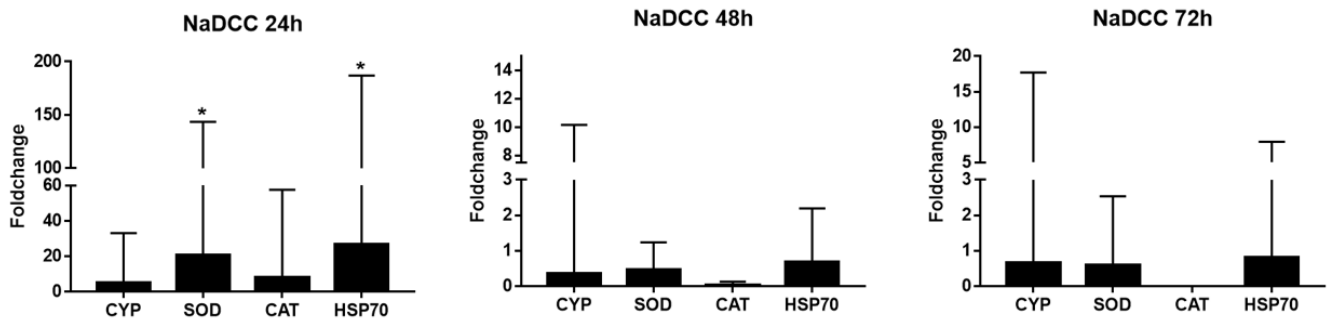


Figure 7 Activity of defence enzymes (CYP, SOD, CAT, HSP70) in the *L. fortunei* gills exposed to NaDCC for 24 hours, 48 hours and 72 hours. [*] Significant differences (p 0.05).

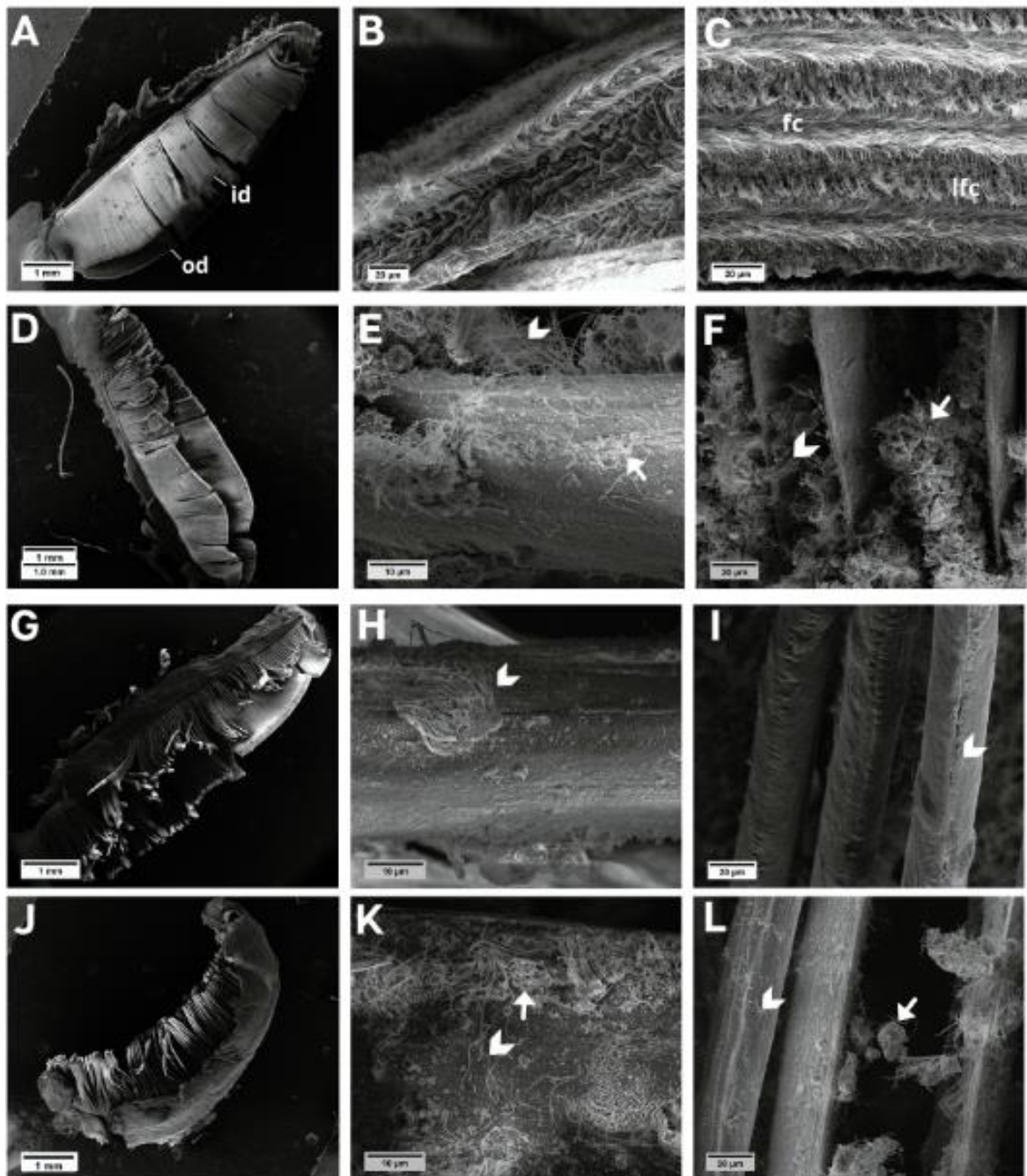


Figure 8 SEM images of the *L. fortunei* gills. (a-c) Group control and (d-l) groups exposed to MXD-100. (a) Ciliated gill with inner [id] and outer demibrach [od]. (b) Dorsal view of gill lamellae showing the frontal region of the filaments, frontal cilia [fc] and laterofrontal cirri [lfc]. (d-f) Group exposed for 24 hours. (g-i) Group exposed for 48 hours. (j-l) Group exposed for 72 hours. Mucus [white arrow], loose cilia [arrow head].

Thickness of the epithelium

MXD-100

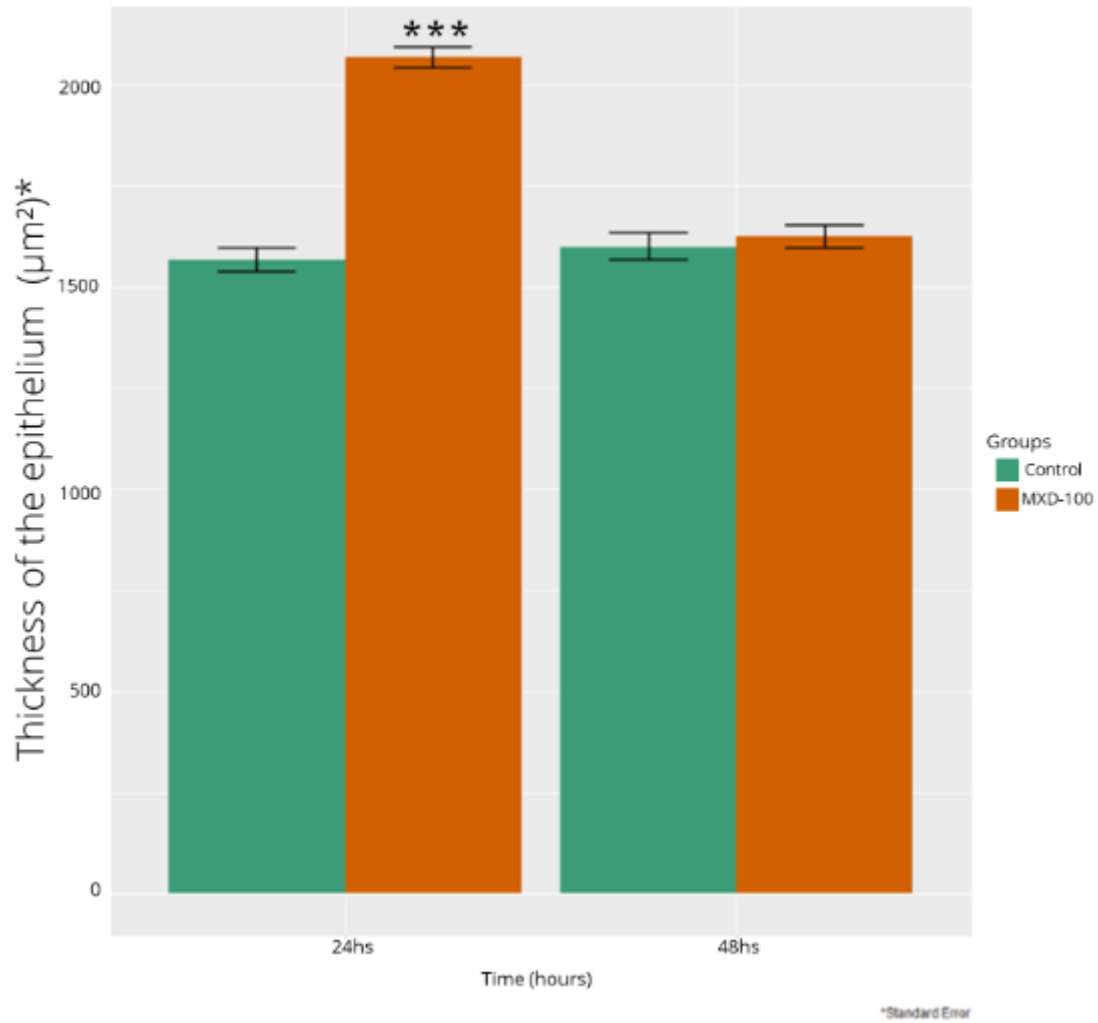


Figure 9 Mean and standard deviation of thickness of the epithelium in 50 branchial filaments exposed to different times of MXD-100 (24 and 48 hours). All individuals died in 72-hour exposition. Significant differences between exposure groups were represented by, $p < 0.01$.

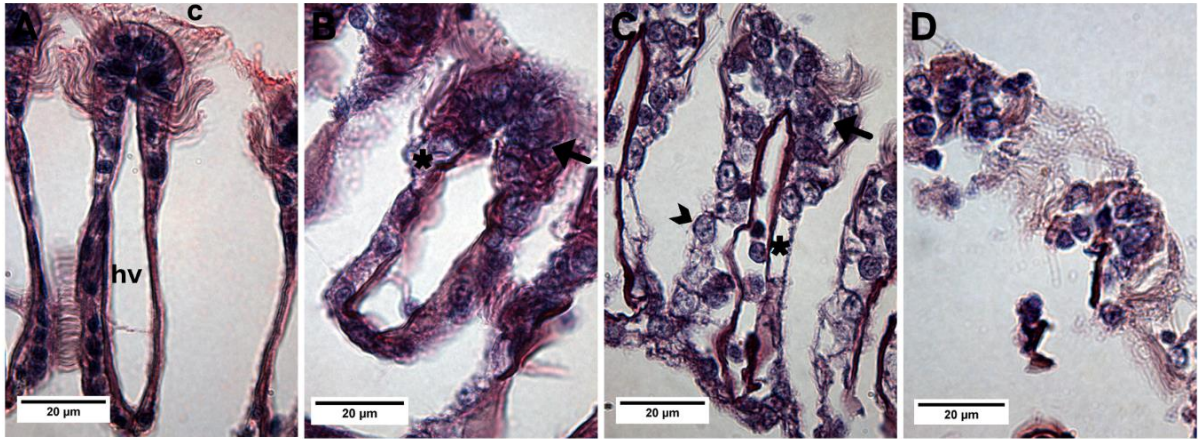


Figure 10 LM images showing the transverse sections of a gill filament of *L. fortunei* exposed to MXD-100. (a) Group control. (b) Group exposed for 24 hours. (c) Group exposed for 48 hours. (d) Group exposed for 72 hours. Cilia [c], hemolymphatic vessel [hv], hyperplasia [arrow], epithelial desquamation [arrow head], epithelium lifting [*].

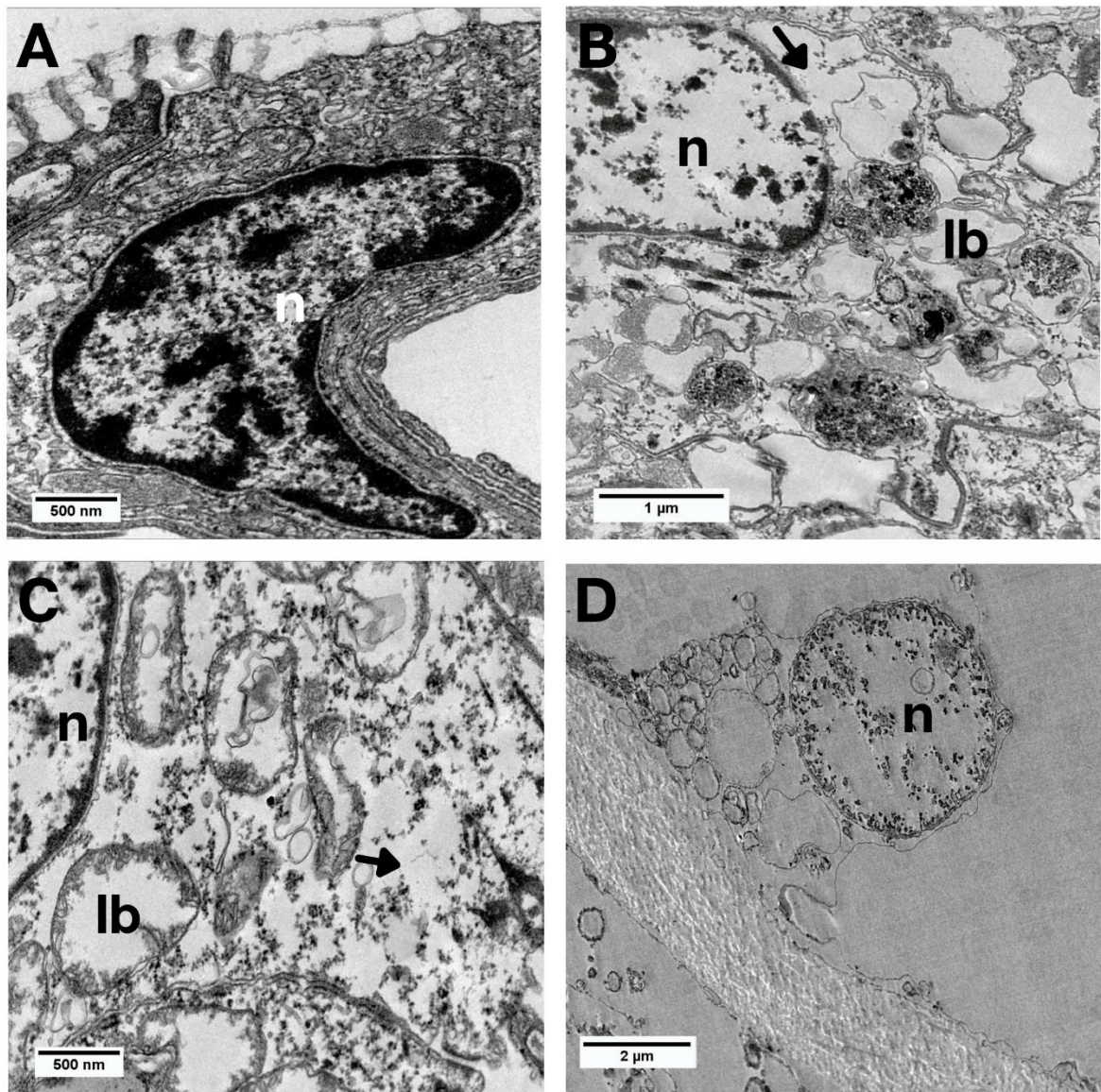


Figure 11 Bright-field TEM images of the epithelial cells of *L. fortunei* with MXD-100. (a) Control group. (b) Group exposed for 24 hours. (c) Group exposed for 48 hours. (d) Group exposed for 72 hours. Lamellar bodies [lb], nuclei [n], cytoplasmic dilatations [arrow head].

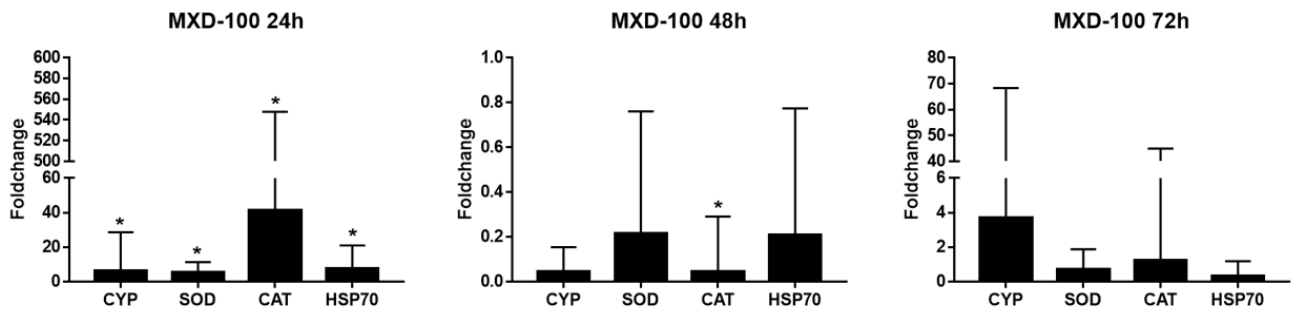


Figure 12 Activity of defence enzymes (CYP, SOD, CAT, HSP70) in the *L. fortunei* gills exposed to MXD-100 for 24 hours, 48 hours and 72 hours. [*] Significant differences (p 0.05).

4.11 TABLES

Table 1. Primers used for the qRT-PCR assays. *CYP*: cytochrome P450; *SOD*: seperoxide dismutase; *CAT*: catalase; *HSP70*: Heath Shock Protein 70. The primer *GAPDH* (Glyceraldehyde 3-phosphate dehydrogenase) was the reference. F: forward primer; R: reverse primer. The annealing temperature of all reactions was 60 °C. bp: base pairs.

Table 1. Primers used for the qRT-PCR assays. *CYP*: cytochrome P450; *SOD*: superoxide dismutase; *CAT*: catalase; *HSP70*: Heat Shock Protein 70. The primer *GAPDH* (Glyceraldehyde 3-phosphate dehydrogenase) was the reference. F: forward primer; R: reverse primer. The annealing temperature of all reactions was 60 °C. bp: base pairs.

Gene	Initial	Sequence	Amplicon (pb)
<i>Cytochrome P450</i>	<i>CYP</i>	F: 5'-GCCAAGGGACACGATTCTAC-3'	292
		R: 5'-CATACAAAGACACCGCCATTC'-3'	
<i>Superoxide dismutase</i>	<i>SOD</i>	F: 5'-TGATTCGTAGGGACTTTGGA-3'	145
		R: 5'-CCTGGTTAGCACAAAGCAACA-3'	
<i>Catalase</i>	<i>CAT</i>	F:5'-CTCTCAAGTCGGTGTATTCTGG-3'	206
		F:5'-CCTGTTTTTCCTTTCGCTGT-3'	
<i>Heat Shock Protein 70</i>	<i>HSP70</i>	F:5'-GAAGCCTACCTCGGACAAAA-3'	269
		F:5'-CGGACCTCAAACAGTGAACC-3'	
<i>Glyceraldehyde 3-phosphate dehydrogenase</i>	<i>GAPDH</i>	F: 5'- TACTGCGAGGCAACAATAGG -3'	135
		R: 5'- GTTTTTCAAGGCACACAGA -3'	

5. CONSIDERAÇÕES FINAIS

As incrustações volumosas formadas pelo mexilhão-dourado geram grandes impactos ambientais e no setor hidrelétrico, sendo importante estudos que abranjam suas características morfológicas, modo de vida, monitoramento e controle de invasão desta espécie. Assim, os resultados apresentados neste trabalho ajudam a compreender, a partir da morfologia e biologia molecular, as atividades fisiológicas do mexilhão e corroboram também com estratégias de controle.

A caracterização das brânquias nos permitiu observar uma complexa organização estrutural e funcional, podendo estes órgãos serem parâmetros biológicos para compreender a plasticidade de *L. fortunei* durante a contenção da invasão.

Além disso, biocidas comumente utilizados no controle (NaDCC e MXD-100) mostraram efeitos sobre a morfologia e expressão gênica das brânquias, o que nos ajuda a compreender a eficiência desses químicos, corroborando com as estratégias de controle de populações desse bivalve.

6. REFERÊNCIAS BIBLIOGRÁFICAS

BOGAN, Arthur E. Global diversity of freshwater mussels (Mollusca, Bivalvia) in freshwater. In: **Freshwater animal diversity assessment**. Springer, Dordrecht, p. 139-147, 2007.

CLOETE, Thomas Eugene; JACOBS, Liesel; BRÖZEL, Volker Siegfried. The chemical control of biofouling in industrial water systems. **Biodegradation**, v. 9, n. 1, p. 23-37, 1998.

DARRIGRAN, GUSTAVO; PASTORINO, GUIDO. Bivalvos invasores en el Río de la Plata, Argentina. **Comunicaciones de la Sociedad Malacológica del Uruguay**, v. 7, n. 64-65, p. 309-313, 1993.

DARRIGRAN, Gustavo Alberto; DAMBORENEA, Maria Cristina. A South American bioinvasion case history: *Limnoperma fortunei* (Dunker, 1857), the golden mussel. 2005.

DE RESENDE, Márcio Figueiredo. A variação das características hidráulicas em condutos forçados devido à infestação do *Limnoperma fortunei*. 2007.

FERNANDES, F. da C. et al. Abordagem conceitual dos moluscos invasores nos ecossistemas límnicos brasileiros. MANSUR, MCD, SANTOS, CP, PEREIRA, D., PAZ, ICP, ZURITA, MLL, RODRIGUEZ, MTR, NEHRKE, MV & BERGONCI, PEA **Moluscos límnicos invasores no Brasil: biologia, prevenção e controle**. Porto Alegre: Redesp, p. 19-23, 2012.

HAUBROCK, Phillip J. et al. Economic costs of invasive alien species across Europe. **NeoBiota**, v. 67, p. 153-190, 2021.

MANSUR, Maria Cristina Dreher et al. Primeiros dados quali-quantitativos do mexilhão-dourado, *Limnoperma fortunei* (Dunker), no Delta do Jacuí, no Lago Guaíba e na Laguna dos Patos, Rio Grande do Sul, Brasil e alguns aspectos de sua invasão no novo ambiente. **Rev. Bras. Zool.**, Curitiba, v. 20, n. 1, p. 75-84, mar. 2003.

MANSUR, M. C. D. Bivalves invasores límnicos: morfologia comparada de *Limnoperna fortunei* e espécies de *Corbicula spp.* **Moluscos Limnicos Invasores no Brasil: Biologia, Prevenção, Controle. Redes Editora, Porto Alegre**, p. 61-74, 2012.

MORTON, Brian. The biology and anatomy of *Limnoperna fortunei*, a significant freshwater bioinvader: blueprints for success. In: *Limnoperna fortunei*. Springer, Cham, p. 3-41, 2015.

OLIVEIRA, Marcia D. et al. Colonization and spread of *Limnoperna fortunei* in South America. In: *Limnoperna fortunei*. Springer, Cham, 2015. p. 333-355.

SILVA, F. A. et al. Mexilhão-Dourado no Brasil: Detecção de um perigoso invasor. **Ciência Hoje**, v. 57, p. 38-42, 2016.

ZANELLA, O.; MARENDA, L. D. Ocorrência de *Limnoperna fortunei* na Central Hidrelétrica de Itaipu. In: **V Congresso Latinoamericano de Malacologia, São Paulo (Brazil)**. 2002.

7. ANEXO 1

Freitas et al. *BMC Zoology* (2022) 7:6
<https://doi.org/10.1186/s40850-022-00107-y>


BMC Zoology

RESEARCH ARTICLE

Open Access



Ultrastructure of the gill ciliary epithelium of *Limnoperna fortunei* (Dunker 1857), the invasive golden mussel

Erico Tadeu Fraga Freitas^{1,2,3*†} , Amanda Maria Siqueira Moreira^{1,4†}, Rayan Silva de Paula^{1,4}, Gabriela Rabelo Andrade¹, Marcela David de Carvalho⁵, Paulo Santos Assis^{1,3}, Erika Cristina Jorge⁴ and Antônio Valadão Cardoso^{1,6*}

Abstract

Background: *Limnoperna fortunei* is a freshwater bivalve mollusc originally from southern Asia that invaded South America in the 1990's. Due to its highly efficient water pumping and filtering, and its capacity to form strong adhesions to a variety of substrates by byssus thread, this invasive species has been able to adapt to several environments across South America, causing significant ecological and economic damages. By gaining a deeper understanding of the biological and ecological aspects of *L. fortunei* we will be able to establish more effective strategies to manage its invasion. The gills of the mollusc are key structures responsible for several biological functions, including respiration and feeding. In this work, we characterized the ultrastructure of *L. fortunei* gills and its ciliary epithelium using light microscopy, transmission and scanning electron microscopies. This is the first report of the morphology of the epithelial cells and cilia of the gill of *L. fortunei* visualized in high resolution.

Results: The analysis showed highly organized and abundant ciliary structures (lateral cilia, laterofrontal cirri and frontal cilia) on the entire length of the branchial epithelium. Mitochondria, smooth endoplasmic reticulum and glycogen granules were abundantly found in the epithelial cells of the gills, demonstrating the energy-demanding function of these structures. Neutral mucopolysaccharides (low viscosity mucus) were observed on the frontal surface of the gill filaments and acid mucopolysaccharides (high viscosity mucus) were observed to be spread out, mainly on the lateral tract. Spherical vesicles, possibly containing mucus, could also be observed in these cells. These findings demonstrate the importance of the mucociliary processes in particle capture and selection.

Conclusions: Our data suggest that the mechanism used by this mollusc for particle capture and selection could contribute to a better understanding of key aspects of invasion and also in the establishment of more efficient and economically viable strategies of population control.

Keywords: Golden mussel, Invasive species, Mussel gill, Suspension-feeding, Branchial epithelium, Electron microscopy

*Correspondence: ericotadeu@ufmg.br; antonio.cardoso@uemg.br

[†]Erico Tadeu Fraga Freitas and Amanda Maria Siqueira Moreira contributed in the same way to the work and share the first authorship.

² Universidade Federal de Ouro Preto (UFOP), FIMAT, 35400-000 Ouro Preto, MG, Brazil

⁴ Escola de Design, Universidade do Estado de Minas Gerais (UEMG), 30140-091 Belo Horizonte, MG, Brazil

Full list of author information is available at the end of the article

Background

Biological invasions of alien animals and plants are one of the most critical threats to biodiversity in aquatic ecosystems. Among the known invasive species, bivalve molluscs are responsible for causing both significant environmental and economic damages [1]. *Limnoperna*



© The Author(s) 2022. **Open Access** This article is licensed under a Creative Commons Attribution 4.0 International License, which permits use, sharing, adaptation, distribution and reproduction in any medium or format, as long as you give appropriate credit to the original author(s) and the source, provide a link to the Creative Commons licence, and indicate if changes were made. The images or other third party material in this article are included in the article's Creative Commons licence, unless indicated otherwise in a credit line to the material. If material is not included in the article's Creative Commons licence and your intended use is not permitted by statutory regulation or exceeds the permitted use, you will need to obtain permission directly from the copyright holder. To view a copy of this licence, visit <http://creativecommons.org/licenses/by/4.0/>. The Creative Commons Public Domain Dedication waiver (<http://creativecommons.org/publicdomain/zero/1.0/>) applies to the data made available in this article, unless otherwise stated in a credit line to the data.

fortunei (Dunker 1857) and *Corbicula fluminea* (Müller 1774) are among those bivalves known to have become established invaders in South America [2, 3]. *Limnoperna fortunei* is a bivalve belonging to the family Mytilidae (subclass Pteriomorpha and order Mytiloida) and is originally native to Southeast Asia (including China and South Korea) [4]. The arrival of this invasive mollusc in South America occurred in the early 1990's, possibly transported by ballast waters from cargo ships originating in Asia due to the increase in trade routes between the two continents [5].

Limnoperna fortunei can inhabit waters with a wide range of temperatures and salinity and cope with long periods of air exposure [6, 7]. Understanding the morphological aspects of *L. fortunei* structures is key to further understanding these biological invasions. Some recent studies focused on the morphology and function of the cilia on the *L. fortunei* foot, used to promote adhesion to substrates [8], and on its shell microstructure in adults [9]. As a prolific suspension feeder, *L. fortunei* has one of the highest reported clearance rates for suspension-feeding bivalves, including other invasive species such as *Dreissena polymorpha* (Pallas 1771), *Dreissena bugensis* (Andrusov 1897) and *C. fluminea*. This filtering capacity was analysed under laboratory conditions using cells from the alga *Chlorella vulgaris*. That also makes *L. fortunei* able to function as a bioindicator and sentinel of metal pollution and pollution monitoring, already observed in other bivalves such as the blue mussel *Mytilus edulis* (Linnaeus 1758) [10–12]. Indeed, this attribute has already been evaluated in studies involving the accumulation and dynamics of microplastics [13] and herbicides, such as glyphosate [14, 15].

Further understanding of the invasive mussels' morphology can reveal their role in varying ecosystems and also provide insight into possible methods of population control in invaded areas [16]. A thorough morphological description of the *L. fortunei* anatomy has been reported by Morton [17]. *Limnoperna fortunei* has a single foot, two pairs of gills (ctenidia) and is gonochoric with external fertilization. Both juvenile and adult individuals have two valves surrounding the body, mainly composed of calcium carbonate [18] and its polymorphs aragonite and amorphous calcium carbonate [9]. The outermost part of the shell has a proteinaceous layer, known as periostracum. Adult shell length can reach 4.5 cm [17].

Limnoperna fortunei adult gills are flat, homorhabdic and filibranchiate [17], being in direct contact with the environment. In the presence of environmental contaminants chemicals, such as chlorothalonil, the bivalve gills are key in xenobiotics biotransformation, antioxidant response, innate immune response and osmoregulation [19]. Moreover, a giant virus belonging to the

Marseilleviridae family was recently found in *L. fortunei* gills, as the morphophysiological structure of the gills favours microorganism bioaccumulation such as amoebas and viruses [20]. Bivalve gills are located in the mantle cavity [21]. After the post larvae stage, the gills are quite well formed in Mytilidae and Pectinidae, although they continue growing and developing until adulthood [22]. Each gill comprises two demibranchs, the outer and inner demibranchs, a double-lamellar macrostructure, namely ascending and descending lamellae [21]. The gill of the *L. fortunei* is type B(I) [17, 23], showing a W-shape in transverse sections, such as in *M. edulis* and other representatives of Mytilidae [22, 23]. The ventral margin of each demibranch has a deep groove, the marginal food groove [23]. Similar to *D. polymorpha* (Dreissenidae), the outer demibranch of *L. fortunei* is longer than the inner [17, 23]. This arrangement increases the efficiency of transfer of material from the marginal food grooves to the labial palps [17]. Each lamella comprises several parallel tubular filaments, the spaces between which form the interfilament channels. On the lateral surface of each individual filament there are ciliary bands, known as water-pumping cilia or lateral cilia (lc), responsible for the main water flow through the gills [17, 24]. Similar to other Mytiloida, there are frontal cilia (fc) at the frontal tract of the filaments, and laterofrontal cirri (lfc) located at the frontal margin of each filament frontal surface, in between the lc and fc. Each laterofrontal cirrus is a compound ciliary structure, and the action of the lfc facilitates particle capture [25, 26]. The fc transfer the captured particles towards the marginal food groove and then to the labial palps [17, 22, 24, 27–30]. Thereby, in addition to its respiratory function, this organ also fulfils the capturing and transportation of particles [17, 22].

Particle transportation on the gill filaments is mediated to a great extent by mucus [30–34]. The contact of captured particles to the fc of the gill filaments in *Ostrea edulis* (Linnaeus 1758) might cause the goblet cells to secrete mucus, trapping the particles within them [30]. Particles that require large amounts of mucus to cover them would be less likely to be ingested, while those demanding less mucus would be more likely to enter the labial palps [31]. In *M. edulis*, *Venerupis pullastra* (Montagu 1803) and *Cerastoderma edule* (Linnaeus 1758) an increase in mucus secretion was observed when particles were added to filtered sea water, and strings of mucus-particles could be observed [32]. Mucus mediating particle selection or rejection would be size dependent. High mass particles caused an instantaneous mucus discharge on the coarse frontal tracts of *Crassostrea virginica* (Gmelin 1791), in which the particles were entangled [33]. Mucus discharge would be triggered by a type of tactile stimulation. The smaller particles, on the other

hand, would not cause such discharge to occur in the fine frontal tract [33]. A detailed mechanism of selection and rejection of mucus-particles strings by the labial palps in bivalves can be found in the works of Foster-Smith [32, 34] and Beninger and colleagues [35]. The mechanisms of particle capture were reviewed and discussed by Riisgård and Larsen [36] and the works of Ward and Shumway [37] and Rosa and colleagues [38] present great reviews of the present understanding of particle processing by suspension feeders.

The mechanism of particle processing and the further understanding of the physiological aspects of suspension-feeding bivalves greatly depend upon the knowledge of their morphology. *Limnoperna fortunei* morphology has been described in Morton [17]. Additionally, Paolucci and colleagues [39] reported the association between genetic variability and macro- and micro-structural morphology of *L. fortunei* populations across South America. However, few information about the ultrastructure of the golden mussel gills is available thus far. In this current work, for the first time, we characterized the ultrastructure of the gills epithelium of adult *L. fortunei*. These results will assist us to better understand the morphological aspects of the gills, which are vital for respiration and feeding.

Results

Gills microstructure

The *L. fortunei* gills of adult individuals have a large surface area fitting the mantle cavity space. Each pair of gills has a leaf-like shape (Fig. 1) and is located at both sides of the viscera. Each gill comprises two demibranchs, known as inner- and outer- demibranchs, in a double lamellar structure joined by the gill axis (Fig. 2a). Each demibranch has nearly 75 filaments. Ventrally, the outer demibranch is longer than the inner, but it shortens laterally, close to the labial palps (Fig. 1).

At the margins of the frontal surface of each filament, different ciliary projections were observed: lc and lfc, and, on the frontal surface, fc (Figs. 1, 3, 4 and 5 and Additional file 1). Each laterofrontal cirrus has approximately 18-28 pairs of cilia (see Additional file 1). Ciliary discs (cd) were observed at the lateral surface of the filaments (Fig. 3), measuring approximately $16 \times 10 \mu\text{m}$ and cross-connecting individual filaments. TEM images showed that lc, lfc, and fc have the type 9+2 axoneme microtubule-based cytoskeleton (Additional files 1, 2 and 3, Figs. 6 and 7). Pro-laterofrontal cirri (p-lfc) could not be observed between the lfc and fc in the SEM and TEM images. Several adhering particles ($<15 \mu\text{m}$) could be observed on the frontal surface of the filaments (Fig. 3). A larger particle (nearly $20 \mu\text{m}$) could be observed at the lateral tract (Fig. 3) and several smaller particles were

observed attached to the lc and lfc (Fig. 3c-d). The smallest particles (200-300 nm) were found to be spherical vesicles and clearly seen on TEM images (Fig. 7b-c, Additional files 1 and 2). Particles of almost $4\text{-}5 \mu\text{m}$ are probably the size of algae cells.

Gills ultrastructure

Light microscopy (LM) images show transverse and longitudinal sections of gill filaments (Fig. 4). The lc, lfc and fc can be clearly observed in the transverse section (Fig. 4a-b). Based on the combined alcian blue and periodic acid Schiff (AB-PAS) staining, we could observe the presence of different types of mucocytes in the gills filaments sections. Acid and neutral mucopolysaccharides were also observed. Larger amounts of neutral mucopolysaccharides (NMPS) were found at the apex of the frontal surface (Fig. 4c-d - stained in pink), while acid mucopolysaccharides (AMPS) were found, in small numbers, spread out in the whole filament (Fig. 4c-d - stained in blue).

TEM image of the transverse section of one filament showed many ciliated epithelial cells (see Additional file 6). Backscattered electron (BSE) SEM images of the longitudinal section of filaments are shown in Fig. 5, with an inverse contrast resembling TEM images. At the dorsal part of the filament epithelium, the basal membrane is smooth (Fig. 5 and Additional file 2). It is supported by a collagenous structure, which also surrounds the hemolymph vessel (Fig. 5). Close to the marginal food groove, a V-shaped collagenous structure could be observed (Fig. 5a). It is apparent that the central hemolymph vessel has no collagenous supporting structure, apart from the marginal food groove. Hemocytes were observed in the central hemolymph (Fig. 5a-b), while more elongated hemocytes could be observed in the region below the basal epithelium (Fig. 5a-c). Three types of cells were observed, Two of them (cells I and II) located at the apical epithelium and the other (cell III) at the basal region (Fig. 5c and Additional file 7). The cell I narrows at the apex of the epithelium and has an elongated dark nucleus that occupies a large volume in the cell and contains more dispersed heterochromatin. Each laterofrontal cirrus arises from a single cell I, as can be seen in the 3D model (see Additional file 7). In between these cells, we could observe the cell II, which has a goblet shape also with an elongated dark nucleus, but with less dispersed heterochromatin. Cell II enlarges at the apex of the epithelium and possesses microvilli, $880 \pm 150 \text{ nm}$ long (Fig. 5c Additional file 7). The microvilli were also observed on the surface of the lateral tract of the filaments, below the lc around the cd (Fig. 3b-c). Numerous mucins were observed in the cells II (Additional file 8). The cells III have a lobed bright nucleus and were mostly found

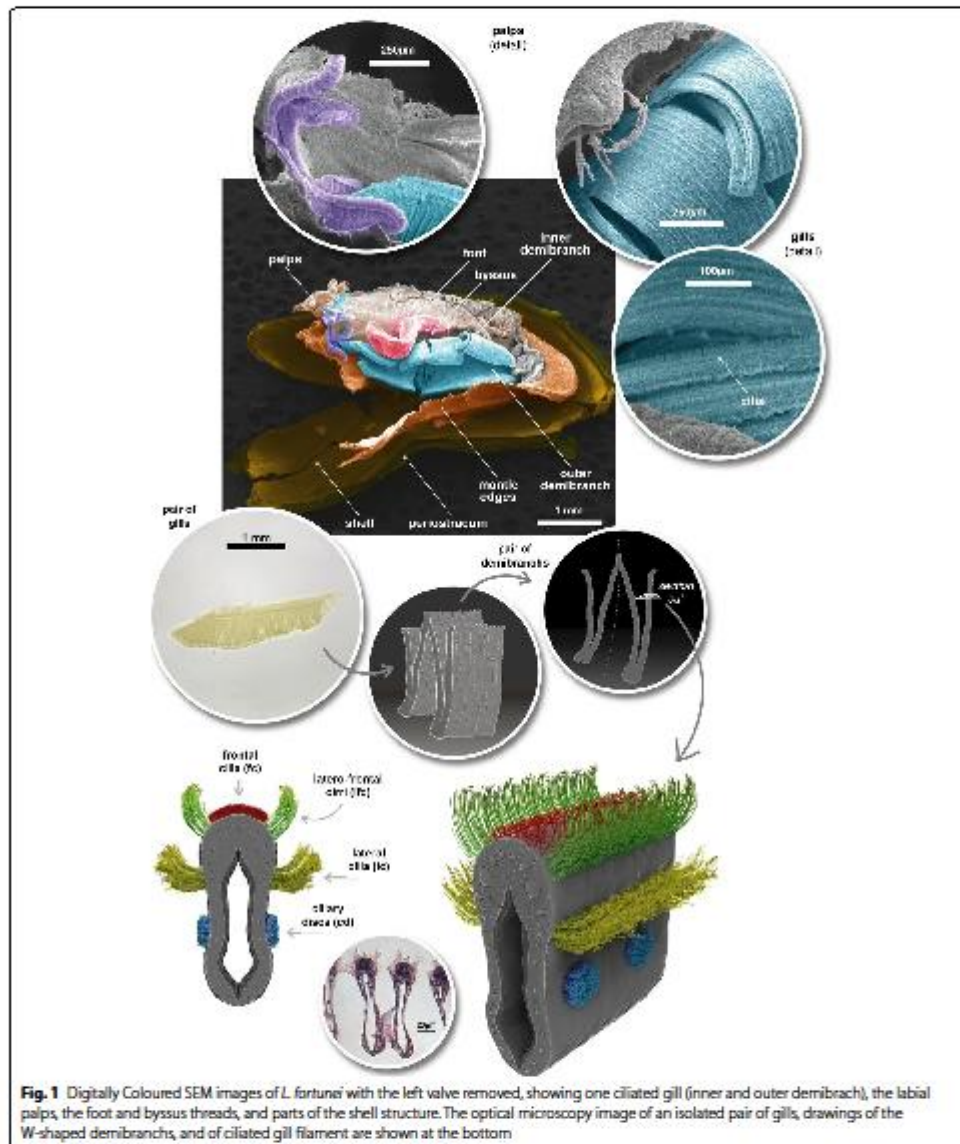
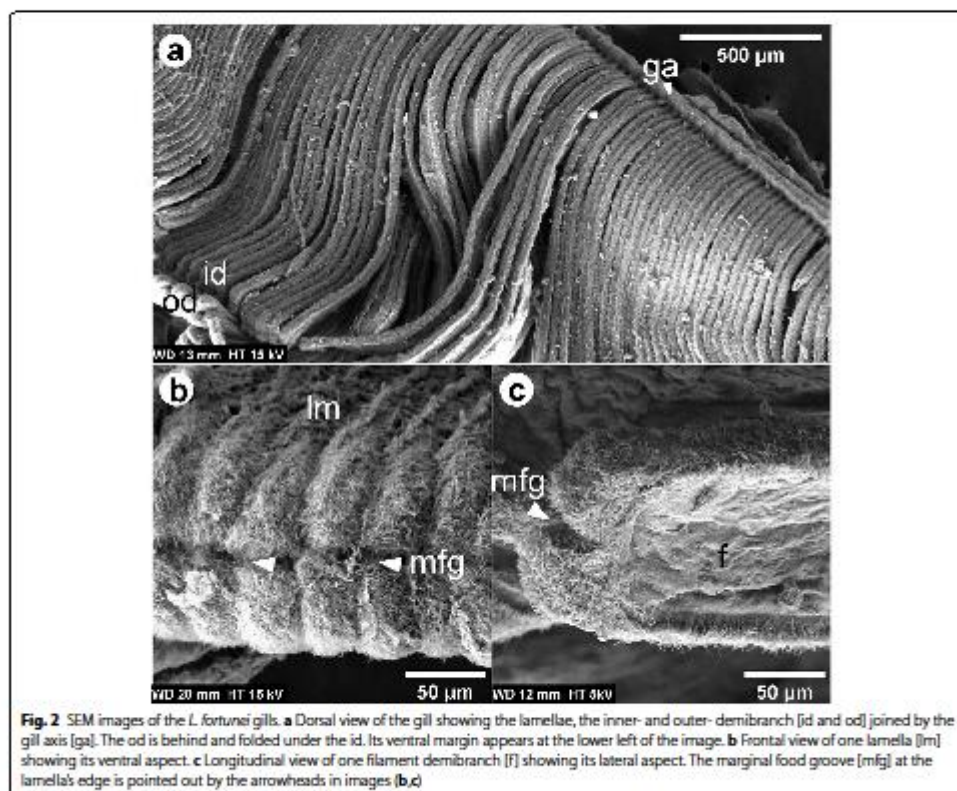


Fig. 1 Digitally Coloured SEM images of *L. fortunei* with the left valve removed, showing one ciliated gill (inner and outer demibranch), the labial palps, the foot and byssus threads, and parts of the shell structure. The optical microscopy image of an isolated pair of gills, drawings of the W-shaped demibranchs, and of ciliated gill filament are shown at the bottom

present at the basal epithelium (Figs. 4d and 5c). Vacuoles occupy a large volume of epithelium and interconnect the basal membrane to the apical region (Fig. 5c).

Gill epithelial cells are shown in Figs. 6 and 7. In Fig. 6a, some fc lay longitudinally to the demibranch filament, suggesting that the fc are stiffer in that

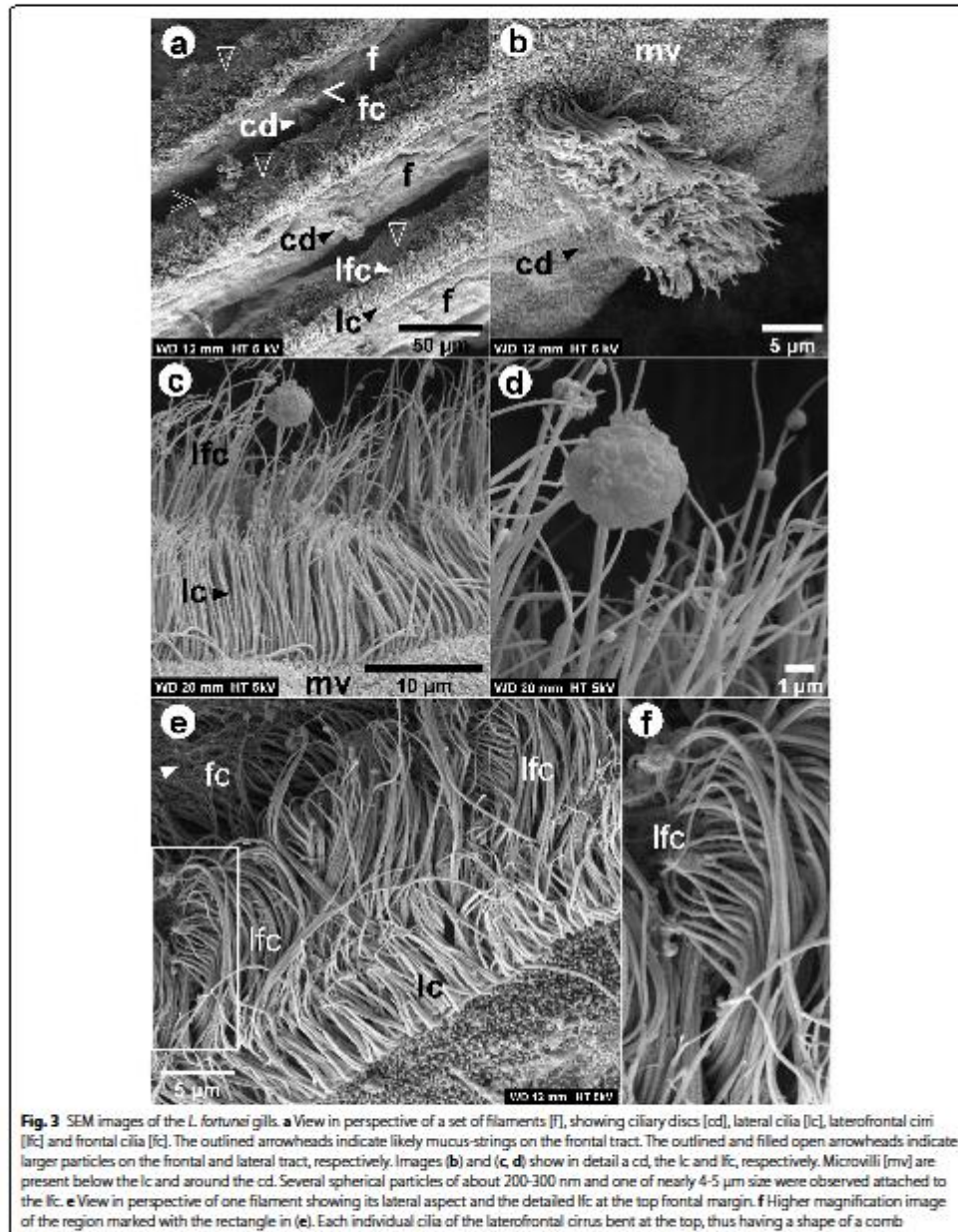


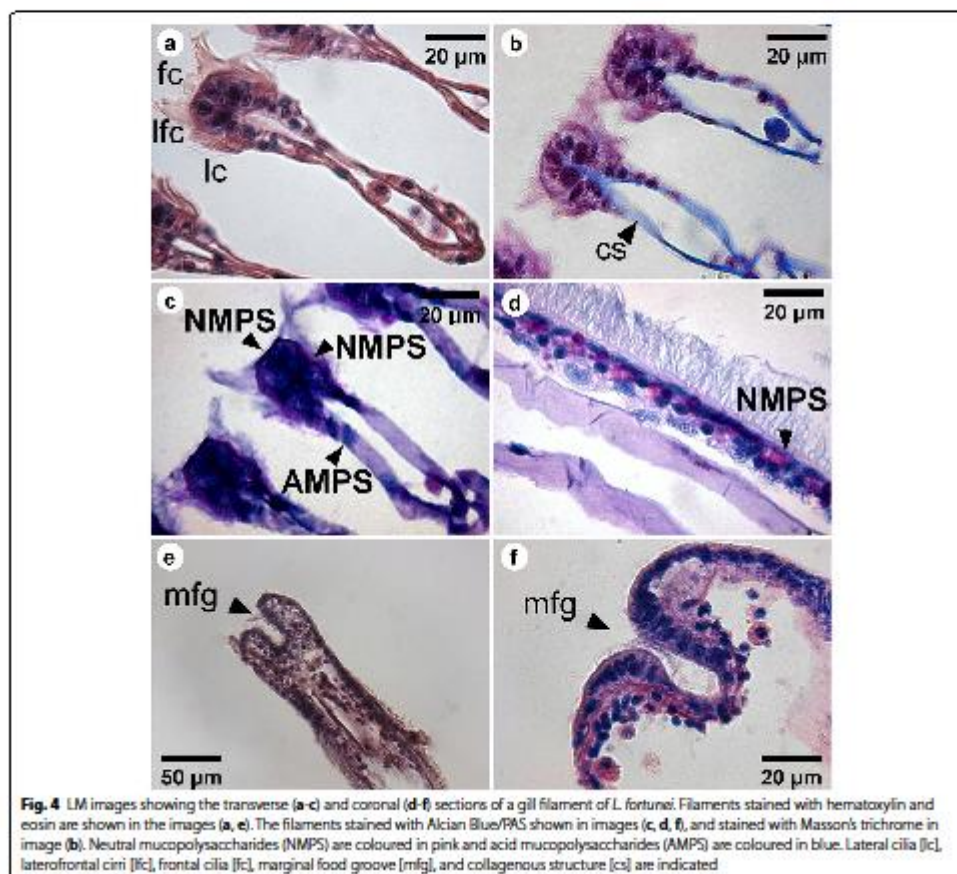
portion of the filament, as also observed in Fig. 3c and Additional file 5. In Fig. 6c, the fc were observed in cross-section, which means most of them are bent. Many mitochondria could be observed, mainly in the region close to the insertion site of gill cilia (Fig. 6c-d), while the smooth endoplasmic reticulum could be found in the apical region (Fig. 6d). Surrounding the smooth reticulum, we could also observe several nearly 70 nm electron dense glycogen granules (Fig. 6d). Cell junctions could clearly be seen in the portion of the epithelium observed in TEM images (Figs. 6 and 7) and several septate junctions were observed adjacent to the region with glycogen granules and smooth endoplasmic reticulum (Figs. 6d and 7b-d). In addition, numerous vesicles (201 ± 29 nm), possibly containing mucus, could also be observed in this region (Figs. 6b-c and 7c-d).

Discussion

In this work, we have characterized the ultrastructure of the mucociliary epithelium of *L. fortunei* gills in order to describe the cellular traits of this important biological structure, mainly responsible for feeding and respiration. The gills of suspension feeders are in direct contact with the environment and understanding their morphology is fundamental to the establishment of new strategies to manage this invasive species in the environment.

Adult gills size from the specimens used in the present work did not significantly differ from the population of *L. fortunei* studied by Paolucci and colleagues [39]. In this work, we could observe a slightly longer mean cilia length of fc of the Volta Grande (VG) specimen, and a slightly lower mean of filament width for the Paranaíba river (PR) one, both compared with *L. fortunei* populations of South America [39]. Morphometric





differences found for both VG and PR specimens might be due to different environmental conditions in which they had grown and adapted to.

Classically, the two main functions of the gills in bivalves are feeding and respiration. The thin structure of the gill epithelium may allow the exchange of gases such as oxygen and carbon dioxide by passive diffusion, in response to partial gas pressures. Also, it allows ion exchange between the external environment and the hemolymphatic vessels [40]. The observed microvilli at the apical pole of goblet cells of *L. fortunei* are now evidence that gills might also present a trophic function. The outermost gill epithelium might have a large surface area due to the microvilli, which may assist the

direct uptake of dissolved or particulate organic matter. This trait was also suggested for the bivalve *Placopecten magellanicus* (Gmelin 1791) [41, 42]. Furthermore, these cells present vacuoles interconnecting the apical region to the basal membrane of the epithelium, which suggests that transport and diffusion of nutrients might be occurring [42]. We also found endoplasmic reticulum and Golgi complex, organelles that produce and excrete mucus in the goblet cells. These cells look similar to the ones found in *M. edulis* [43] and *P. magellanicus* [42]. As described for the Brazilian endemic bivalve *Diplodon expansus* (Küster 1856) [44], the production of mucus in this apical region of the gills might be associated with lubrication, in order to reduce the frictional resistance

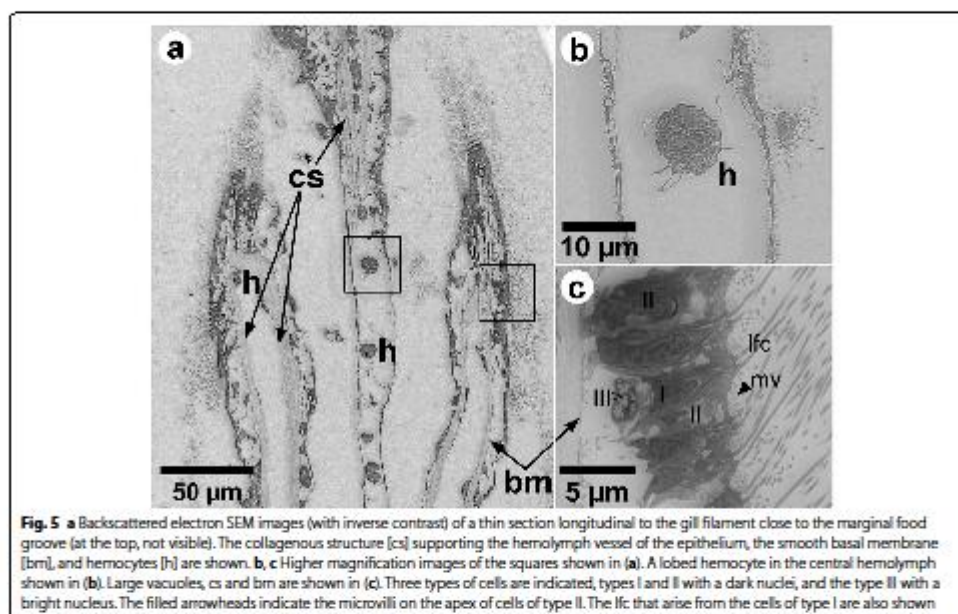
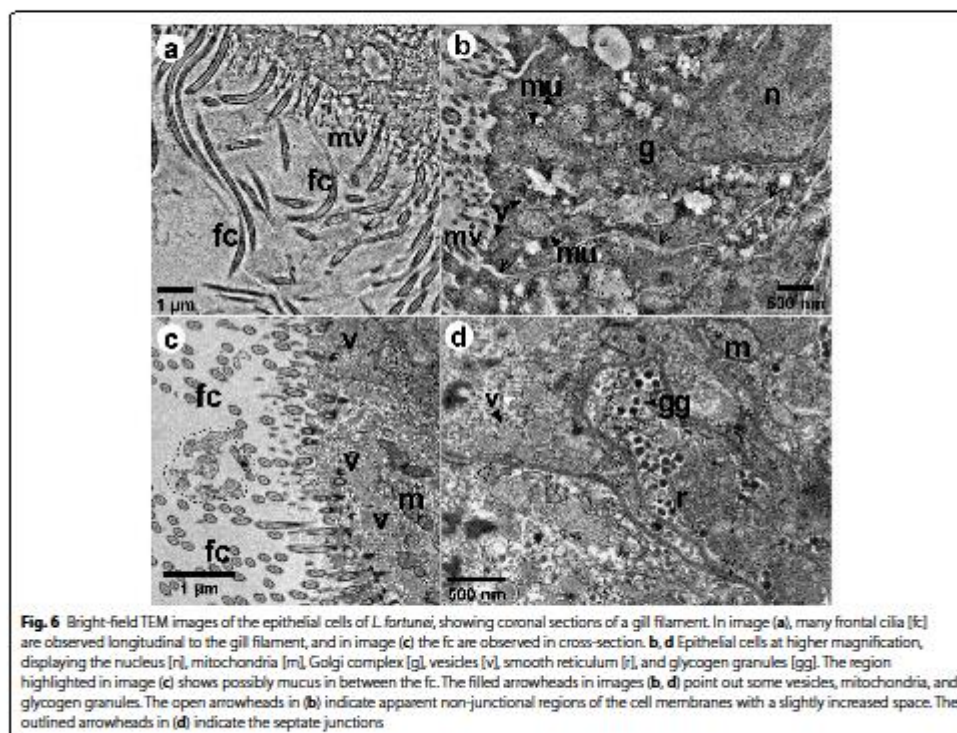


Fig. 5 **a** Backscattered electron SEM images (with inverse contrast) of a thin section longitudinal to the gill filament close to the marginal food groove (at the top, not visible). The collagenous structure [cs] supporting the hemolymph vessel of the epithelium, the smooth basal membrane [bm], and hemocytes [h] are shown. **b, c** Higher magnification images of the squares shown in **(a)**. A lobed hemocyte in the central hemolymph shown in **(b)**. Large vacuoles, cs and bm are shown in **(c)**. Three types of cells are indicated, types I and II with a dark nuclei, and the type II with a bright nucleus. The filled arrowheads indicate the microvilli on the apex of cells of type II. The lfc that arise from the cells of type I are also shown

in water flow along the epithelium. In *D. expansus*, the mucus layer is highly viscous and difficult to hydrate, ensuring the efficiency of the mucus as a lubricant. The mucus associated with the ciliary tracts might change the local fluid mechanical properties and, in fact, only a small amount of mucus is needed for the viscosity of the medium transport [45]. It is unlikely that captured particles can be kept in this confined local current produced by the cilia beating without the intervention of mucus in mytiloids homorhabdic gills [36, 46]. Particles covered by intermediate-viscosity mucus are transported close to the frontal gill epithelium in *M. edulis*, in such enclosed space [32, 44]. Our own results are evidence of that in *L. fortunei*. Numerous vesicles, mucus and likely mucus strings were observed in the fc tract of *L. fortunei*. The LM images of sections stained with AB-PAS showed mixed-secreted (neutral and acid) mucopolysaccharide in the gill filaments, with NMPS being abundant on the frontal surface of the filaments. This result corroborates other studies in *M. edulis* [45] and in the oyster *Crassostrea gigas* (Thunberg 1793) [47]. The particles bound to NMPS or mixed (acid + neutral) mucopolysaccharides are transferred to the marginal groove by the frontal cilia and then transported to the labial palps, where they are sorted and either ingested or rejected as pseudofeces.

The mechanisms of particle capture and their transport in suspension-feeding molluscs are almost exclusively ciliary dependent. The lc are responsible for pumping water through the gill interfilament channels towards the suprabranchial cavity [24, 27, 42]. One of the functions of the lfc in Mytilidae and Pectinidae is ascribed to the particle capture [13, 22, 24, 27], which is accomplished by the lfc [27, 28], or through currents produced as the lfc beat against the main water current [24]. Captured particles are then transported towards the marginal food groove by the action of fc, which seems to be autonomous mechanical processes. However, *in vivo* endoscopic observations in many bivalves have shown that the transportation of particles depends either on mucociliary and hydrodynamic mechanisms [25, 26]. Particle rejection or ingestion, on the other hand, is based on physicochemical interactions that can be sensed in the labial palps [13, 42].

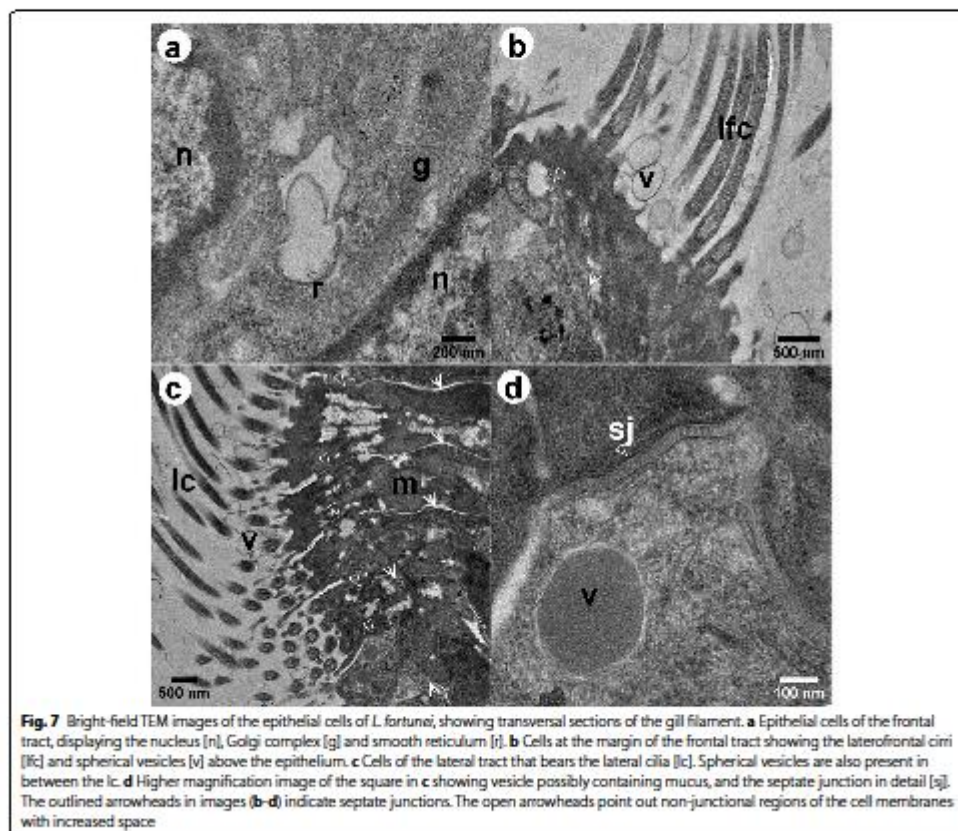
Particle selection mechanism is not fully resolved. Some works show that it depends on particle characteristics such as size, shape and surface properties, which affect their ingestion or rejection [37, 38]. Rejected particles are bound to cohesive mucus, deposited in specific sites of the mantle and then transported to the cilia, for their expulsion as pseudofeces [25, 48]. Additionally, the mucus covering feeding organs might mediate particle



selection [13, 33, 49]. For *P. magellanicus*, it has been shown that reduced mucus-particles viscosity are more likely to be ingested, while high viscosity mucus-particles are more likely rejected (AMPS) [49]. Our own results show evidence that the mucus produced and excreted in the gills epithelium also plays a role in the mechanism of particle capture itself.

Our data suggested that the mucus in *L. fortunei* gill filaments might be correlated to the fc beating. A larger number of mucus-containing vesicles in the epithelium cells were observed when the fc were bent and, conversely, less mucus-containing vesicles were observed when fc were stiffer, being longitudinal to the gill filament. Such correlation is rather difficult to ensure based on images of TEM sections only and it would need to be investigated by volume electron microscopy. TEM images suggested that the mucus are packed and sent to the apical region. Indeed, we observed mucus and spherical vesicles above the epithelial cells in between the fc and lfc and also mucus covering a food particle. This might be an ongoing process, in which the mucus carried

by vesicles towards the gill cilia might be available to interact with the surface of an upcoming particle that will be captured and further transported to the labial palps to be physicochemically sensed and discriminated [13, 42], and then rejected or selected by the feeding organs [13]. The mucus produced by epithelial cells is modified by the Golgi complex, near the nucleus, playing a key role in sorting newly synthesized and recycled molecules towards their final destinations [50], the apical region of the epithelium. TEM images also showed mitochondria with extensive lamellar cristae, arranged in parallel juxtaposed sheets that occupy most of the organelle volume, which is common of high energy-demanding tissues [51] such as the gill ciliary epithelium [52]. The smooth reticulum was also present and among several cellular functions, it participates in glycogen metabolism [53]. The glycogen granules are important components for the bivalve metabolism [54]. Indeed, several septate junctions were observed interconnecting the cell rich in mucus vesicles to the cell where glycogen granules and smooth reticulum were observed. The presence of the septate



junctions in this portion of the epithelium is evidence of the active intercellular communication and transport of molecules between them [55, 56]. This energetic apparatus is related to the morpho-functional structure of the ciliary epithelium and its analysis allowed us inferring the correlation between the mucus in gill filaments to the beat of the cilia. Such correlation is quite hard to confirm by single TEM sections, though. This would require a 3D reconstruction of the ciliary epithelium at high spatial resolution. This will be further investigated by volume electron microscopy techniques, to better understand such dynamical processes as this.

Conclusions

Understanding the *L. fortunei* morphology is the first step towards the establishment of strategies to control this invasive species and, to the authors' knowledge, this is the first time high-resolution ultrastructure of *L. fortunei* gills epithelium have been reported. Our data showed the microstructure of the gill filaments and cilia in high spatial resolution and also evidence of the production and release of mucus and spherical vesicles in ciliary cells. This might have implications to the process of selection and discrimination of particles to be ingested or rejected by mussels.

Methods

Gills preparation

Specimens of adult *L. fortunei* were collected in February 2019 in the fish farming reservoir of the Volta Grande (VG specimen), on the border between the states of Minas Gerais and São Paulo, Brazil (20°01'54.0"S, 48°13'10.0"W), where measured water parameters were 29.2 °C, pH 7.5, dissolved oxygen 3.2 mg L⁻¹, and turbidity 0.1 NTU. Specimens were packed in cloth bags (to decrease overlapping individuals) and during transport, they were submerged in water at constant aeration. In the laboratory at the *Centro de Bioengenharia de Espécies Invasoras de Hidrelétricas* (CBEIH), nearly 200 animals were acclimated for 3 weeks in an aquarium with 36 L capacity containing artesian water well, pH 7.7, dissolved oxygen 6.8 mg L⁻¹ and turbidity 1.68 NTU, at constant aeration and temperature of 18 to 20 °C to minimize stress. After acclimation, the molluscs were kept under the same conditions and temperature of 22 ± 1 °C.

Light microscopy

Adult *L. fortunei* specimens (n=10) were taken out of the aquarium and immersed in Bouin's fixative for 24 h. After this, the gills were dissected, dehydrated in a progressive series of ethanol, cleared in xylene and then embedded in paraffin. Longitudinal and transverse histological sections of the gills were cut with 5 µm thickness, using a MRS 3500 Microtome. Sections were dewaxed in xylene, hydrated in graded ethanol and stained accordingly: to determine the general structure of gills filaments, sections were stained with hematoxylin-eosin [57]; to demonstrate the existence of polysaccharides, periodic acid Schiff (PAS), combined with alcian blue (AB), at pH 2.5, were used [58], which allowed us differentiating between neutral (stained pink) and acid polysaccharides (stained blue). In addition, the Masson's trichrome method [59] was used to allow the identification of structures that had connective tissue.

Electron microscopy

For the purpose of this work, an adult specimen, with a shell length of approximately 1.5 cm long, was taken out of the aquarium so its valves could be kept partially open with the help of a short piece of metal (1 mm diameter). Next, the specimen was rapidly submerged in a 1.5 mL Eppendorf® tube, filled with modified Karnovsky fixative solution (2% paraformaldehyde and 2.5% glutaraldehyde), and incubated for 3 days. The valves were then carefully opened and the gills dissected using forceps, to further process for scanning electron microscopy (SEM) and transmission electron microscopy (TEM). Dissected

gills were placed into 1.5 mL Eppendorf® tubes containing phosphate buffer solution (PBS). In this present work, we also used unreported TEM and SEM data of the gills from another pristine adult specimen that was collected in Paranaíba river (PR), downstream the confluence with Barreiro's river, near the municipality of Paranaíba (Mato Grosso do Sul, Brazil). Sample preparation details about this latter specimen can be found in Andrade et al. [8]. The two specimens used in the work were named after the place they were collected, as VG and PR specimens.

Scanning electron microscopy (SEM)

Immediately before the secondary fixation, PBS excess volume was first removed and replaced by an appropriate volume of a fresh PBS and incubated for 10 min. This washing process was performed three times. PBS was then replaced by an appropriate volume of 1% osmium tetroxide (OsO₄) in PBS (pH 7.3 ± 0.1) in the fume hood and incubated for 1 h in darkness and room temperature (RT). The sample was washed with PBS and incubated for 10 min, three times. Excess PBS was removed and replaced by 1% tannic acid (C₇₆H₅₂O₄₆) solution and incubated for 20 min at RT. After washing with PBS three times, the solution was replaced by 1% OsO₄ solution and incubated for 1 h in darkness and RT. The samples were then washed in distilled water three times and dehydrated in a sequence of alcohol solutions (35%, 50%, 70%, 85%, 95% and 100%), 10 min each. The last step with absolute alcohol was performed twice. The sample was critical point dried with CO₂ (using a Leica EM CPD 030), placed on an aluminium SEM stub with a carbon tape and finally coated with gold nanoparticles (5 nm thickness) in a sputter coater (Bal-tec MED 020). The VG sample was analysed in a field emission scanning electron microscope (FEI Quanta 200), operated at 5 kV and 15 kV.

Transmission electron microscopy (TEM)

For TEM analysis, samples were firstly washed three times in PBS, for 10 min each time. PBS was replaced by 2% OsO₄ in PBS (pH 7.3 ± 0.1) and incubated for 2 h in darkness at RT. Samples were then washed with deionized water four times, for 10 min each time. Distilled water was then replaced by 2% uranyl acetate (C₄H₈O₆U) solution and incubated overnight at 6°C in darkness. Samples were again washed with deionized water, three times, for 5 min each, followed by dehydration in a sequence of alcohol solutions (35%, 50%, 70%, 85%, 95% and 100%). Absolute alcohol was replaced by acetone and incubated for 20 min. Acetone was then replaced by Epon™ resin in three steps, using different dilutions of acetone in resin (2:1, 1:1, and 1:2). In each of these three

steps, the tube was enclosed and homogeneously agitated (using a Norte Científica NH2200) for at least 2 h. After drying the excess acetone/resin with a filter paper, samples were transferred to a new polypropylene tube containing Epon™ resin prepared with DMP-3 (Sigma Aldrich) and incubated at 40°C for 1 h. Samples were carefully embedded to obtain longitudinal sections of the lateral surface of the gills' filament. Ultrathin Sect. (60 nm) were obtained using an ultramicrotome (Leica EM UC6) and a diamond knife Ultra 45* (Diatome), with the sections being transferred to C-film Cu-TEM grids. Series of ultrathin Sect. (100 nm) array was also obtained and deposited in a clean silicon wafer. The surface of the silicon wafer was previously glow discharged so to become more hydrophilic. Sections were post-stained using a 2% uranyl acetate and lead citrate. TEM analysis was performed in a thermionic W-filament transmission electron microscope (FEI Tecnai Spirit G2-12 BioTwin), operated at 120 kV. SEM and TEM samples preparations and their analysis were performed at the Center of Microscopy at the Universidade Federal de Minas Gerais (UFMG).

Structural analysis

The micro-morphological analysis of the *L. fortunei* gills structure was performed using SEM images. Electron microscopy of thin sections was used to describe the ultrastructural morphology of the ciliary gill epithelium. When suitable, measurements of the gill filaments were performed using transmitted light microscopy images (Additional file 4), taken in a Leica DM4500 microscope, with the same plastic embedded blocks for TEM preparation. Filament width, interfilament space, and filament linear density (number of filaments per linear distance) were obtained from SEM images. Data are shown in the Additional file 9. Cilia length was obtained in SEM images and the cilia diameter and linear density (number of cilia onto the filament over the linear distance along the filament) using the TEM images. Measurements were performed using the free software Fiji / ImageJ v. 1.52p (Wayne Rasband - National Institutes of Health, USA) and the DigitalMicrograph® v. 3.41.2916.1 (Gatan, Inc).

Abbreviations

3D: Three dimensional; AB-PAS: Alcian blue and periodic acid Schiff; AMPS: Acid mucopolysaccharides; BSE: Backscattered electron; CBEIH: Centro de Biogenharia de Espécies Invasoras da Hidrolétricas; cd: Ciliary discs; fc: Frontal cilia; lc: Lateral cilia; lf: Laterofrontal cilia; LM: Light Microscopy; NMPS: Neutral mucopolysaccharides; PBS: Phosphate buffer solution; p-lf: Pro-laterofrontal cilia; PR: Paranaíba river; SEM: Scanning Electron Microscopy; TEM: Transmission Electron Microscopy; VG: Volta Grande.

Supplementary Information

The online version contains supplementary material available at <https://doi.org/10.1186/s40850-022-00107-y>.

- Additional file 1.** TEM bright field images showing coronal section of a filament of *L. fortunei*'s gill. The laterofrontal cilia (lf) are shown in cross-section view.
- Additional file 2.** Montage of TEM bright field images showing longitudinal view of the whole gill epithelium. Legend: cs - collagenous supporting structure, n - nucleus, vc - vacuoles, mu - mucin, mw - microvilli, lf - laterofrontal cilia, fc - frontal cilia, v - vesicle.
- Additional file 3.** TEM bright field images showing the detail microtubule cytoskeleton of laterofrontal cilia in cross-section (c) and longitudinal (b) views.
- Additional file 4.** Transmitted light microscopy of the plastic embedded block of the mussel gill in Volta Grande (VR) specimen.
- Additional file 5.** SEM images of the frontal and lateral tract of gill filament. The white arrowhead points a 4-5 µm particle on the frontal tract. Legend: ms - mucus string, fc - frontal cilia, lf - laterofrontal cilia, cd - ciliary discs.
- Additional file 6.** Montage of bright-field TEM images of a thin section transversally to a gill filament of *L. fortunei* showing its frontal portion. Lateral cilia (lc), laterofrontal cilia (lf), and frontal cilia (fc) are observed in cross-section view. Spherical vesicles (v), vacuoles (vc), the collagenous structure (cs) of the hemolymph, and a hemocyte (h) are indicated.
- Additional file 7.** Three dimensional reconstruction of a portion of the *L. fortunei* gill epithelium showing three different types of cells. Cell I shows a colored green nucleus and bears the laterofrontal cilia (in light gray). Cell II shows a colored orange nucleus. It possesses microvilli (in red) and is positioned in between cell I. Cell III shows a colored dark green and is located at basal region of the epithelium. Spherical vesicles are located inside cell II (in yellow) and outside (in beige). The reconstruction was carried out by serial-sectioning array BSE-SEM images and using the Free-D software: Andrey P, Maurin Y. (2005). *J Neurosci Methods*. 145(1-2):233-44. doi:10.1016/j.jneumeth.2005.01.006.
- Additional file 8.** Bright-field TEM images showing coronal thin section of the gill epithelium of *L. fortunei*. The laterofrontal cilia (lf) are shown in cross-section view. Mucins (mu) and vacuoles (vc) are observed in the cells that possess microvilli (mw). Spherical vesicles (v) are present close to the lf and septate junctions (sj) and nuclei (n) are indicated.
- Additional file 9.** Measurements of the gills structure variables (mean ± standard deviation) of the Volta Grande (VG) and Paranaíba River (PR) specimens. Errors were estimated from measurements performed in different parts of the image.

Acknowledgements

This work was supported by the Companhia Energética de Minas Gerais (Cemig) GT/ANEEL R&Ds GT-0604. Erico T. F. Freitas received a scholarship from the Universidade Federal de Ouro Preto / Cemig GT S.A. Erika C. Jorge received a scholarship from Conselho Nacional de Desenvolvimento Científico e Tecnológico (CNPq). Authors are grateful for the support given by Mr. Renato Brito and Mrs. Kally Carneiro at the CBEIH laboratory, and by Mrs. Altair Mendes dos Santos, Mrs. Flávia Kelly Moreira da Silva, and Mrs. Marlene Lúcia de Oliveira for the sample preparation assistance at the Center of Microscopy at UFMG. This work is dedicated to the memory of Brian Morton (1942-2021), professor emeritus of marine ecology, The University of Hong Kong.

Authors' contributions

Mr. EFFF performed the electron microscopy analyses and compiled the data. Ms. AMSM collected the samples at the CBEIH laboratory and did the pre-fixation. Mr. EFFF, Ms. AMSM, and Mr. RSdP contributed to the data analysis and to the written part of the manuscript. Ms. GRA helped in the image treatment, manuscript review and agreed to give non-published electron microscopy images of *L. fortunei* gills she investigated earlier. Professor Mr.

PSA, the coordinator of the R&D Annel/Cernig GT-604, contributed to the design of the work. Professor Mr. AVC, the research group leader, had the idea of studying the *L. fortunei* gills and revised this manuscript. Professor Mrs. ECJ did the throughout review of the manuscript. Professors PSA, AVC, ECJ, and Mrs. MDdC provided useful insights to the work. All the authors read and approved the manuscript.

Funding

This work was supported by Agência Nacional de Energia Elétrica (Anel) / Cernig-GT SA, under the Project GT-604. The funder supported the CBEH laboratory infrastructure and all the experiments performed to carry out this work.

Availability of data and materials

The datasets used and analysed during the current study are available from the corresponding author on reasonable request.

Declarations

Ethics approval and consent to participate

The experiments have been conducted in compliance with the Brazilian law nº 11.794, of 08/10/2008, (available at http://www.planalto.gov.br/ccivil_03/_ato2007-2010/2008/lei/l11794.htm), that concerns laboratory and field experiments involving animals and following the orientation of the Ethical Committee of the Universidade Federal de Minas Gerais (UFMG), which follows the Brazilian regulations on the matter (available at <https://www.ufmg.br/bioetica/ceua/>). The law ruling the animal experiment is concerned about those animals pertaining to the Phylum Chordata and the subphylum Vertebrata. For all the other cases, the submission of the proposal to the above-mentioned ethical committee is waived. Even though there are no specific rules about experiments using Invertebrates, our work was carried out in compliance with International standards in ethical research and recent scientific concerns, as those expressed in Driukwater et al. (*Methods Ecol Evol*, 2019, 10(8):1265–1273. doi:<https://doi.org/10.1111/2041-210X.13208>), and ASAB (*Animal Behaviour*, 2020, 159:1–XL. doi:<https://doi.org/10.1016/j.anbehav.2019.11.002>). Our experiments were performed using adult *L. fortunei* specimens (which are molluscs of the class Bivalvia). The collection, transport and maintenance of the molluscs in the laboratory have been authorized by the environmental agency ICMBio, linked to the Ministry of the Environment under code 72222-2 (and can be accessed in <https://drive.google.com/file/d/15VsAic1gh7wzr1m7pywU9JhEwX0deMGQ/view?usp=sharing>).

Consent for publication

Not applicable.

Competing interests

We declare no competing interests.

Author details

¹Centro de Biongenharia de Espécies Invasoras de Hidrelétricas (CBEH), 31035-536 Belo Horizonte, MG, Brazil. ²Centro de Microscopia, Universidade Federal de Minas Gerais (UFMG), 31270-901 Belo Horizonte, MG, Brazil. ³Universidade Federal de Ouro Preto (UFOP), FIMAT, 35400-000 Ouro Preto, MG, Brazil. ⁴Instituto de Ciências Biológicas, Universidade Federal de Minas Gerais (UFMG), 31270-901 Belo Horizonte, MG, Brazil. ⁵Companhia Energética de Minas Gerais SA (CEMIG), 30190-131 Belo Horizonte, MG, Brazil. ⁶Escola de Design, Universidade do Estado de Minas Gerais (UEMG), 30140-091 Belo Horizonte, MG, Brazil.

Received: 17 September 2020 Accepted: 31 December 2021

Published online: 17 January 2022

References

- Fernandes FdC, Mansur M, Pereira D, Fernandes L, Campos S, Danielos O. Abordagem conceitual dos moluscos invasores nos ecossistemas límnicos brasileiros. In: Mansur MCD, Santos CPd, Pereira D, Paz ICP, Zurita MLL, Rodriguez MTR, Nehrka MV, Bergonci PEA, organizadores. Moluscos límnicos invasores no Brasil: biologia, prevenção, controle. Porto Alegre: Redes Editora; 2012. pp. 61–74.

- Ituarte C. Primera noticia acerca de la Introducción de pelecipodos asiáticos en el área rioplatense (Mollusca: Corbiculidae). Neotropica. 1981;27(77):79–82.
- Darrigran G, Pastorino G. Bivalvos Invasores en el Río de la Plata, Argentina. Comun Soc Malacol Urug. 1993;7:309–13.
- Xu M. Distribution and spread of *Limnoperna fortunei* in China. In: *Invasive nature – Springer series in invasion ecology*. Springer; 2015. doi:https://doi.org/10.1007/978-3-319-13494-9_17.
- Oliveira MD, Campos MC, Paolucci EM, Mansur MC, Hamilton SK. Colonization and spread of *Limnoperna fortunei* in South America. In: *Invasive nature – Springer series in invasion ecology*. Springer; 2015. doi:https://doi.org/10.1007/978-3-319-13494-9_19.
- Ulliano-Silva M, Americo JA, Brindairo R, Dondoro F, Prosdociimi F, de Freitas Rebelo M. Gene discovery through transcriptome sequencing for the invasive mussel *Limnoperna fortunei*. PLoS One 9. 2014; doi:<https://doi.org/10.1371/journal.pone.0102973>.
- de Andrade JTM, Cordleiro NIS, Montresor LC, da Luz DMR, de Faria Viana EM, Martinez CB, Vidigal THDA. Tolerancia de *Limnoperna fortunei* (Dunker, 1857) (Bivalvia: Mytilidae) to aerial exposure at different temperatures. Hydrobiologia. 2020. doi:<https://doi.org/10.1007/s10750-020-04191-4>.
- Andrade GR, de Araújo JLF, Nakamura Filho A, Guarabens AC, Carvalho MDd, Cardoso AV. Functional Surface of the golden mussel's foot: morphology, structures and the role of cilia on underwater adhesion. Mat Sci Eng C. 2015. doi:<https://doi.org/10.1016/j.msec.2015.04.032>.
- Nakamura Filho A, Almeida ACd, Riera HE, Araújo JLFd, Gouveia VJP, Carvalho MDd, Cardoso AV. Polymorphism of CaCO₃ and microstructure of the shell of a Brazilian invasive mollusc (*Limnoperna fortunei*). Mater Res. 2014. doi:<https://doi.org/10.1590/S1516-14392014005000044>.
- Sylvester F, Dorado J, Boltovskoy D, Juárez Á, Cataldo D. Filtration rates of the invasive pest bivalve *Limnoperna fortunei* as a function of size and temperature. Hydrobiologia. 2005. doi:<https://doi.org/10.1007/s10750-004-1322-3>.
- Waykar B, Deshmukh G. Evaluation of bivalves as bioindicators of metal pollution in freshwater. Bull Environ Contam Toxicol. 2012. doi:<https://doi.org/10.1007/s00128-011-0447-0>.
- Schäyon M, Allan II, Ruus A, Håvardstun J, Hjørnmann D, Bøyer J. Comparison of caged and native blue mussels (*Mytilus edulis* spp.) for environmental monitoring of PAH, PCB and trace metals. Mar Environ Res. 2017. doi:<https://doi.org/10.1016/j.marenvres.2017.07.025>.
- Ward JE, Rosa M, Shumway SE. Capture, ingestion, and egestion of microplastics by suspension-feeding bivalves: a 40-year history. Anthropolocene Coasts. 2019. doi:<https://doi.org/10.1139/anc-2018-0027>.
- Di Fiori E, Pizarro H, dos Santos Afonso M, Cataldo D. Impact of the invasive mussel *Limnoperna fortunei* on glyphosate concentration in water. Ecotox Environ Safte. 2012. doi:<https://doi.org/10.1016/j.ecoenv.2012.04.024>.
- Vargas RPF, Saad JF, Graziano M, dos Santos Afonso M, Izaguirre I, Cataldo D. Bacterial composition of the biofilm on valves of *Limnoperna fortunei* and its role in glyphosate degradation in water. Aquat Microb Ecol. 2019. doi:<https://doi.org/10.3354/ame01907>.
- Mansur M. Bivalves Invasores límnicos: morfologia comparada de *Limnoperna fortunei* e espécies de Corbicula spp. In: Mansur MCD, Santos CPd, Pereira D, Paz ICP, Zurita MLL, Rodriguez MTR, Nehrka MV, Bergonci PEA, organizadores. Moluscos límnicos invasores no Brasil: biologia, prevenção, controle. Porto Alegre: Redes Editora; 2012. pp. 61–74.
- Morton B. The biology and anatomy of *Limnoperna fortunei*, a significant freshwater bioinvasive: blueprints for success. In: *Invasive nature – Springer series in invasion ecology*. Springer; 2015. doi:https://doi.org/10.1007/978-3-319-13494-9_1.
- Bogan AE. Global diversity of freshwater mussels (Mollusca, Bivalvia) in freshwater. In: Ballan EV, Lévêque C, Segers H, Martens K, editors. Freshwater animal diversity assessment. Springer; 2008. doi:https://doi.org/10.1007/978-1-4020-8259-7_16.
- Guareiro AdS, Monteiro JS, Medeiros ID, Sandini JZ. First evidence of transcriptional modulation by chlorothalonil in mussel *Perna perna*. Chemosphere. 2020. doi:<https://doi.org/10.1016/j.chemosphere.2020.126947>.

20. dos Santos RN, Campos FS, de Albuquerque NRM, Finkatti F, Corra RA, Cano-Ortiz L, Assis FL, Arantes TS, Roehle PM, Franco AC. A new marshallivirus isolated in Southern Brazil from *Limnoperna fortunei*. *Sci Rep*. 2016. doi:<https://doi.org/10.1038/srep35237>.
21. Ridewood WD. On the structure of the gills of the lamellibranchia. *Philos Trans R Soc B*. 1903. doi:<https://doi.org/10.1098/rstb.1903.0005>.
22. Cannuel R, Beninger PG, McComble H, Boudry P. Gill development and its functional and evolutionary implications in the blue mussel *Mytilus edulis* (Bivalvia: Mytilidae). *Biol Bull*. 2009. doi:<https://doi.org/10.1086/BBLv217n2p173>.
23. Atkins D. On the ciliary mechanisms and interrelationships of lamelli-branchia. Part II: types of lamellibranch gills and their food currents. *J Cell Sci*. 1937. doi:<https://doi.org/10.1242/jcs.2-79.315.375>.
24. Risgård HU, Funch P, Larsen PS. The mussel filter-pump—present understanding, with a re-examination of gill preparations. *Acta Zool*. 2015. doi:<https://doi.org/10.1111/azo.12110>.
25. Ward JE. Biodynamics of suspension-feeding in adult bivalves molluscs: particle capture, processing and fate. *Invert Bio*. 1996. doi:<https://doi.org/10.2307/3226932>.
26. Ward JE, Sanford LP, Newell RIE, MacDonald BA. A new explanation of particle capture in suspension-feeding bivalve molluscs. *Limnol Oceanogr*. 1998. doi:<https://doi.org/10.4319/lo.1998.43.5.0741>.
27. Atkins D. On the ciliary mechanisms and interrelationships of lamelli-branchia. Part VI: latero-frontal cilia of the gill filaments and their phylogenetic value. *J Cell Sci*. 1938. doi:<https://doi.org/10.1242/jcs.2-80.319.345>.
28. Sivarman H, Lynn JW, Achberger EC, Dietz TH. Gill structure in zebra mussels: bacterial-sized particle filtration. *Am Zool*. 1996. doi:<https://doi.org/10.1093/ncb/36.3.373>.
29. Owen G. Classification and the bivalve gill. *Phil Trans R Soc Lond B*. 1978. doi:<https://doi.org/10.1098/rstb.1978.0075>.
30. Yonge C. Structure and physiology of the organs of feeding and digestion in *Ostrea edulis*. *J Mar Biol Assoc UK*. 1926. doi:<https://doi.org/10.1017/S002531540000789X>.
31. Atkins D. On the ciliary mechanisms and interrelationships of lamelli-branchia. Part II: sorting devices on the gills. *J Cell Sci*. 1937. doi:<https://doi.org/10.1242/jcs.2-79.315.339>.
32. Foster-Smith RL. The role of mucus in the mechanism of feeding in three filter-feeding bivalves. *Proc Malac Soc Lond*. 1975. doi:<https://doi.org/10.1093/oxfordjournals.molus.a065307>.
33. Ribelin BW, Collier A. Studies on the gill ciliation of the American oyster *Crassostrea virginica* (Gmelin). *J Morph*. 1977. doi:<https://doi.org/10.1002/jmor.1051510308>.
34. Foster-Smith RL. The function of the pallial organs of bivalves in controlling ingestion. *J Moll Stud*. 1978; doi:<https://doi.org/10.1093/oxfordjournals.molus.a065419>.
35. Beninger PG, Le Pennec M, Dorval A. Mode of particle ingestion in five species of suspension-feeding bivalve molluscs. *Mar Biol*. 1991. doi:<https://doi.org/10.1007/BF01344340>.
36. Risgård HU, Larsen PS. Particle capture mechanisms in suspension-feeding invertebrates. *Mar Ecol Prog Ser*. 2010. doi:<https://doi.org/10.3354/meps08755>.
37. Ward JE, Shumway SE. Separating the grain from the chaff: particle selection in suspension- and deposit-feeding bivalves. *J Exp Mar Biol Ecol*. 2004. doi:<https://doi.org/10.1016/j.jembe.2004.03.002>.
38. Rosa M, Ward JE, Shumway SE. Selective capture and ingestion of particles by suspension-feeding bivalve molluscs: a review. *J Shellfish Res*. 2018. doi:<https://doi.org/10.2983/035.037.0405>.
39. Paolucci E, Sardiña P, Sylvester F, Peropeltzin PV, Zhan A, Ghabooli S, Cristescu ME, Oliveira MD, MacIsaac HJ. Morphological and genetic variability in an alien invasive mussel across an environmental gradient in South America. *Limnol Oceanogr*. 2014. doi:<https://doi.org/10.4319/lo.2014.59.2.0400>.
40. Rodriguez C, Prieto GI, Vega IA, Castro-Vazquez A. Functional and evolutionary perspectives on gill structures of an obligate air-breathing aquatic snail. *PeerJ*. 2019. doi:<https://doi.org/10.7717/peerj.7342>.
41. Beninger PG, Le Pennec M, Salatin M. New observations of the gills of *Placopecten magellanicus* (Mollusca: Bivalvia), and implications for nutrition. I. General anatomy and surface microanatomy. *Mar Biol*. 1988. doi:<https://doi.org/10.1007/BF00392659>.
42. Le Pennec M, Beninger PG, Herry A. New observations of the gills of *Placopecten magellanicus* (Mollusca: Bivalvia), and implications for nutrition. II. Internal anatomy and microanatomy. *Mar Biol*. 1988. doi:<https://doi.org/10.1007/BF00391199>.
43. Owen G. Studies on the gill of *Mytilus edulis*: the eu-latero-frontal cilia. *Proc R Soc Lond B*. 1974. doi:<https://doi.org/10.1098/rspb.1974.0062>.
44. Nogaol LR, Brassi-Garcia AL, de Oliveira David JA, Fontanetti CS. Morphological and Histochemical Characterization of Gill Filaments of the Brazilian Endemic Bivalve *Diplodon expansus* (Küster, 1856) (Mollusca, Bivalvia, Hyridae). *Microsc Microanal*. 2012. doi:<https://doi.org/10.1017/S1431927612013992>.
45. Beninger PG, Decottignies P. Worth a second look: gill structure in *Hemipecten forbesianus* (Adam & Reeve, 1849) and taxonomic implications for the Pectinidae. *J Molluscan Stud*. 2008. doi:<https://doi.org/10.1093/mollus/eyn001>.
46. Beninger PG, St-Jean S, Poussart Y, Ward JE. Gill function and mucocyte distribution in *Placopecten magellanicus* and *Mytilus edulis* (Mollusca: Bivalvia): the role of mucus in particle transport. *Mar Eco Prog Ser*. 1993. doi:<https://doi.org/10.3354/meps098275>.
47. Beninger PG, Cannuel R, Jaunet S. Particle processing on the gill plcae of the oyster *Crassostrea gigas*: fine-scale mucocyte distribution and functional correlates. *Mar Eco Prog Ser*. 2005. doi:<https://doi.org/10.3354/meps295191>.
48. Garrido M, Chaparro O, Thompson R, Garrido O, Navarro J. Particle sorting and formation and elimination of pseudofaeces in the bivalves *Mulinia edulis* (siphonate) and *Mytilus chilensis* (asiphonate). *Mar Biol*. 2012. doi:<https://doi.org/10.1007/s00227-012-1879-8>.
49. Beninger PG, Le Pennec M. Scallop structure and function. *Dev Aquacult Fish Sci*. 2016. doi:<https://doi.org/10.1016/B978-0-444-62710-0.00003-1>.
50. Zappa F, Falli M, Mattioli MA. The Golgi complex in disease and therapy. *Curr Opin Cell Biol*. 2018. doi:<https://doi.org/10.1016/j.cob.2018.03.005>.
51. Fontanesi F. Mitochondria: structure and role in respiration. *eLS*. 2001. doi:<https://doi.org/10.1002/9780470015902.a0001380.pub2>.
52. Jones HD, Richards OG, Hutchinson S. The role of ctenidial abfrontal cilia in water pumping in *Mytilus edulis* L. *J Exp Mar Biol Ecol*. 1990. doi:[https://doi.org/10.1016/0022-0981\(90\)90108-Q](https://doi.org/10.1016/0022-0981(90)90108-Q).
53. Alberts B, Dennis B, Karen H. *Fundamentos da Biologia Celular 4. Porto Alegre: Artmed Editora*; 2006.
54. Berthelin C, Kallner K, Mathieu M. Histological characterization and glucose incorporation into glycogen of the Pacific oyster *Crassostrea gigas* storage cells. *Mar Biotechnol*. 2000. doi:<https://doi.org/10.1007/s101269900017>.
55. Gilula NB, Satir P. Septate and gap junctions in molluscan gill epithelium. *J Cell Biol*. 1971. doi:<https://doi.org/10.1083/jcb.51.3.869>.
56. Alexander DB, Goldberg GS. Transfer of biologically important molecules between cells through gap junction channels. *Curr Med Chem*. 2005. doi:<https://doi.org/10.2174/0929867033456927X1>.
57. Bancroft JD, Layton C. 10 - The hematoxylin and eosin, Editors: Suvarna SK, Layton C, Bancroft JD. *Bancroft's theory and practice of histological techniques*. 2012; doi:<https://doi.org/10.1016/B978-0-7020-4226-3.00010-X>.
58. Yamabayashi S. Periodic acid-Schiff-Alcian Blue: A method for the differential staining of glycoproteins. *Histochem J*. 1987. doi:<https://doi.org/10.1007/BF01687364>.
59. Forno AB, Alves I, Silva MA, Camujo O. Otimização da técnica do tricrômio de Masson. *Micron*. 2006; <http://hdl.handle.net/10400.21/5458>.

Publisher's Note

Springer Nature remains neutral with regard to jurisdictional claims in published maps and institutional affiliations.